INTRODUCTION TO SAR REMOTE SENSING

Thuy Le Toan

10 May 2021

Introduction to SAR remote sensing

Thuy Le Toan
Centre d'Etudes Spatiales de la Biosphère (CESBIO)
Toulouse, France
Thuy.Letoan@cesbio.cnes.fr

Contents


Lsynth

The electromagnetic spectrum

Synthetic Aperture Radar (SAR)

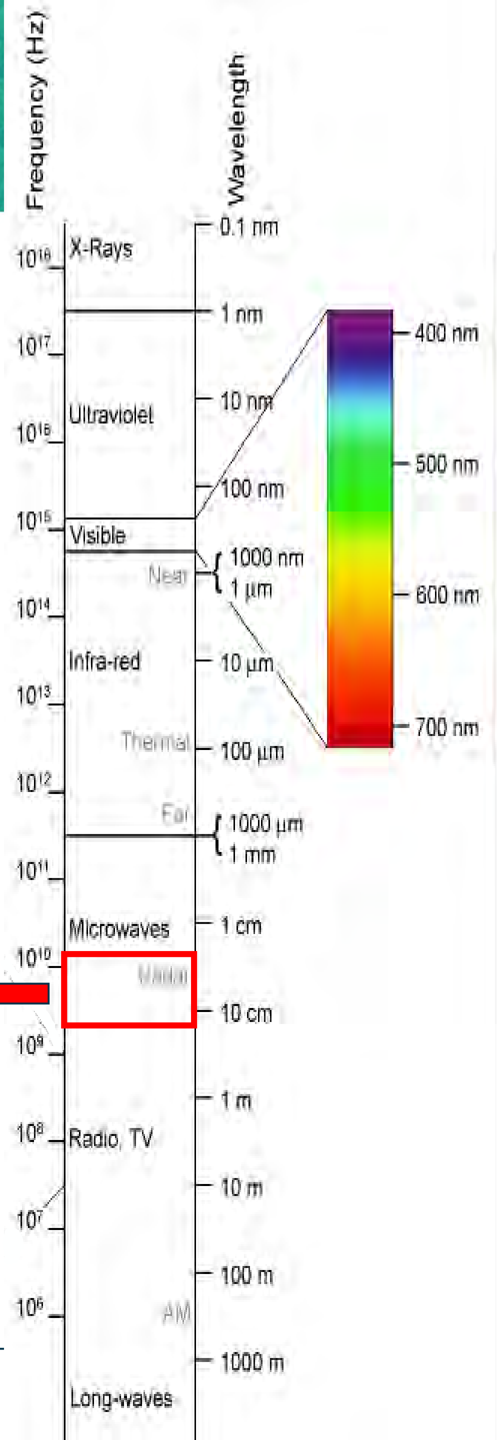

The electromagnetic spectrum

Visible (VIS) + Near Infrared (NIR) = Optical

Thermal Infrared (TIR)

Synthetic Aperture Radar (SAR)

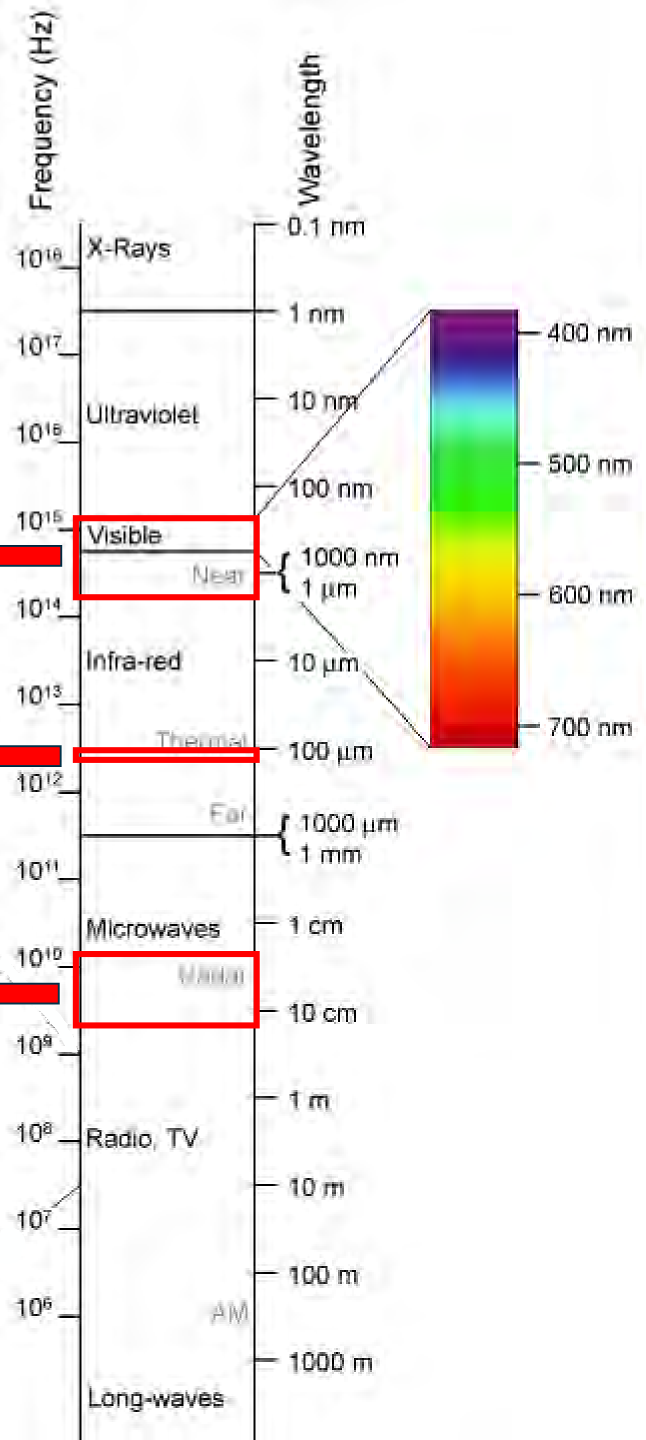

SAR: all-weather observing system

Forest loss in Cameroon

Sentinel-1

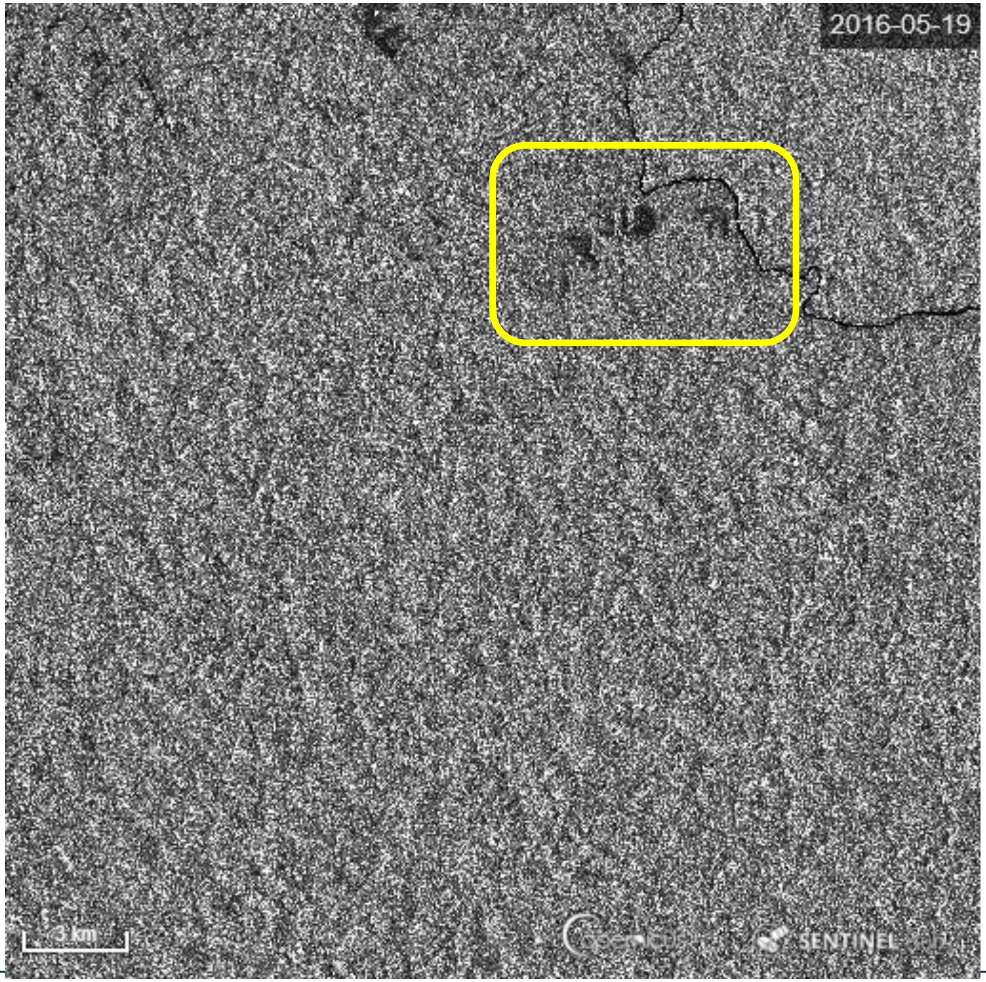

Sentinel-2

Marginal atmospheric effects

Strong attenuation

Low attenuation

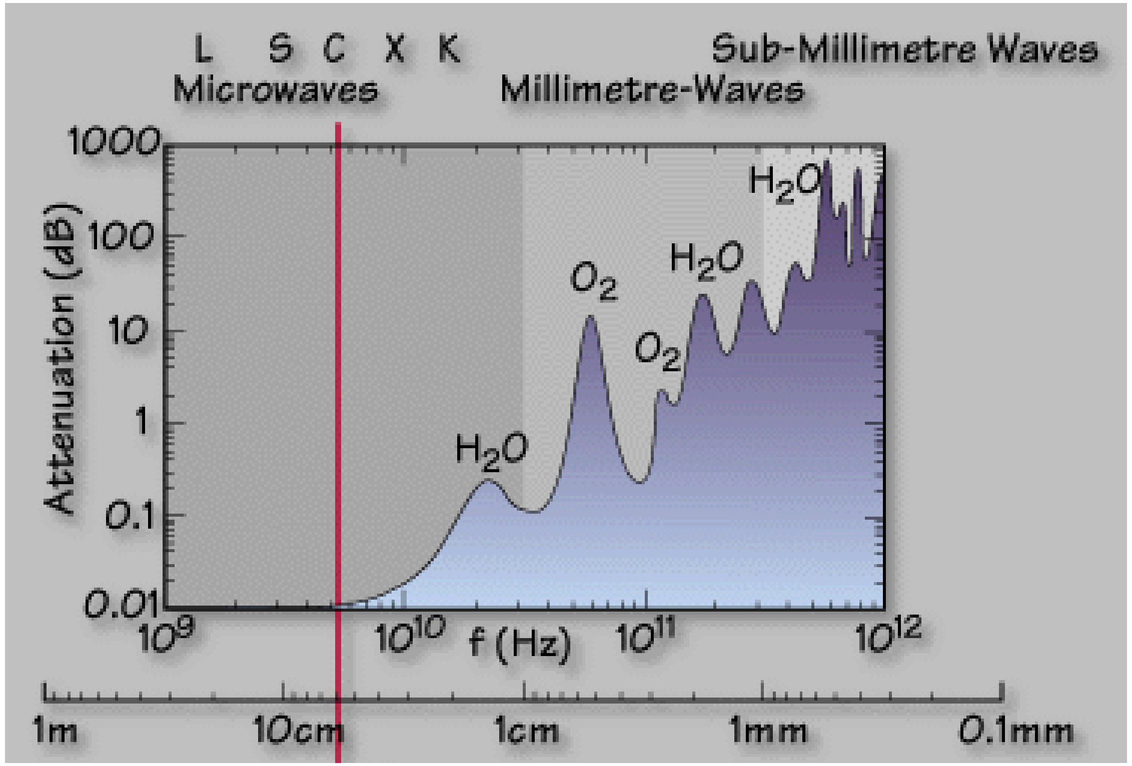

Very low attenuation by atmospheric constituents for λ > ~5 cm

Principle of imaging radar

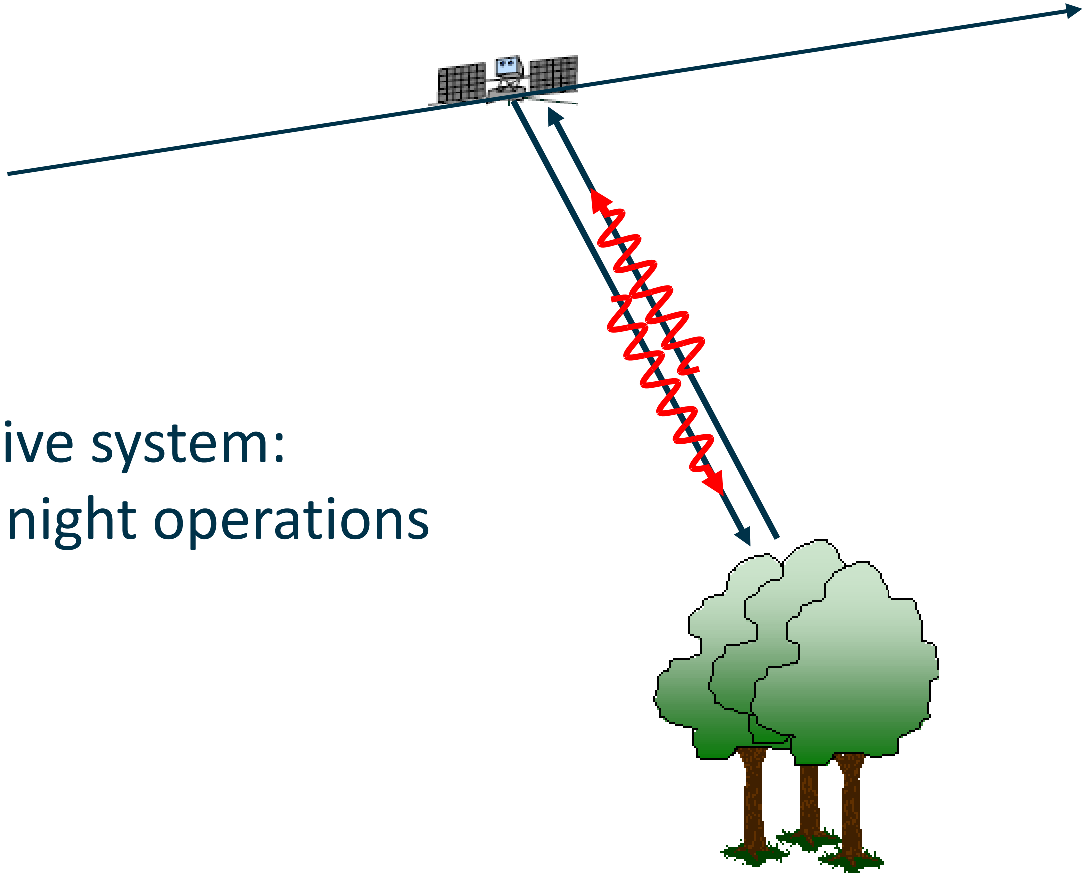

Active system:
day and night operations

Side Looking Radar

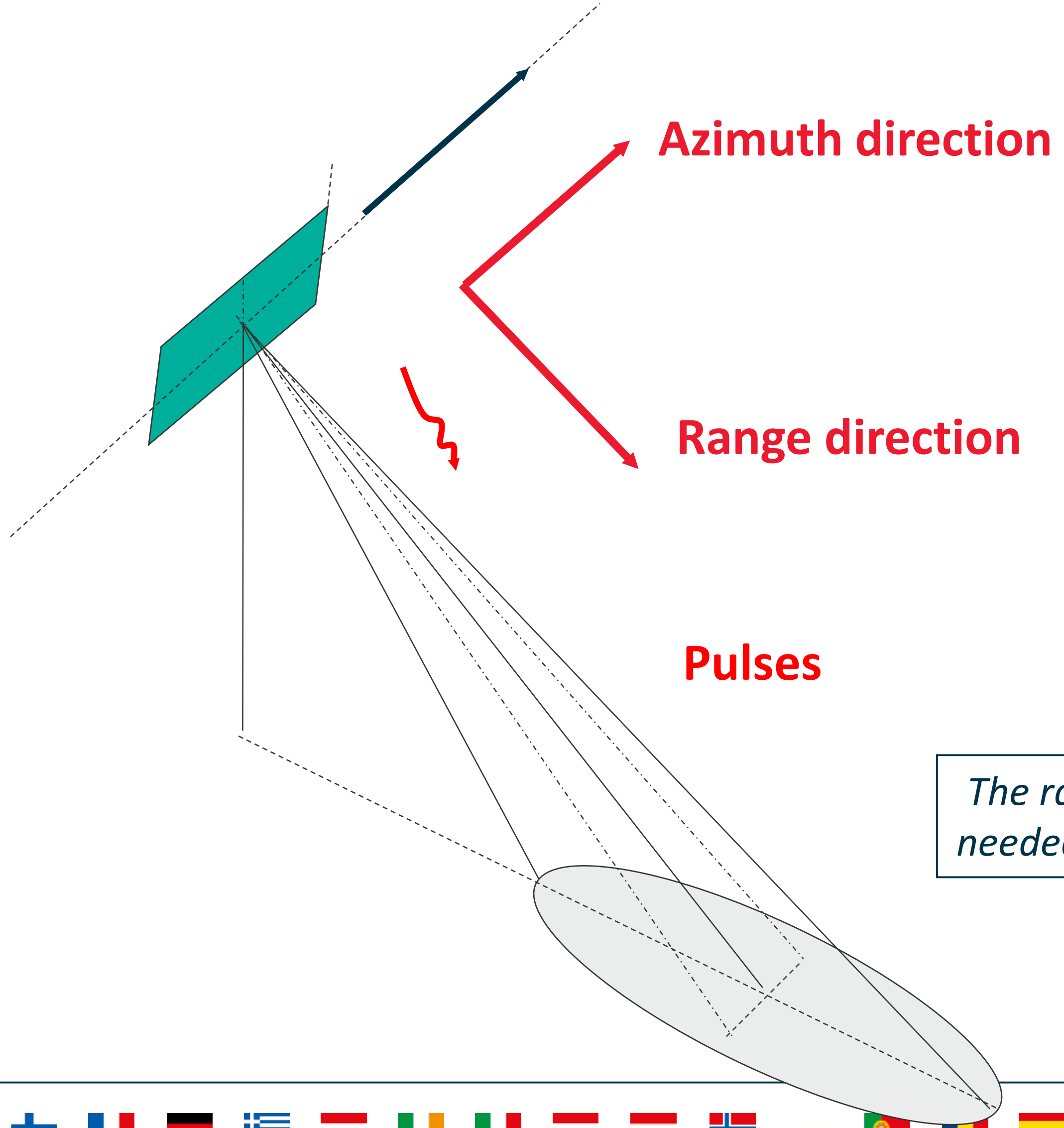

Linear displacement of the antenna along the track

The range information comes from the time needed by the pulse to travel way and back

Why side looking ?

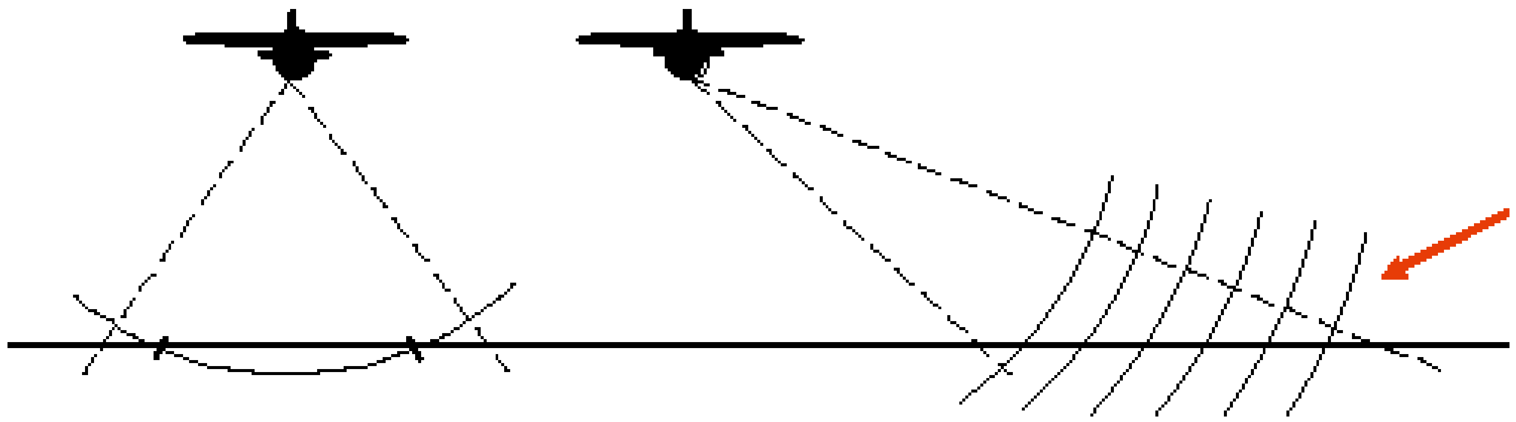

Antenna scattering

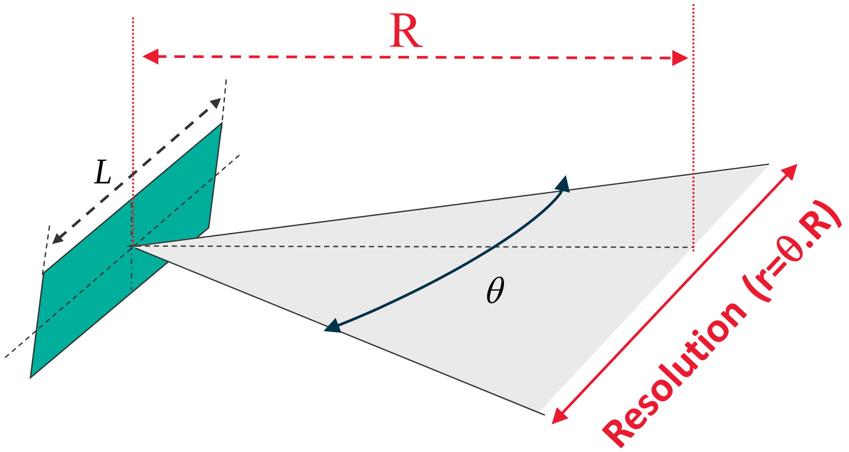

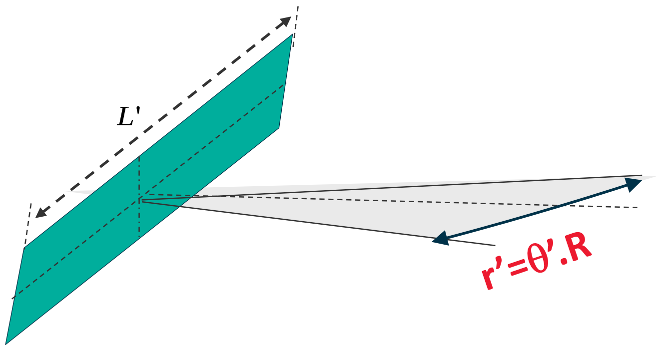

$$\theta = \frac{\lambda}{L}$$

- λ: Wavelength
- θ: Angular aperture (horizontal plane)
- L: Antenna length (horizontal direction)

The larger the antenna, the narrower the aperture (finer resolution)

$$\text{Resolution} = \frac{\lambda R}{L}$$

<u>Numerical example:</u>

L ≈10m, R ≈1000 km (spaceborne radar), λ ≈5 cm (C band) ➔ **resolution ≈ 5 km**

Synthetic aperture technique

An array of antennas is equivalent to a single antenna moving along the flight line L_S if the received signals are coherently recorded and added, and the target assumed to be static during the period

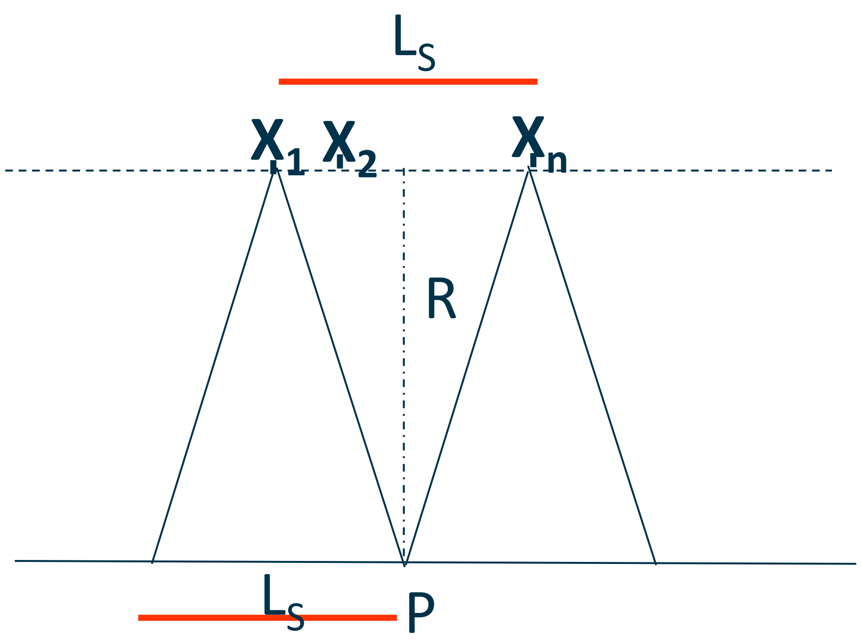

The echoes from X_1, X_2, ..X_n are recorded coherently (amplitude and phase as a function of time)

Azimuth resolution

$$Ra = \frac{\lambda R}{L_S}$$

The SAR image

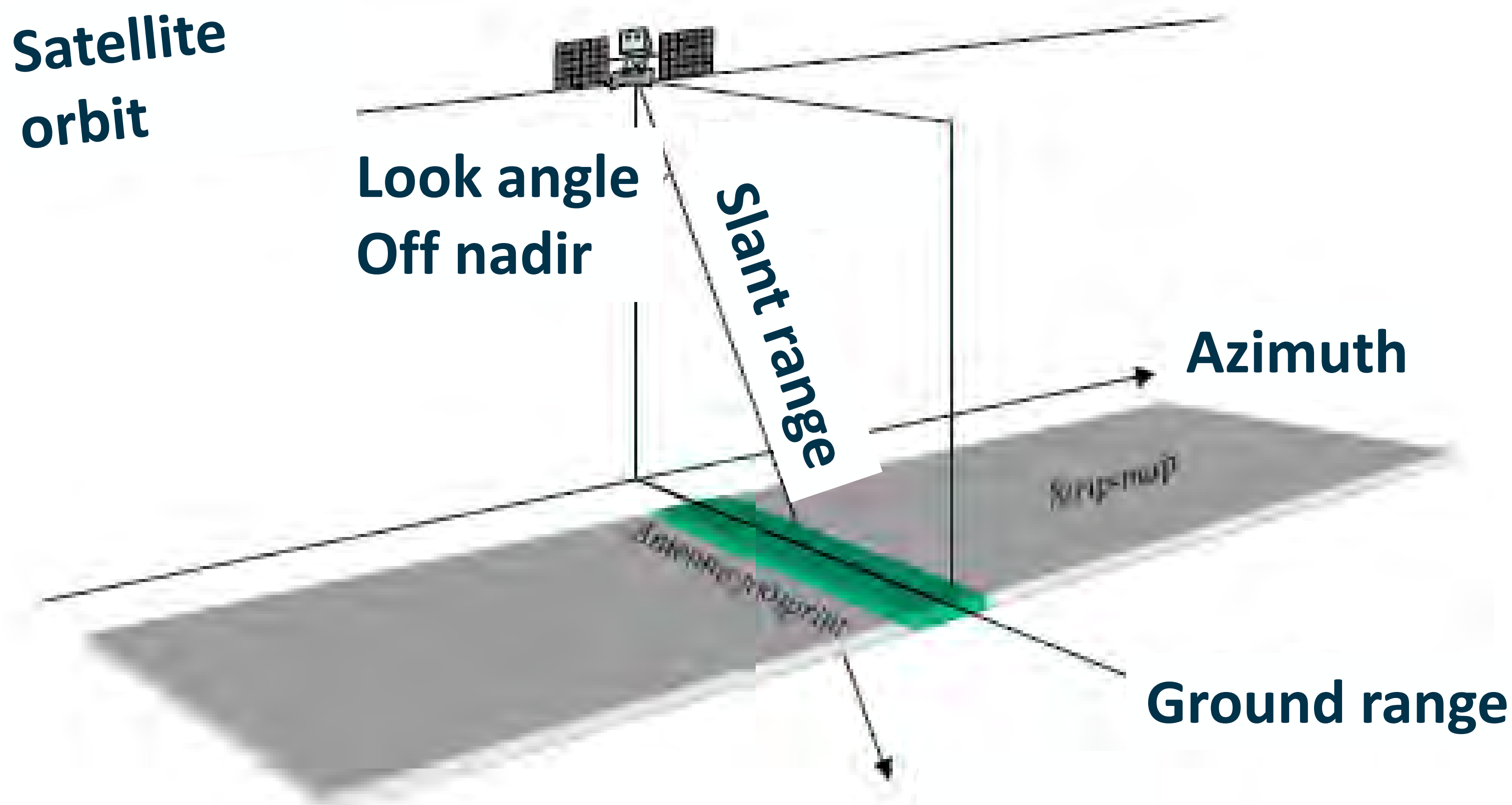

What does the SAR measure ?

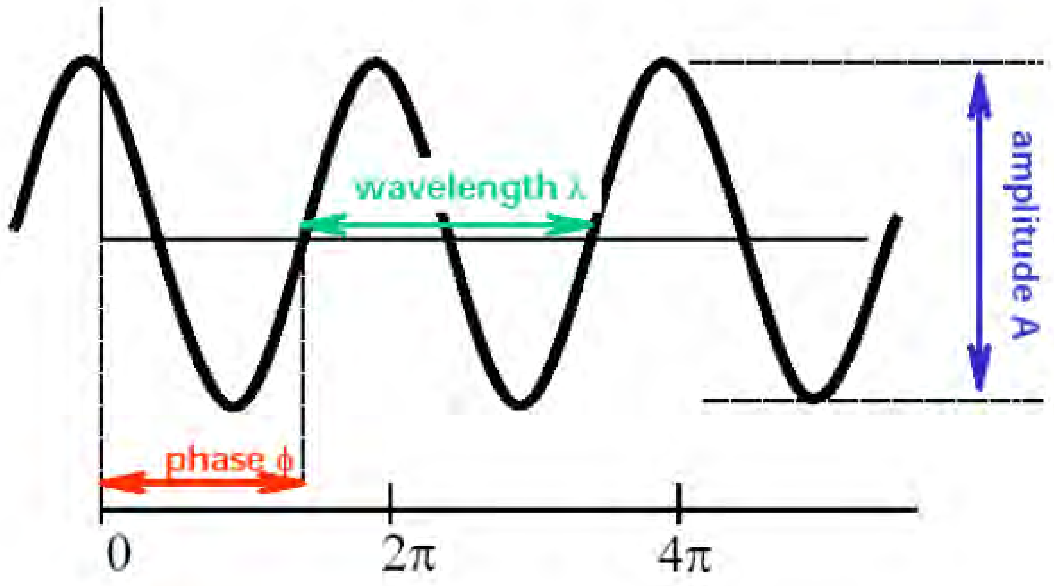

1. **Amplitude** which depends on the target properties (dielectric and geometric properties)

2. **Phase** which is function of the sensor-target distance and target properties

SAR measurement modes-BIOMASS

PolSAR

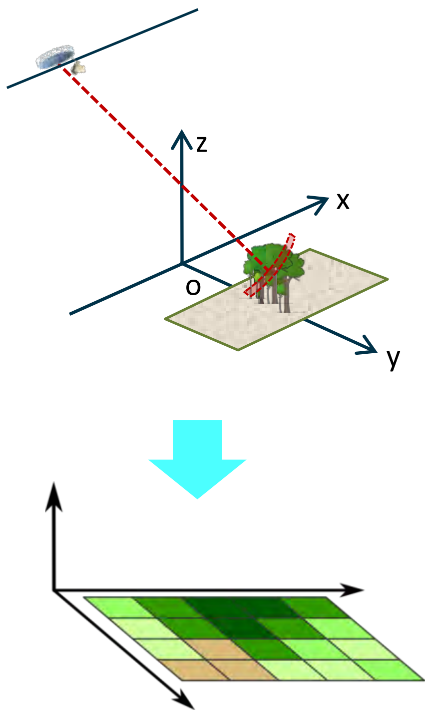

Pol-InSAR

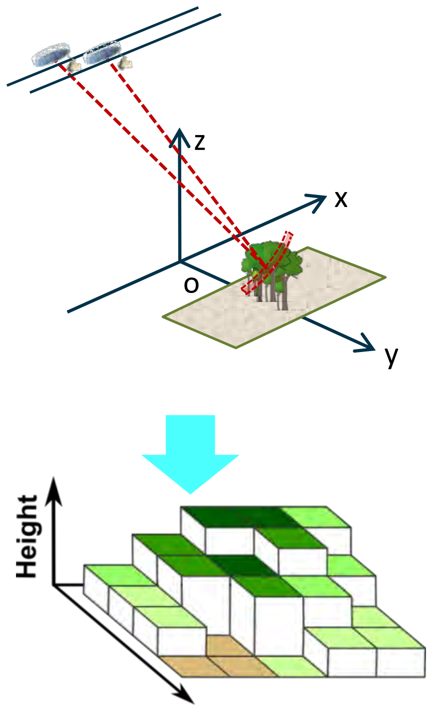

TomoSAR

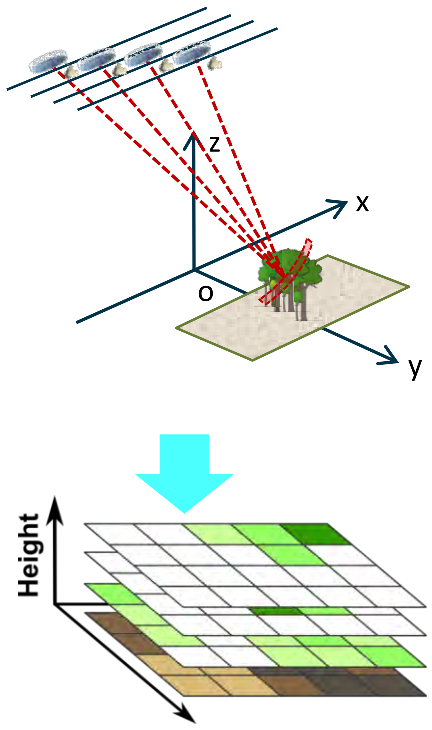

Tree height inversion

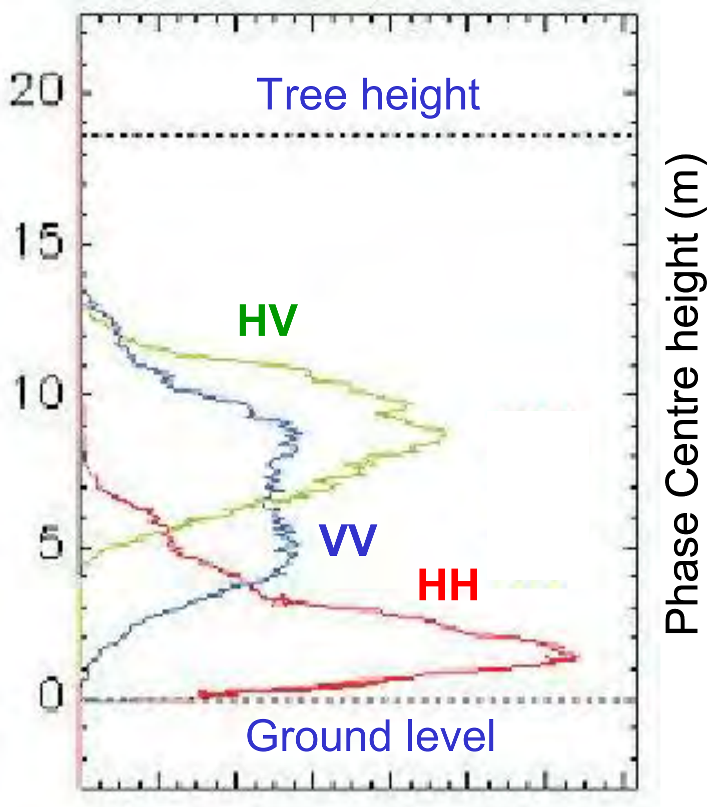

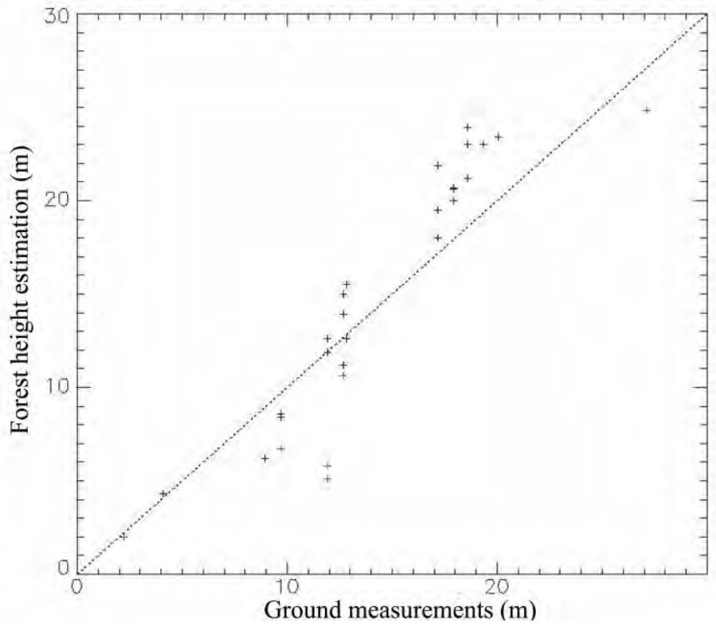

Garestier, 2006

Radar Interferometry

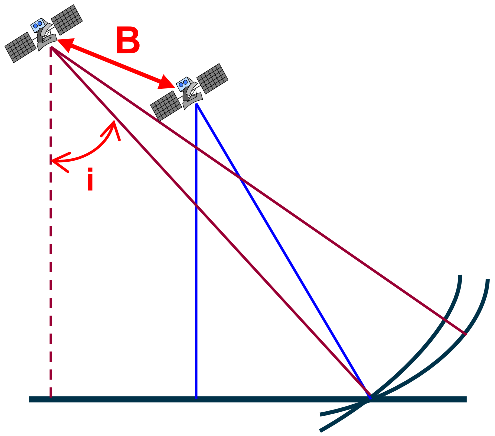

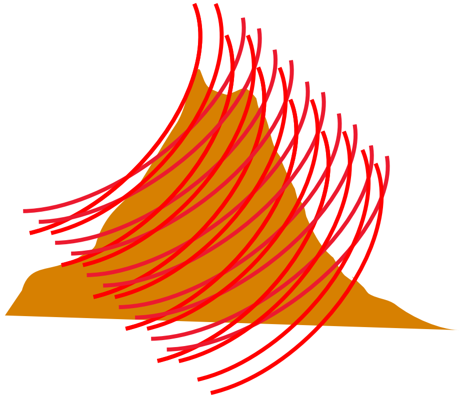

Relief

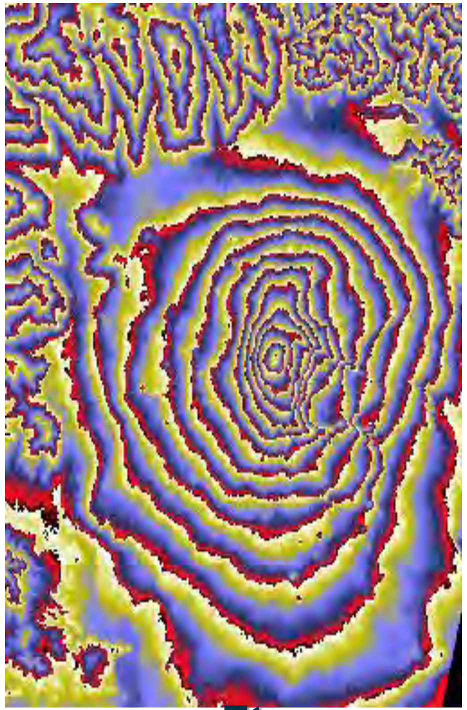

Etna
iso-altitude curves

Digital elevation models

Terrain displacement

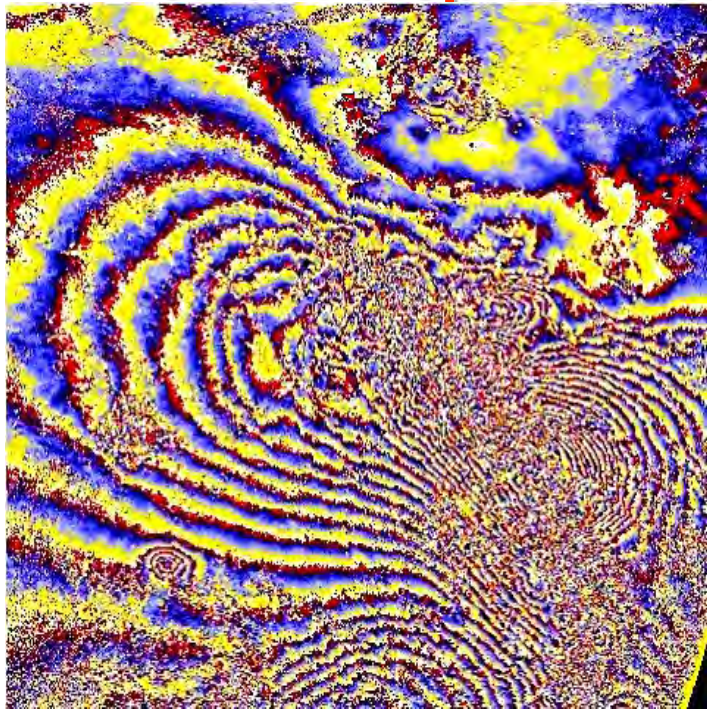

Landers
iso-displacement curves

Cartography of terrain displacements

Radar Interferometry

ERS intensity image

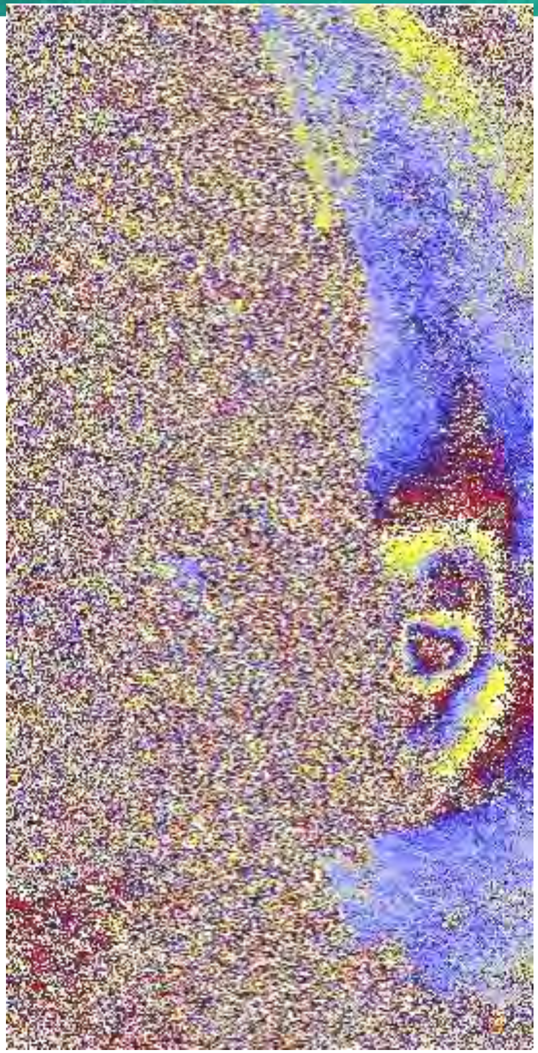

Interferogramme

ERS Interferometry

Mesa, USA/ Mexico border

• *Impact of a geothermal plant on the environment. Interferogram processed from two ERS images, acquired at two years interval. The fringes characterize the ground subsidence around the plant. One observe a subsidence of about 6 cm (2 fringes) which covers 17km x 8km.*

CENTRE NATIONAL D'ETUDES SPATIALES

Principal available SAR data

Satellite	Life-time	Frequen-cy	Polarisation	Resolution	Frame	Repeat cycle	Access
TerraSAR-X **TanDEM-X**	2007- 2010-	**X-band** **λ= 3.5cm**	Single HH,VV Dual: HH/VV,HH/HV VV/VH	Spotlight: <1m,1.7x3.5m Stripmap: 3x3m ScanSAR:18x40m	Spotlight:3x10km Stripmap:50x30km ScanSAR:150x100, 200x200km	11days	Restrained Scientific, Commercial
COSMO-Skymed	2007-	**X-band** **λ= 3.5cm**	Single: HH, VV, HV,VH Dual	Spotlight < 1m Stripmap: 3x15m ScanSAR:30x100m	Spotlight:10x10km Stripmap:40x40km ScanSAR:100x100, 200x200km	Sat: 16 d Constellation: hrs	Commercial Limited scientific.
Radarsat-2	2007-	**C-band** **λ= 5.6cm**	Single: HH, VV, HV,VH Dual: HH/HV,VV/VH Quad	Spotlight : 1.5m Stripmap: 3x3m 25x25m ScanSAR:35x35m 100x100 m	Spotlight:18x8km Stripmap: 20x170km ScanSAR:300x300, 500x500km	24 days	Commercial
ALOS-2 **PALSAR-2**	2014-	**L-band** **λ= 24.6cm**	Single: HH, VV, HV,VH Dual: HH/HV,VV/VH Quad	Spotlight : 1x3m Stripmap: 3x10m ScanSAR:25x100m	Spotlight:25x25km Stripmap:50x70km 70x70km ScanSAR: 355x355km	14days	Commercial Limited proposal-based Scientific.
Sentinel-1	2014-	**C-band** **λ= 5.6cm**	Single: HH, VV Dual: HH/HV,VV/VH	Stripmap: 5x5m Interferometric Wide Swath (IW): 5x20m Extra Wide Swath (EW): 20x40m	Stripmap: 375km IW:250 km EW:400 km	12days S1 &S2: 6 days	Free & Open Access

Principal SAR missions

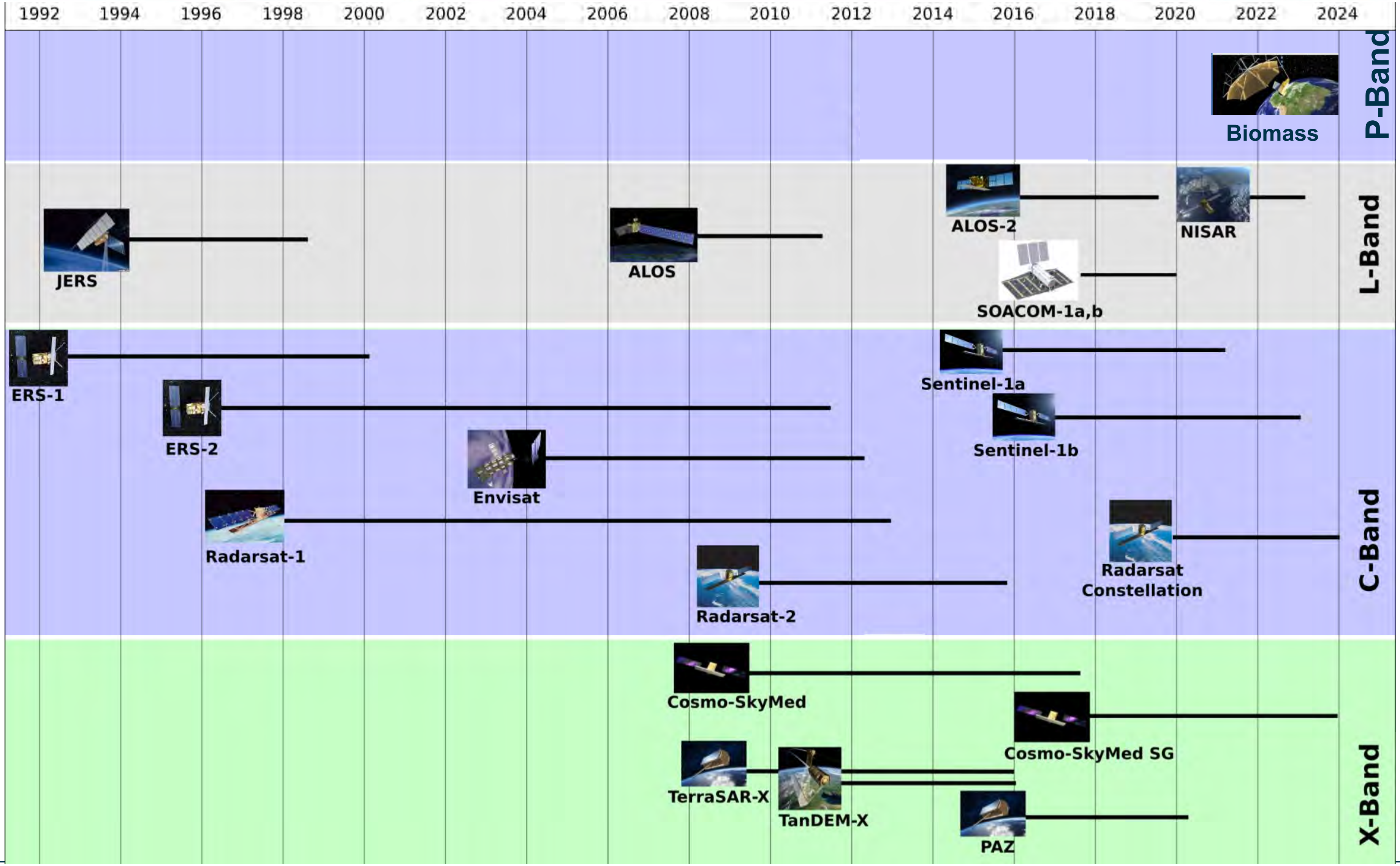

Radar frequency bands

Frequency band	Wavelength (cm)	Frequency (GHz)
Ka	0.8-1.1	40 - 26.5
K	1.1-1.7	26.5 - 18
Ku	1.7-2.4	18 - 12.5
X	2.4-3.8	12.5 -8
C	3.8-7.5	8 - 4
S	7.5-15	4 - 2
L	15 -30	2 - 1
P	30 -100	1 - 0.3

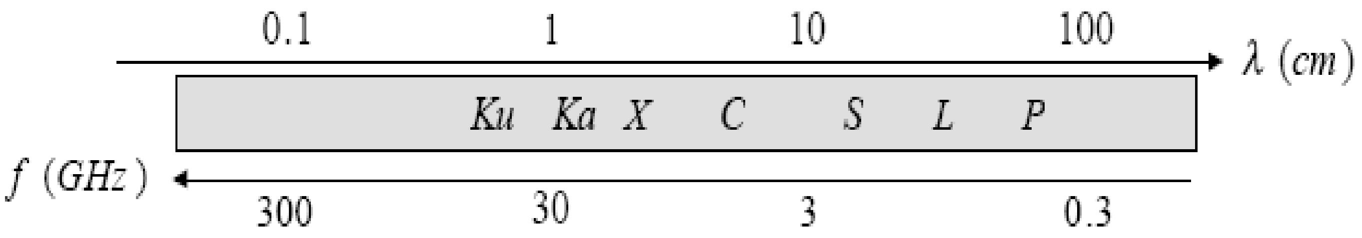

f (in Hertz)=C/λ

C=3.10[8] m

λ =wavelength in m

Polarisation

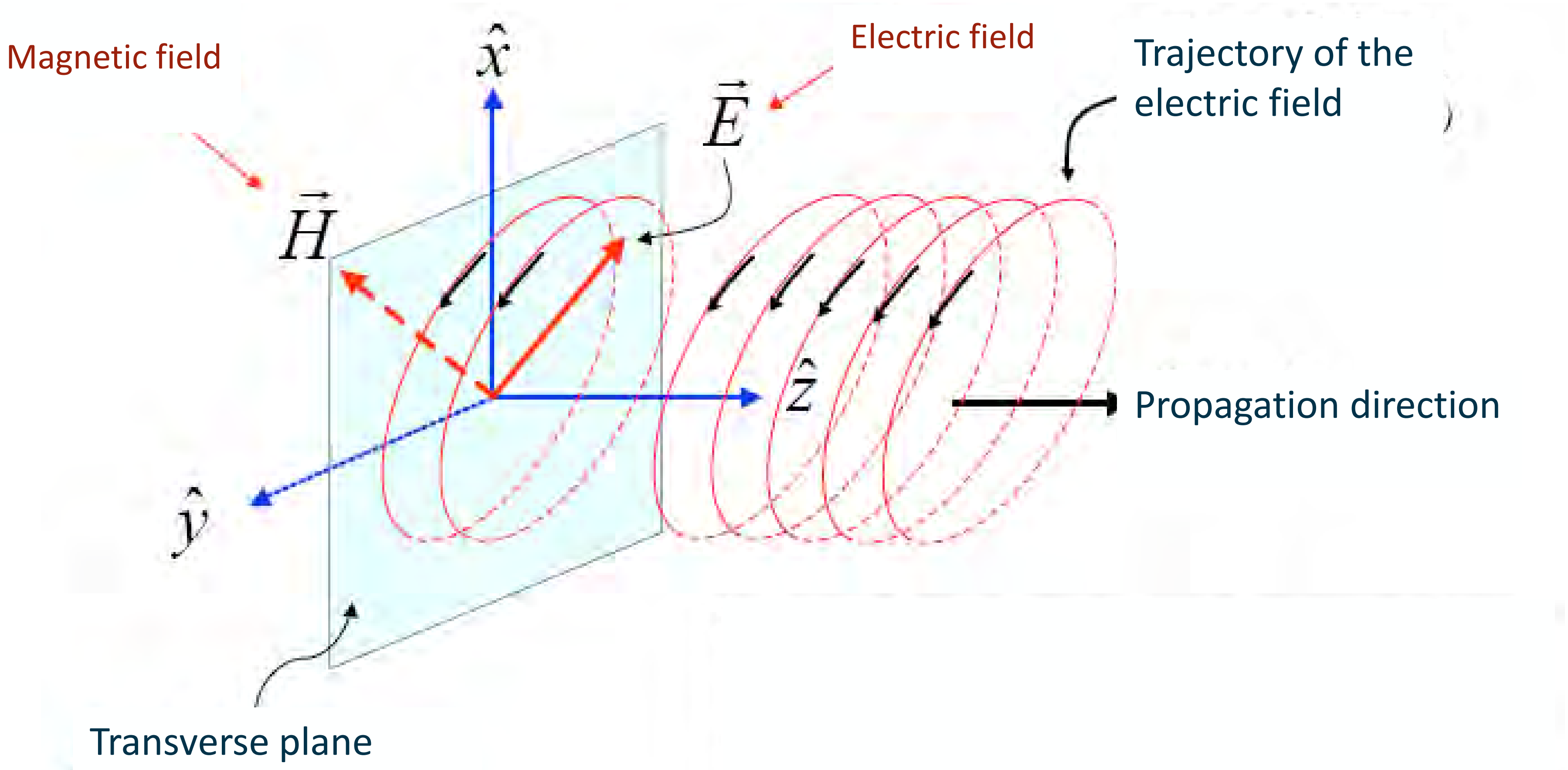

Polarisation

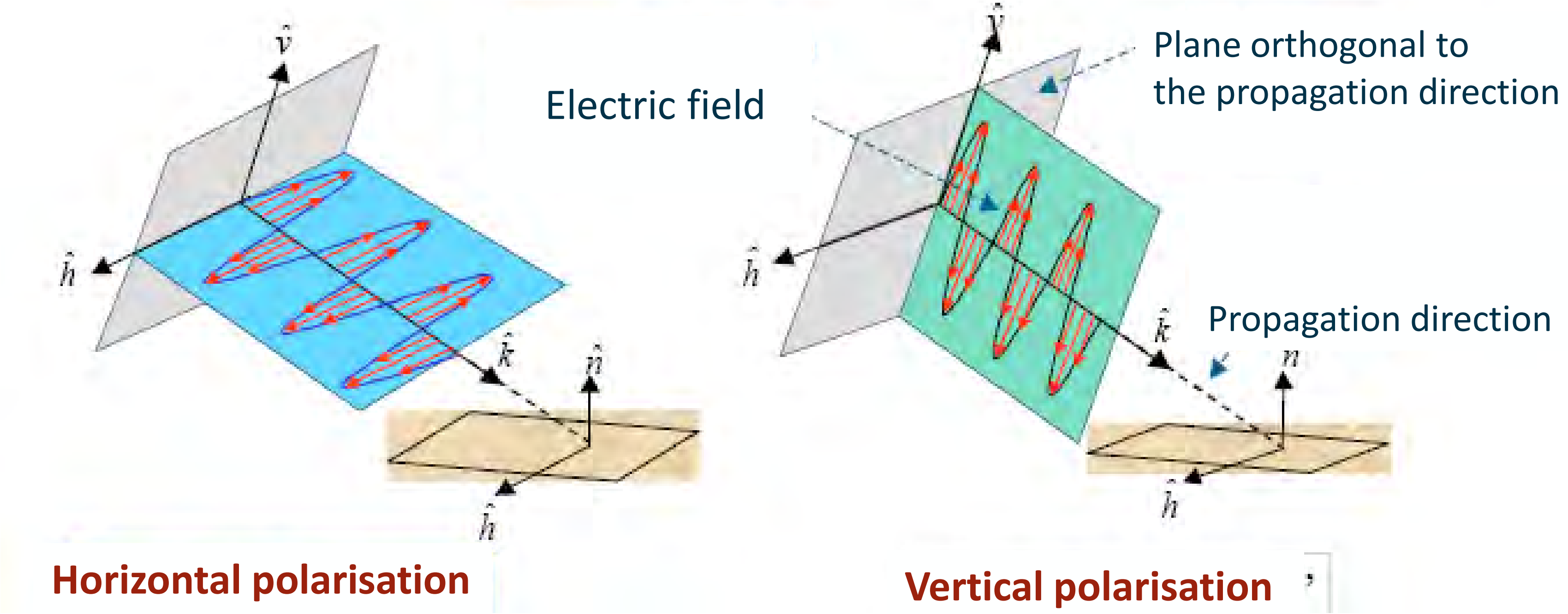

Polarisation

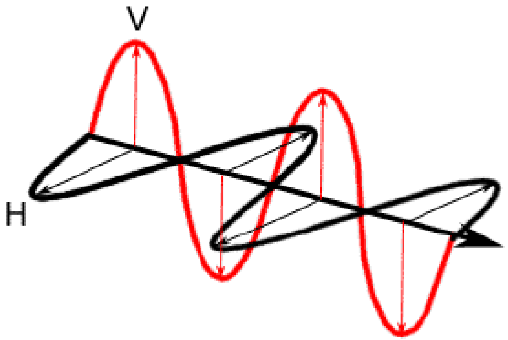

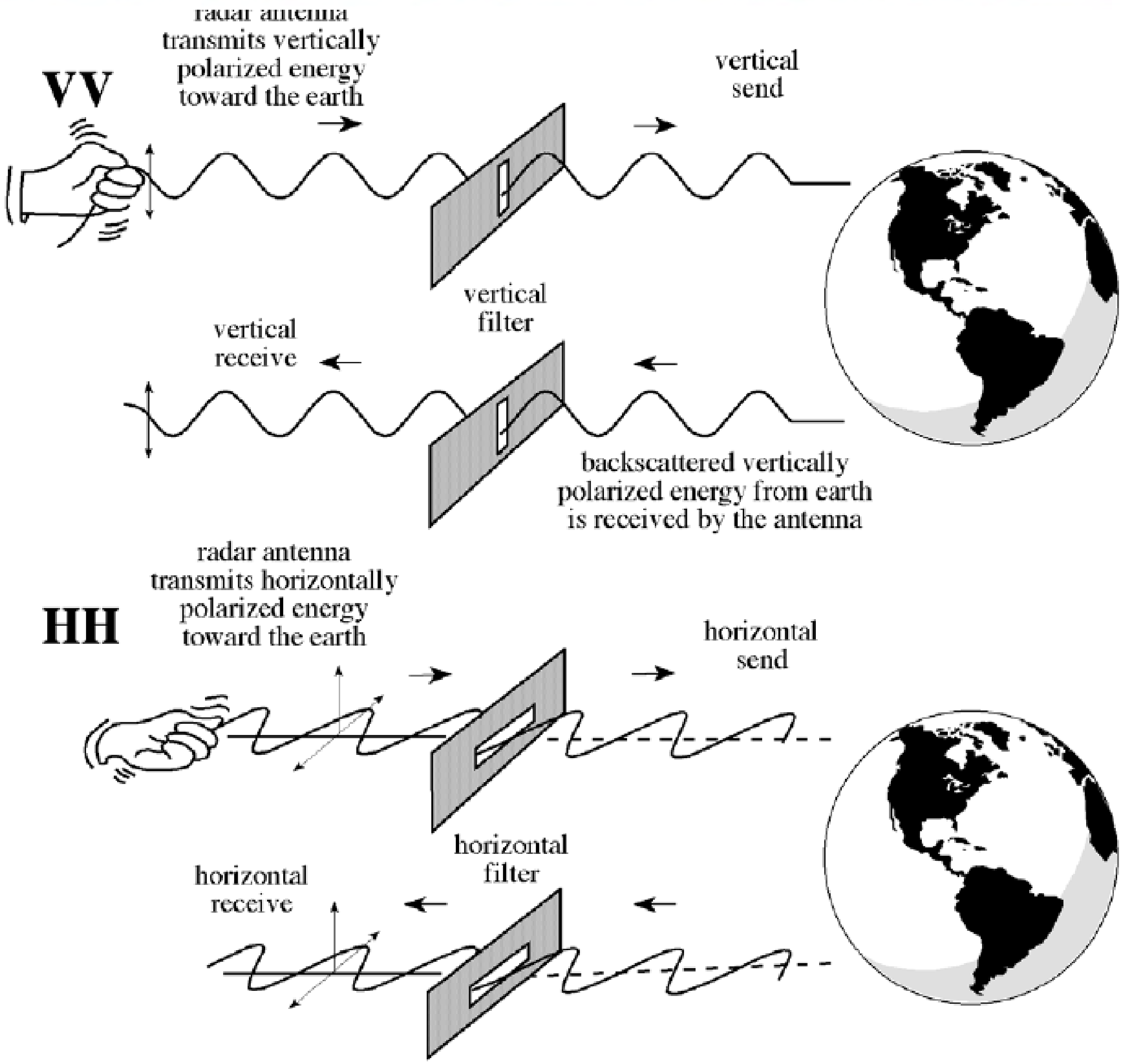

The radar scattering

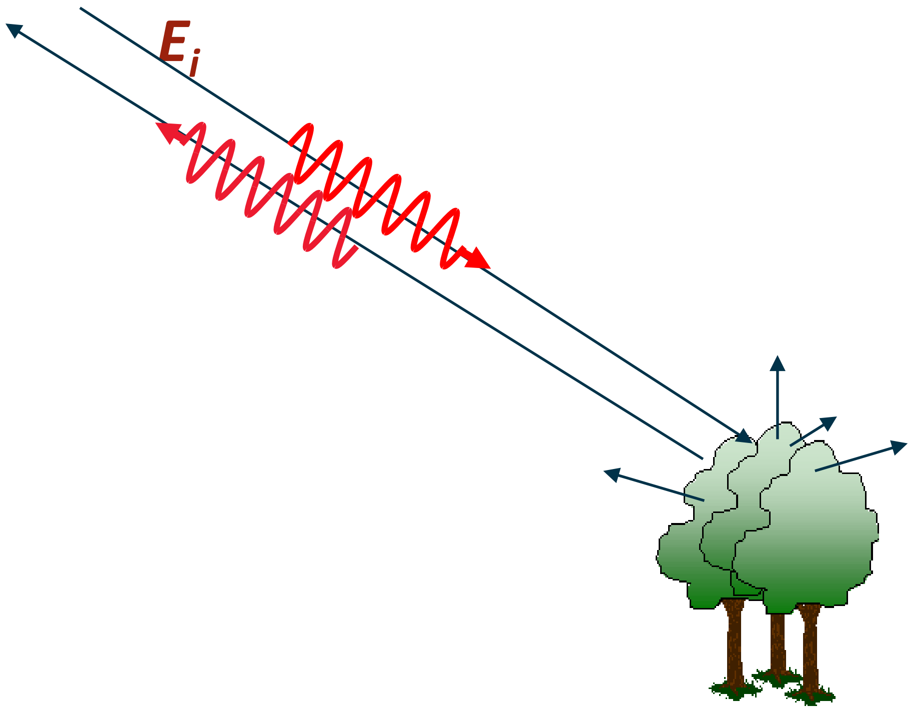

the amplitude, phase and polarisation of E_s are modified with respect to E_i

Basic measurement

The basic measurement made by a SAR is called S (amplitude and phase). This is the complex image.

Main types of images:

A is the amplitude image.
$I = A^2$ is the intensity image.
(the phase of a single image is not exploitable)

The radar cross section

The radar cross-section (RCS) is defined as

$$\sigma_{pq} = 4\pi \left| S_{pq} \right|^2 = 4\pi R^2 \frac{P_s}{P_i} \qquad [\mathrm{m}^2]$$

R is the radar-target distance
P_i is the incident power,
P_s is the power scattered by the target.

The backscattering coefficient

For distributed targets each resolution cell contains many scatterers and the phase varies rapidly with position.

The differential backscattering coefficient, σ^o, is

$$\sigma^o = \frac{4\pi R^2}{\Delta A} \frac{P_s}{P_i} \qquad [m^2/m^2]$$

where ΔA is the area of the illuminated surface over which the phase can be considered constant.

Slant and ground range

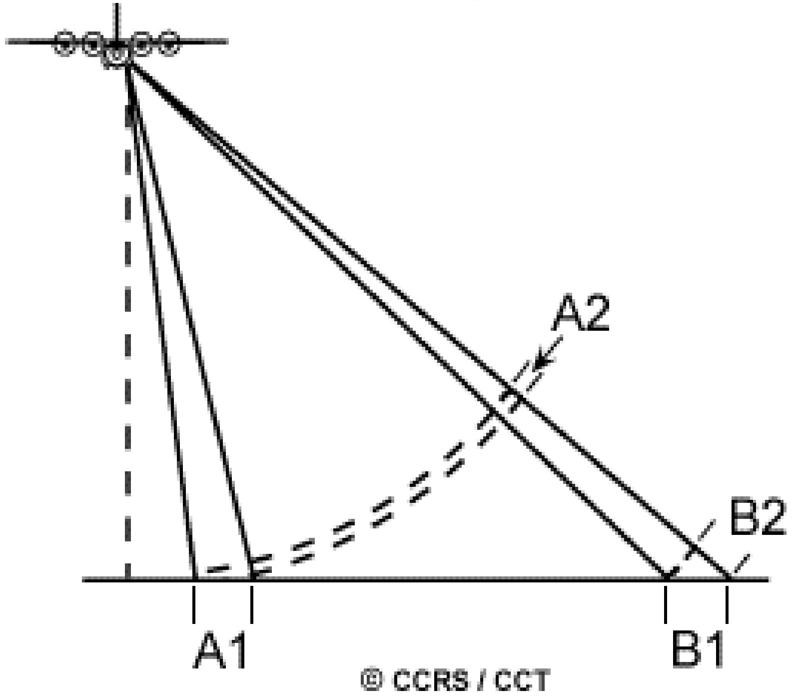

Source: CCRS tutorials

Slant range

Ground range

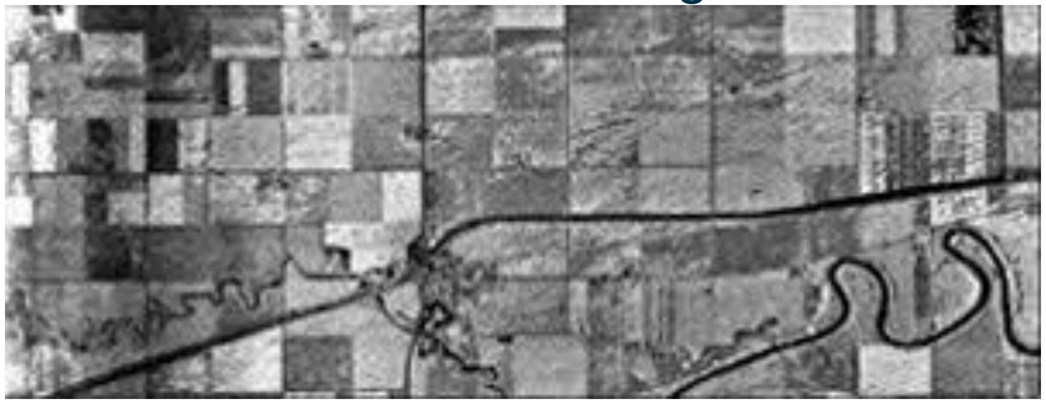

Contents

What is a SAR image?

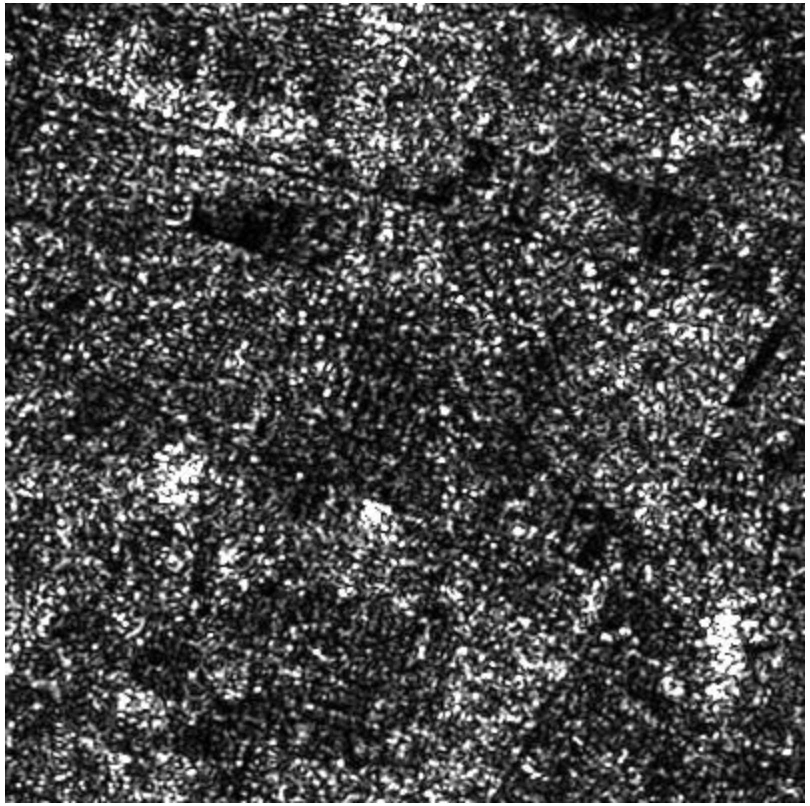

Example of an intensity image
APP HH image 400 x 400 pixels (of 12.5m)
Gaoyou, Jiangsu province, China, 2004 05 24

The image is seen as a **picture**.

Pixels are **numbers**.

Image is affected by **speckle** noise

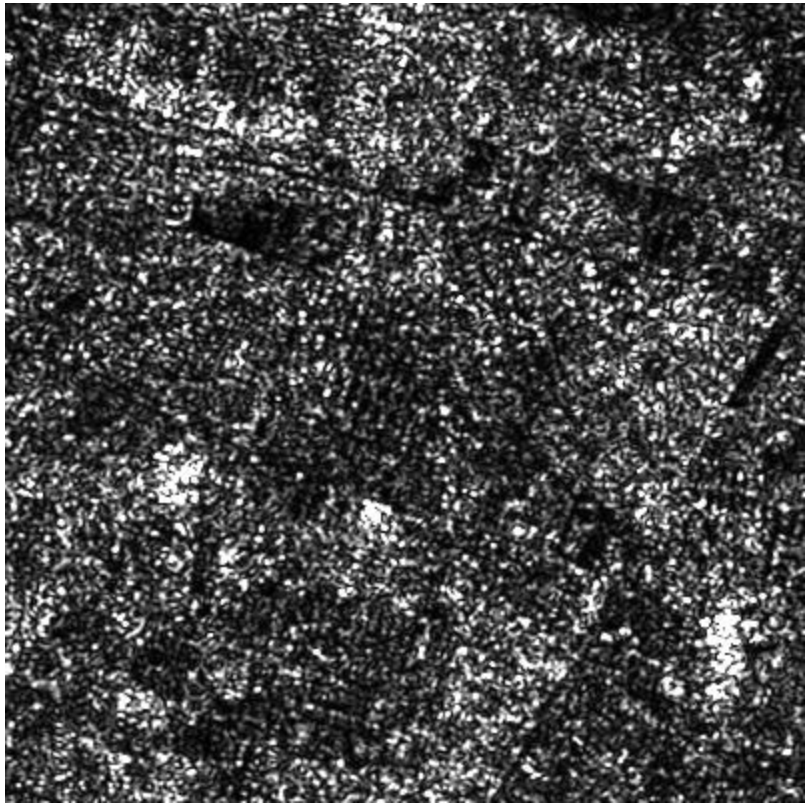

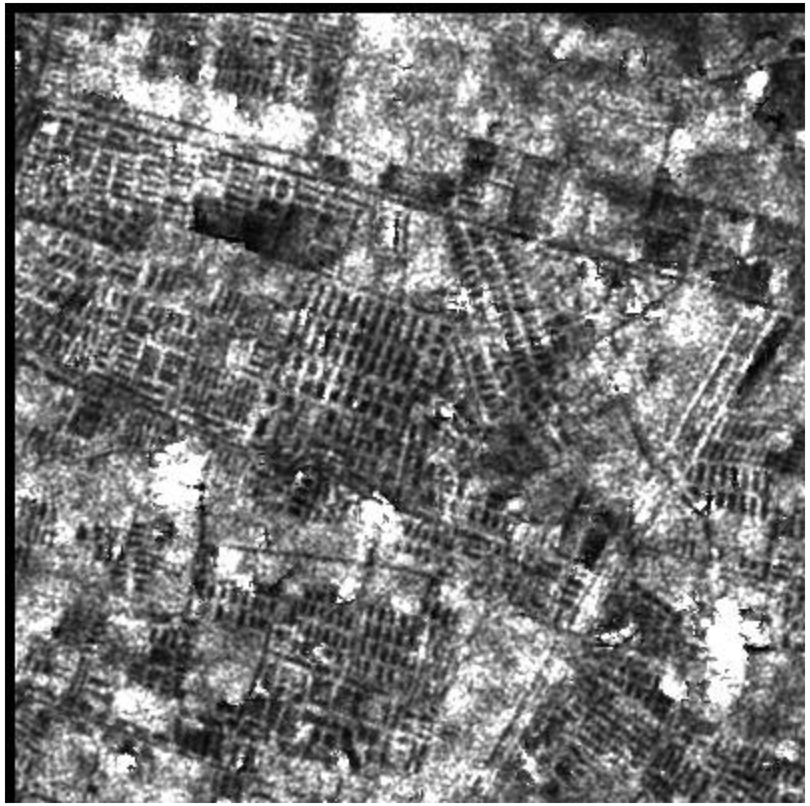

Same image, after speckle filtering

Initial HH and VV images

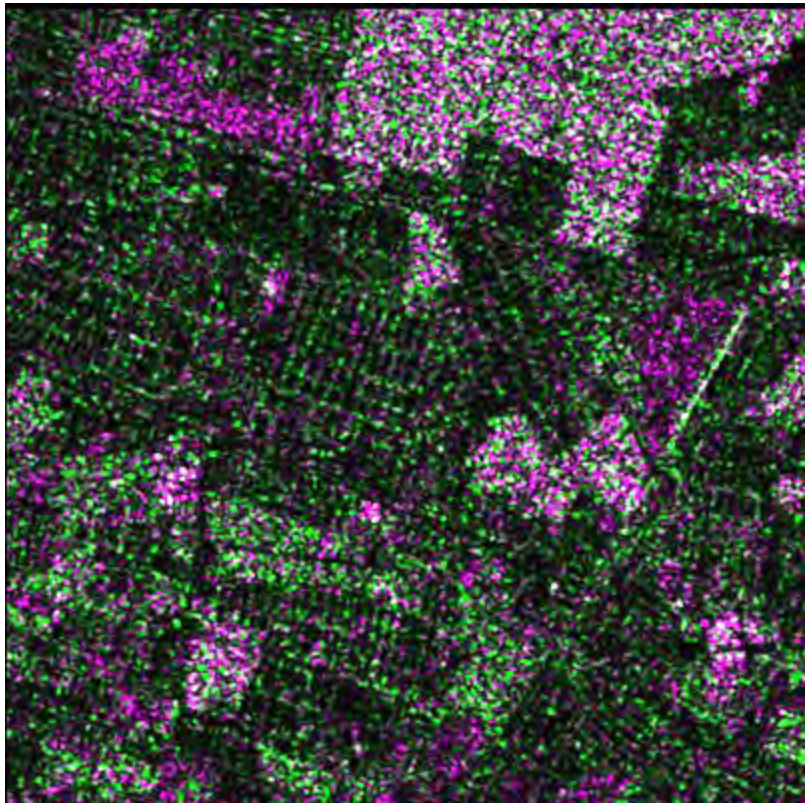

HH and VV image after filtering

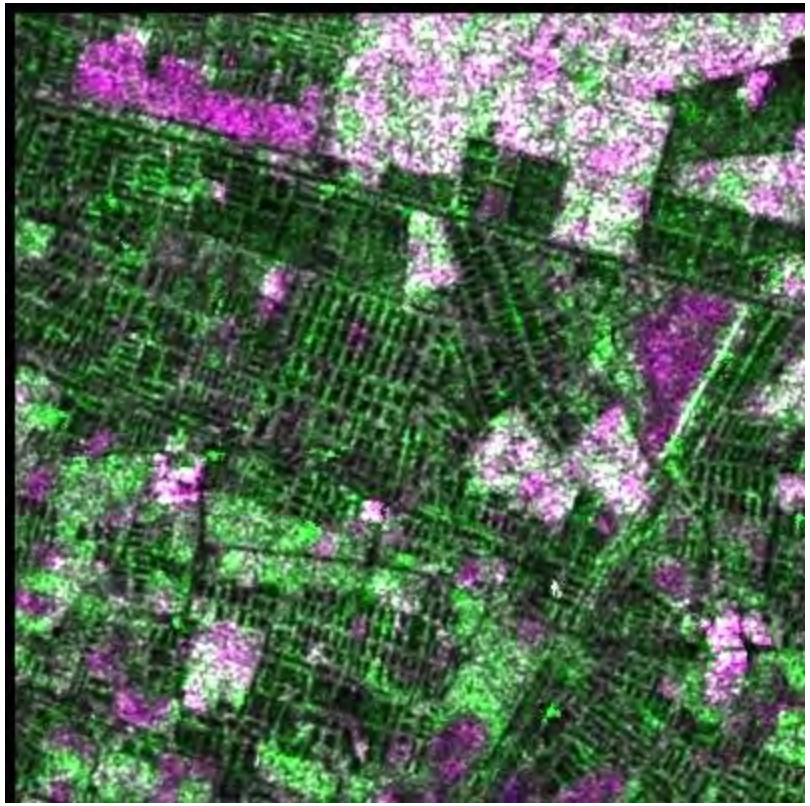

HH (magenta) and VV (green) images
400 x400 pixels
Gaoyou, Jiangsu province, 2004 09 06

Origin of speckle noise

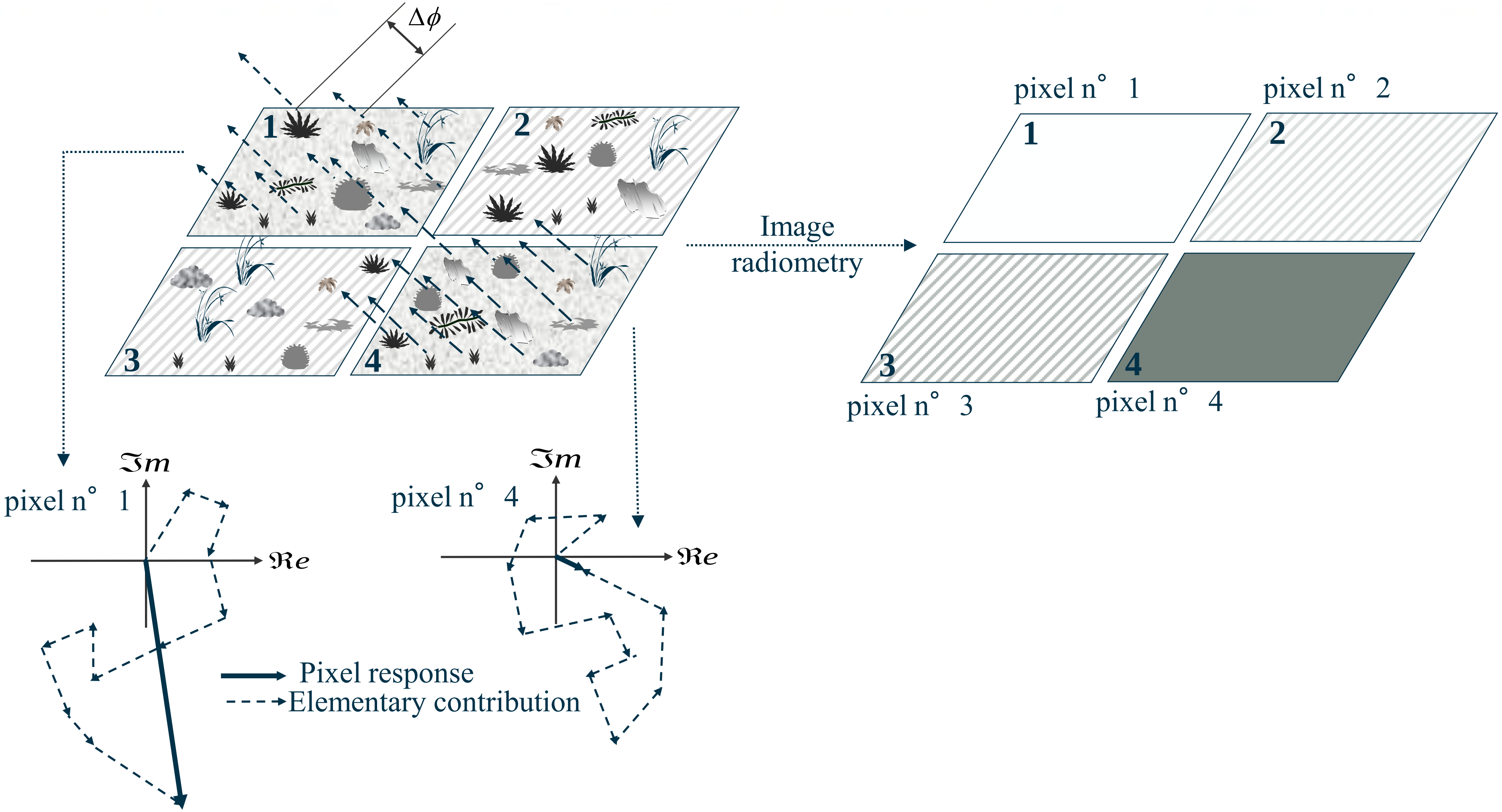

Speckle noise must be reduced…

Before speckle filtering

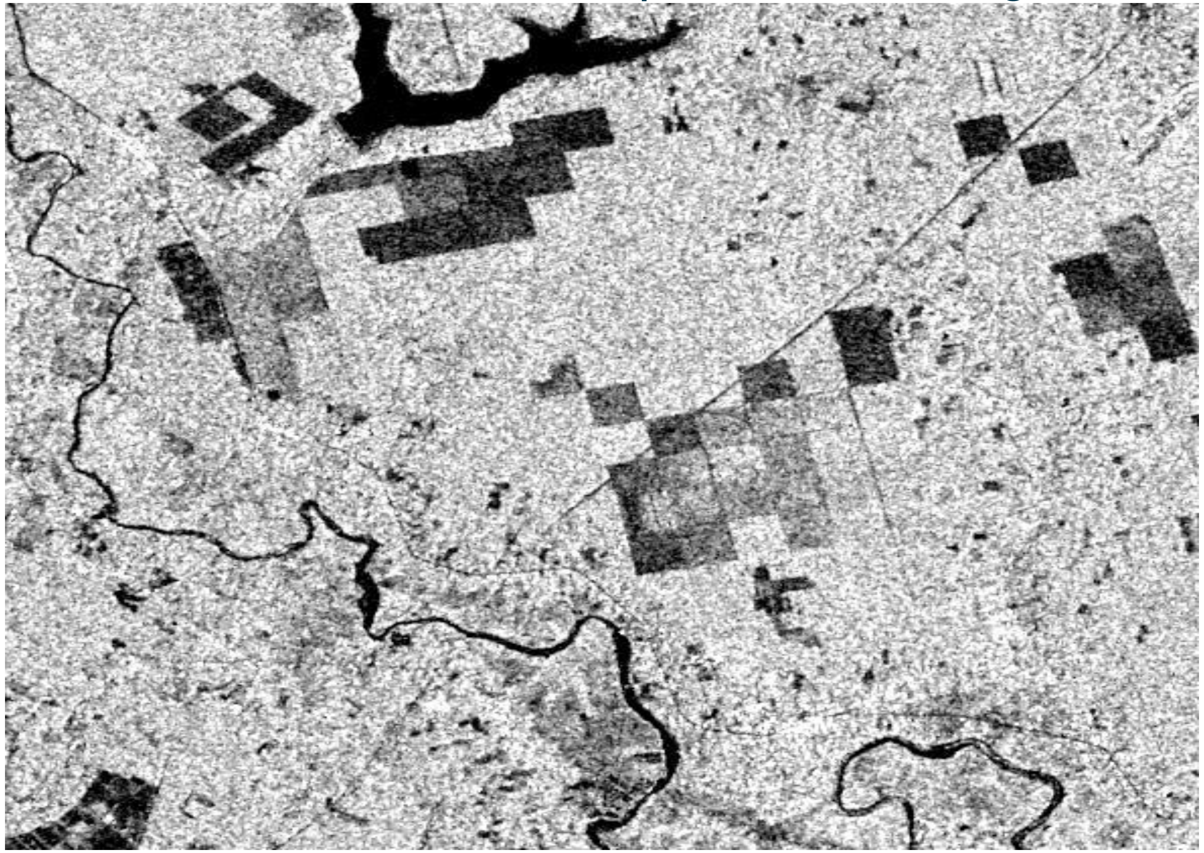

After speckle filtering

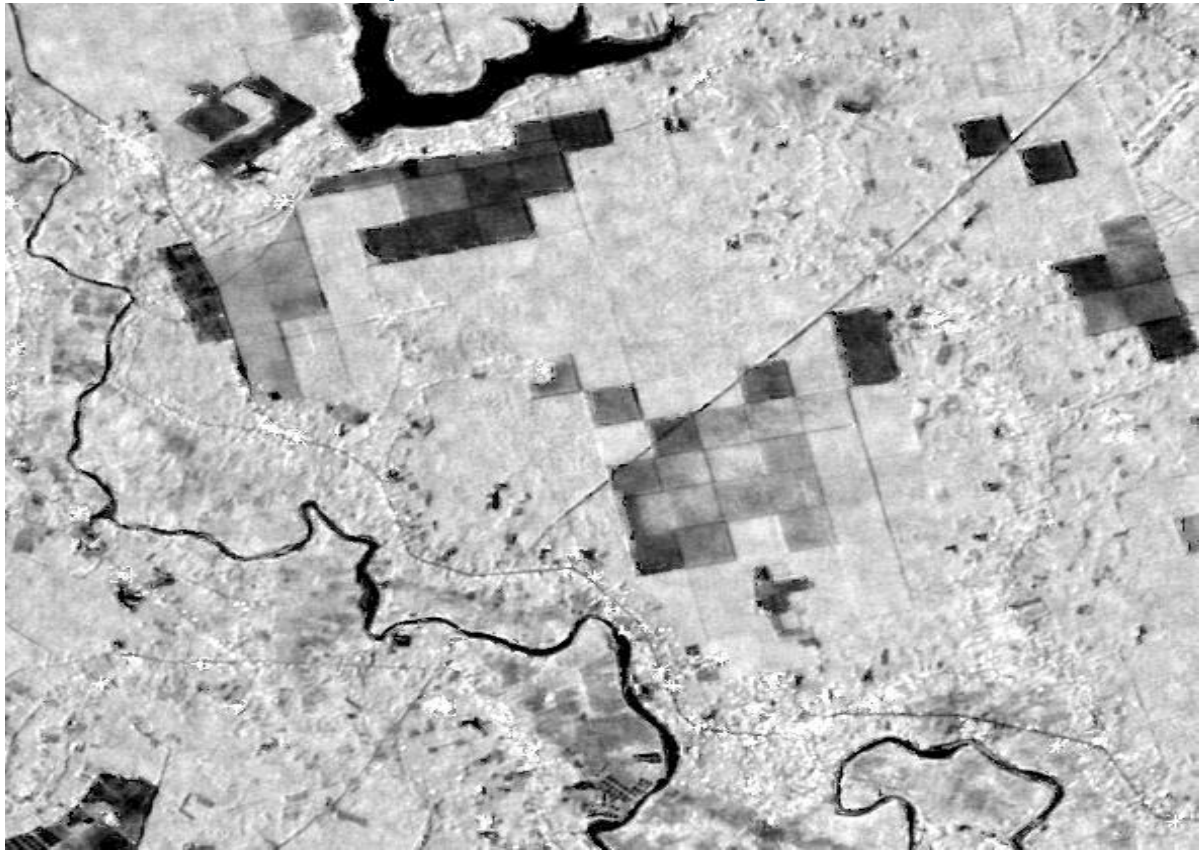

…to start analysing SAR images content

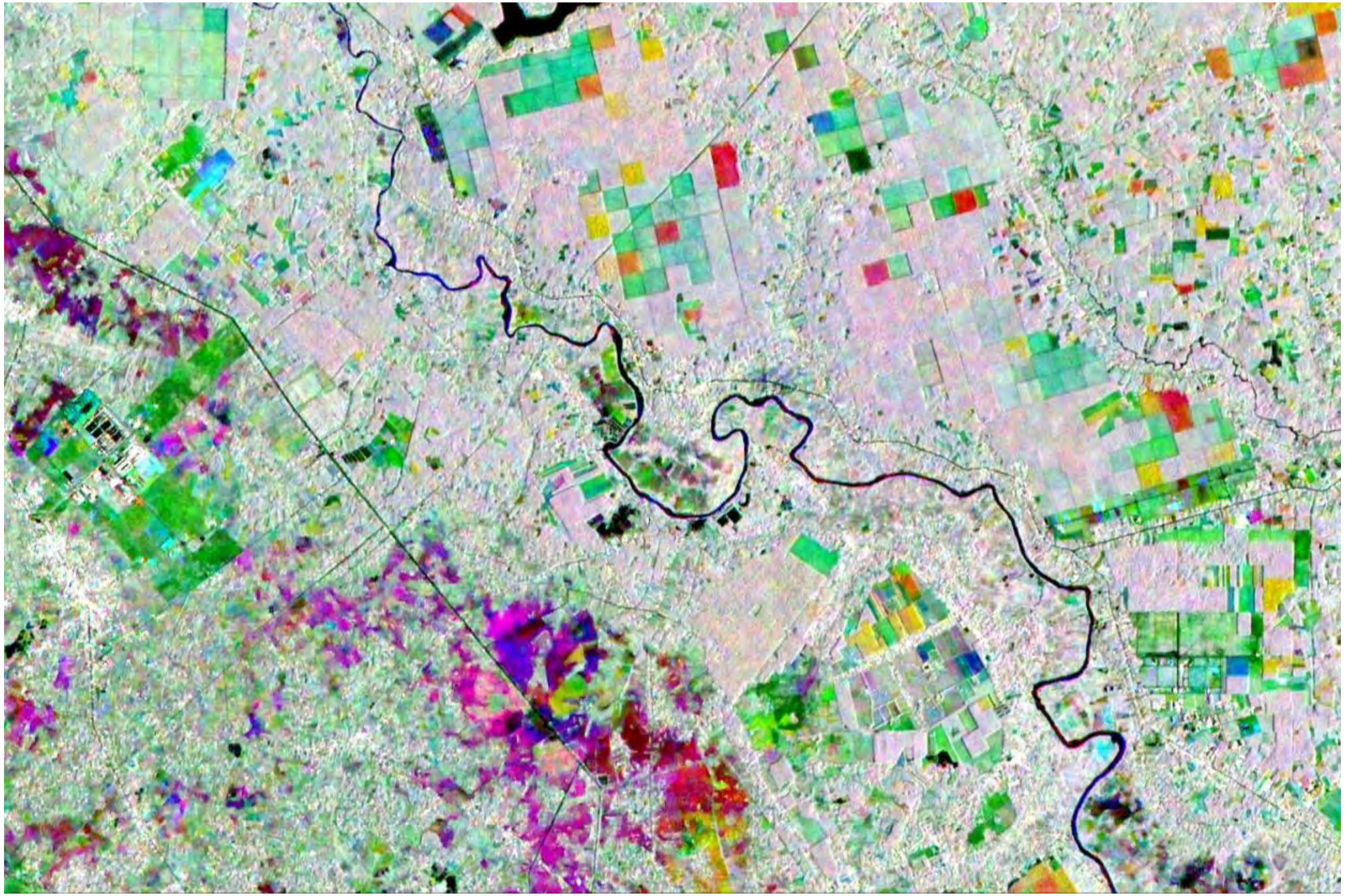

Statistics of speckle

Probability density distribution of speckle:
- **Intensity** image: **Gamma** distribution
- **Amplitude** image: **Rayleigh** distribution

$$\mathrm{var}(I) = \frac{\sigma^2}{L}$$

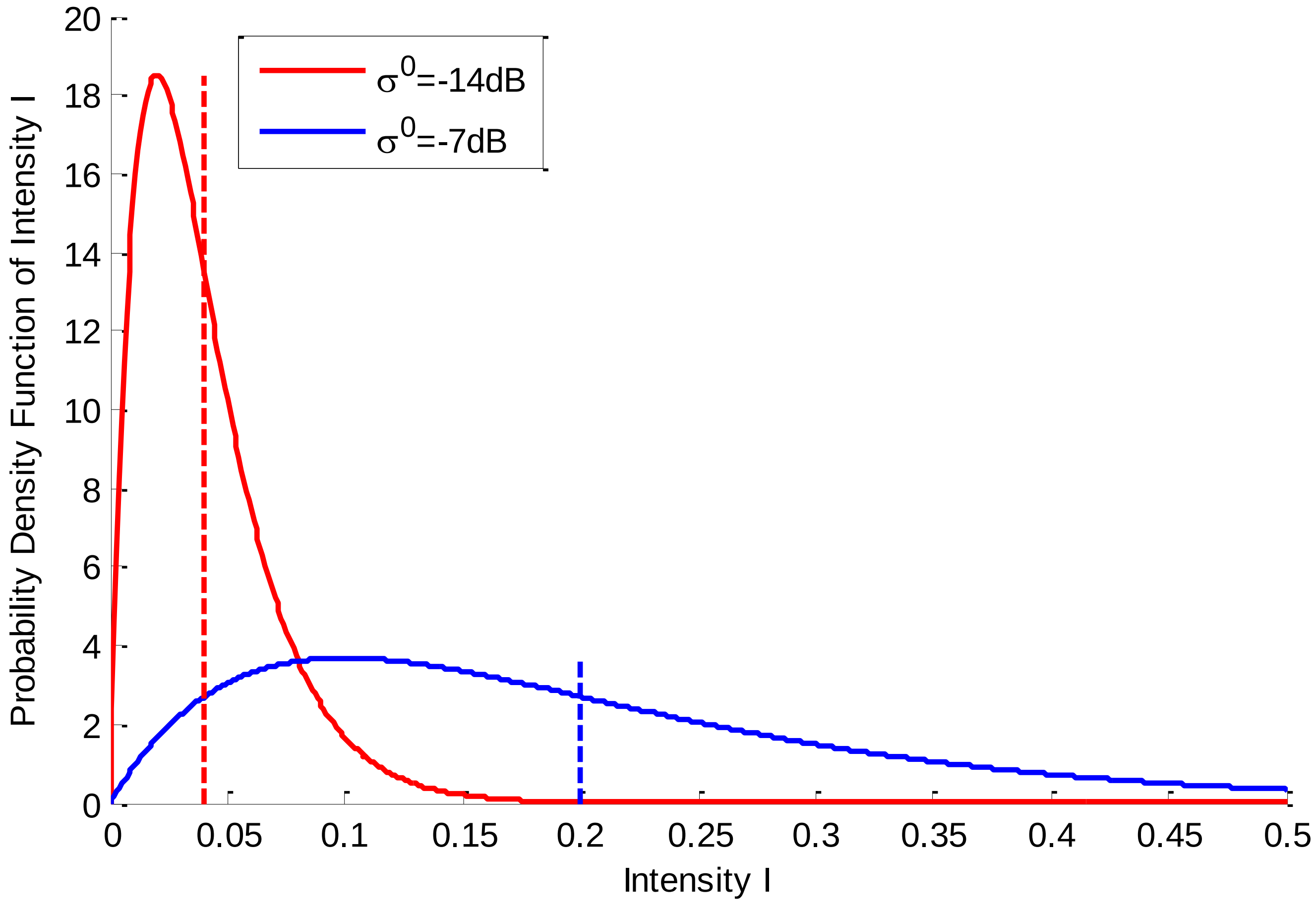

The gamma distribution

Multilooking reduces the effect of speckle.
The distribution tends to normality as L increases.

$$\mathrm{var}(I) = \frac{\sigma^2}{L}$$

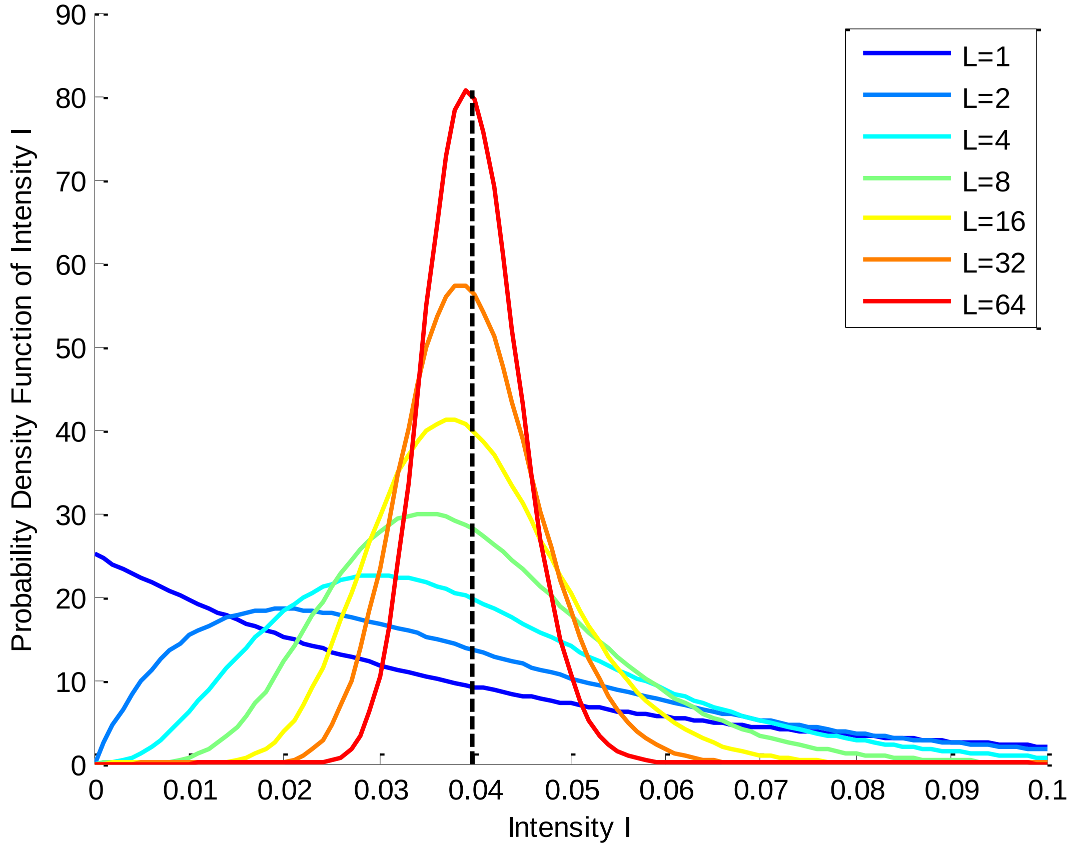

Speckle filtering reduces variance and preserves radiometry

γ^{o}_{HV}

-8 dB

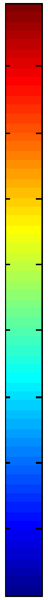

-20 dB

Non filtered – 4 looks

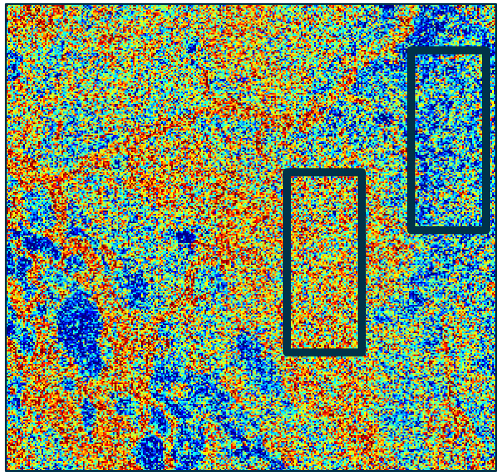

Filtered – 20 looks

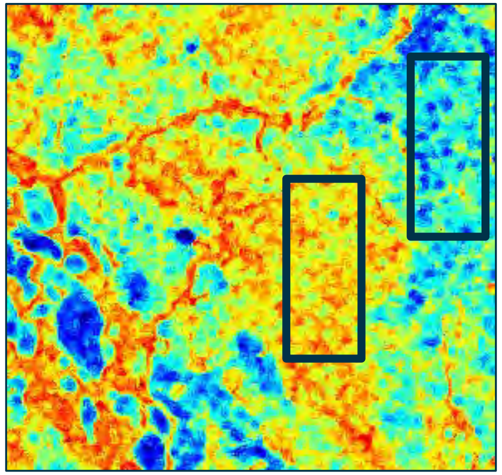

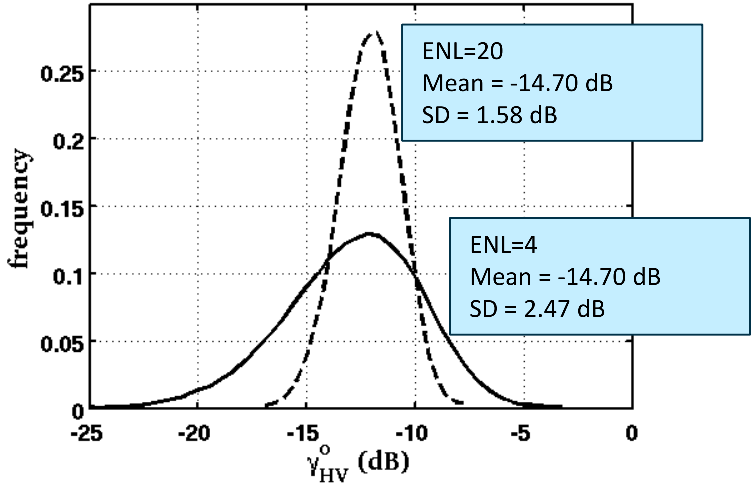

Blue area

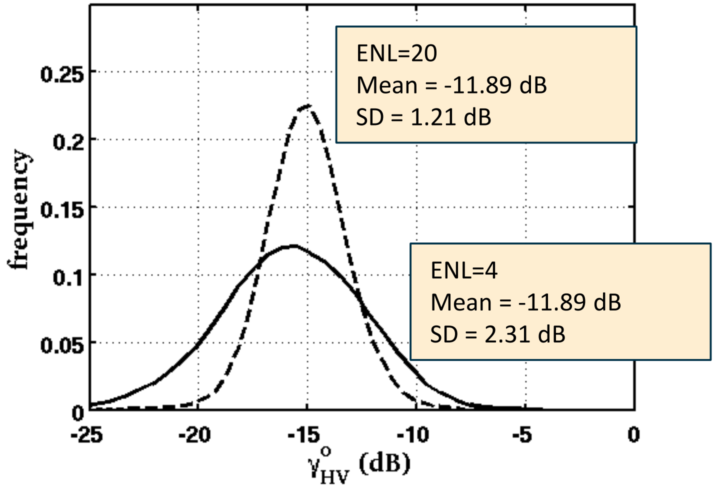

Yellow area

Mermoz et al., 2016

Speckle filtering

$$I = \sigma . v$$

I: measured intensity
σ : scene reflectivity (what we want to measure)
v: speckle noise
L: number of looks

$$\bar{I} = \sigma$$

$$\mathrm{var}(I) = \frac{\sigma^2}{L}$$

Speckle filtering consists in **assessing σ from I** by **reducing the variance of I** (and therefore increasing the Equivalent Number of Looks).

1. **Frequency filtering**: spectral filtering during SAR processing (production of multi-look images)

2. **Spatial filtering**: local estimations using moving kernels
   Filters of Lee, Kuan, Frost, MAP widely available

3. **Multi channel filtering**: applied on multiple images of the same scene
   Multi polarisation, multi temporal, and multi frequency

Multi-image intensity filtering (temporal and polarisation)

Purpose of filter:

(1) Preserve radiometry $\Rightarrow$ unbiased

$$\langle I_k(x,y)\rangle = \langle J_k(x,y)\rangle \qquad 1 \le k \le M$$

(2) Minimise the variance of J_k

Contents

Scattering Mechanisms

- The backscattered signal results from:
  - surface scattering
  - volume scattering
  - multiple volume-surface scattering

- The relative importance of these contributions depends on geometric and dielectric properties of the medium (surface and volume)

- All of these factors depend on
  - the radar frequency
  - the polarisation
  - the incidence angle

Scattering mechanisms

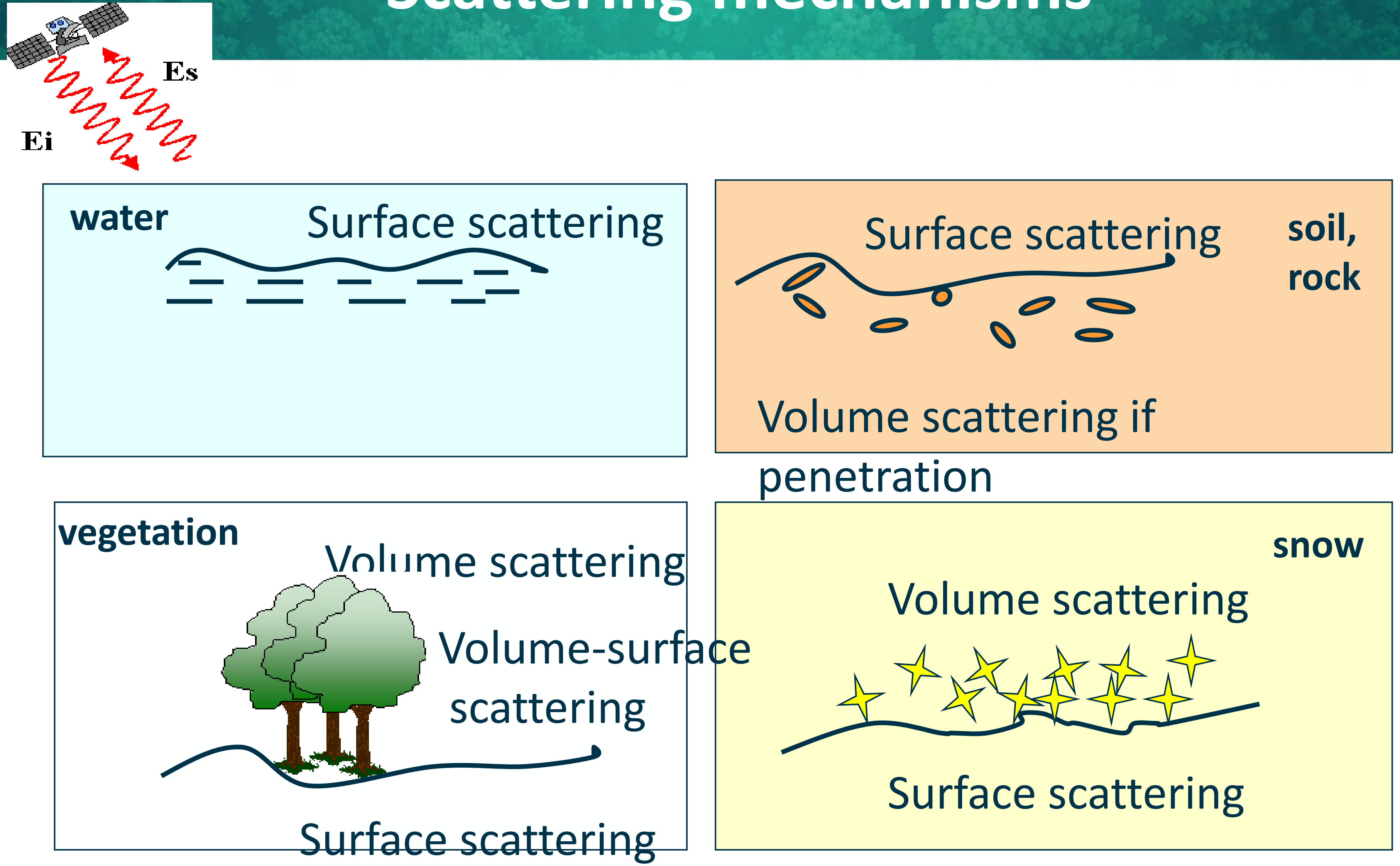

Interactions between radar wave and vegetation cover

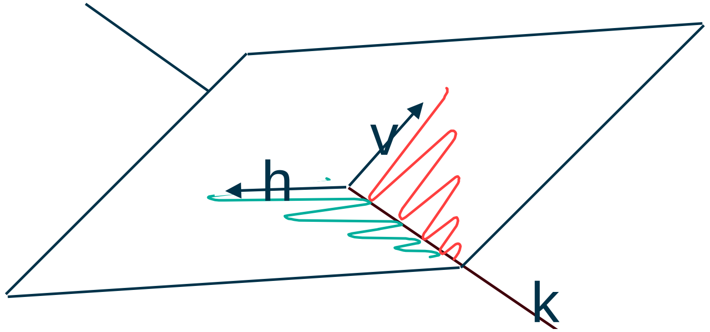

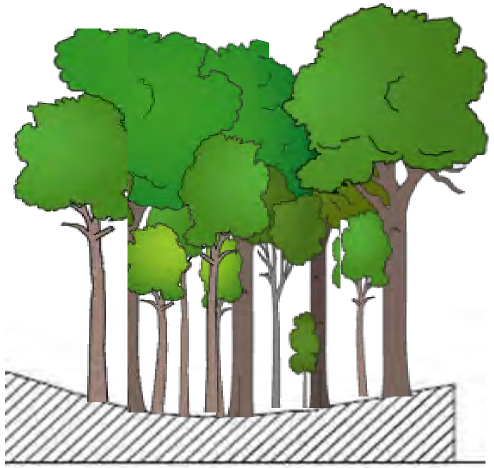

Geometric, structural properties

scatterers size

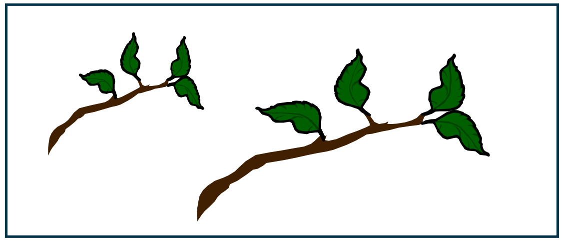

scatterers orientation

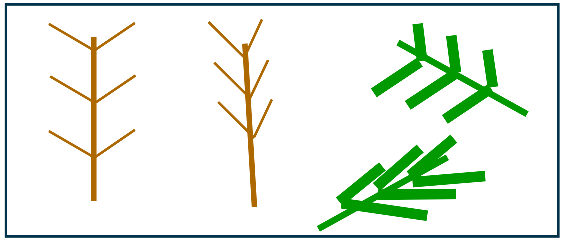

scatterers density

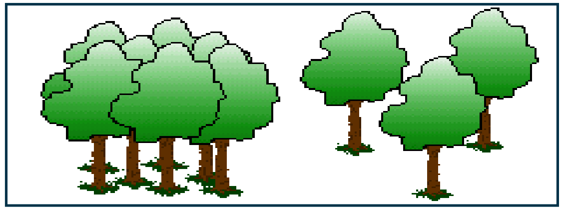

soil roughness

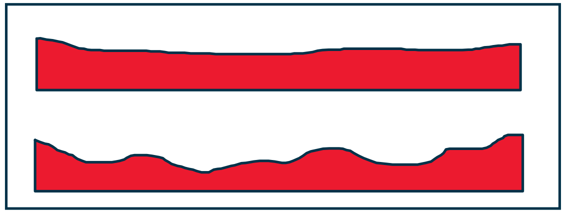

Dielectric properties

scatterers water content

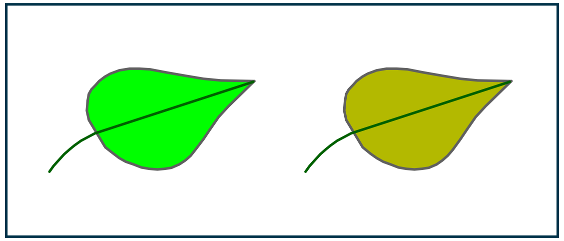

soil moisture

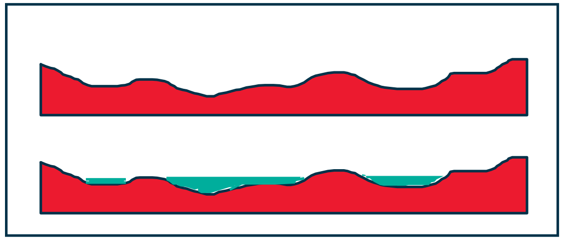

Surface scattering

Smooth surface

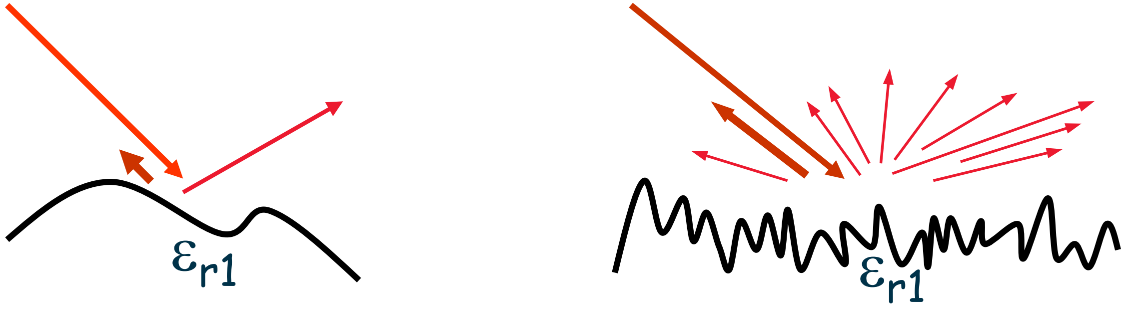

Rough surface

The roughness of the surface (wrt to the wavelength) governs the scattering pattern

$\varepsilon_{r2} > \varepsilon_{r1}$ medium 2 is wetter than medium 1

Wetter media

The dielectric constant (moisture content) of the medium governs the strength of the backscatter

Contents

Scattering from soil surface

Radar backscatter depends on the dielectric and geometry of the target, and on the frequency, polarisation and incidence angle of the wave

e.g. Small Perturbation Method for surface scattering

$$\sigma_{pp}^{0} = 4(ks)^2 (kl)^2 \cos^4\theta \left|\alpha_{pp}\right|^2 \left[1 + 2(kl\sin\theta)^2\right]^{-3/2}$$

$$\sigma_{hv}^{0}(\theta) = 0$$

Here

k = $2\pi/\lambda$ (Wave number)

pp = HH or VV

θ = incidence angle

s = surface RMS height

l = surface autocorrelation length

$$\alpha_{hh} = \frac{\cos\theta - \sqrt{\epsilon - \sin^2\theta}}{\cos\theta + \sqrt{\epsilon - \sin^2\theta}} \qquad \alpha_{vv} = (\epsilon - 1)\frac{\sin^2\theta - \epsilon\left(1 + \sin^2\theta\right)}{\left(\epsilon\cos\theta + \sqrt{\epsilon - \sin^2\theta}\right)}$$

ε = dielectric constant

σ^0 is the backscattering coefficient

Agricultural surface roughness statistics

Seedbed

Harrowed

Ploughed

Tillage	Rms (mean)	Rms (std)	Corr. Length (mean)	Corr. Length (std.)
Seedbed	0.6	0.3	3.7	2.6
Harrowed	1.6	0.7	3.8	2.9
Ploughed	2.7	1.0	6.9	2.7

RMS heights s and correlation length l (mean and std in cm)

Soil dielectric constant

Dielectric constant as a function of soil volumetric water content

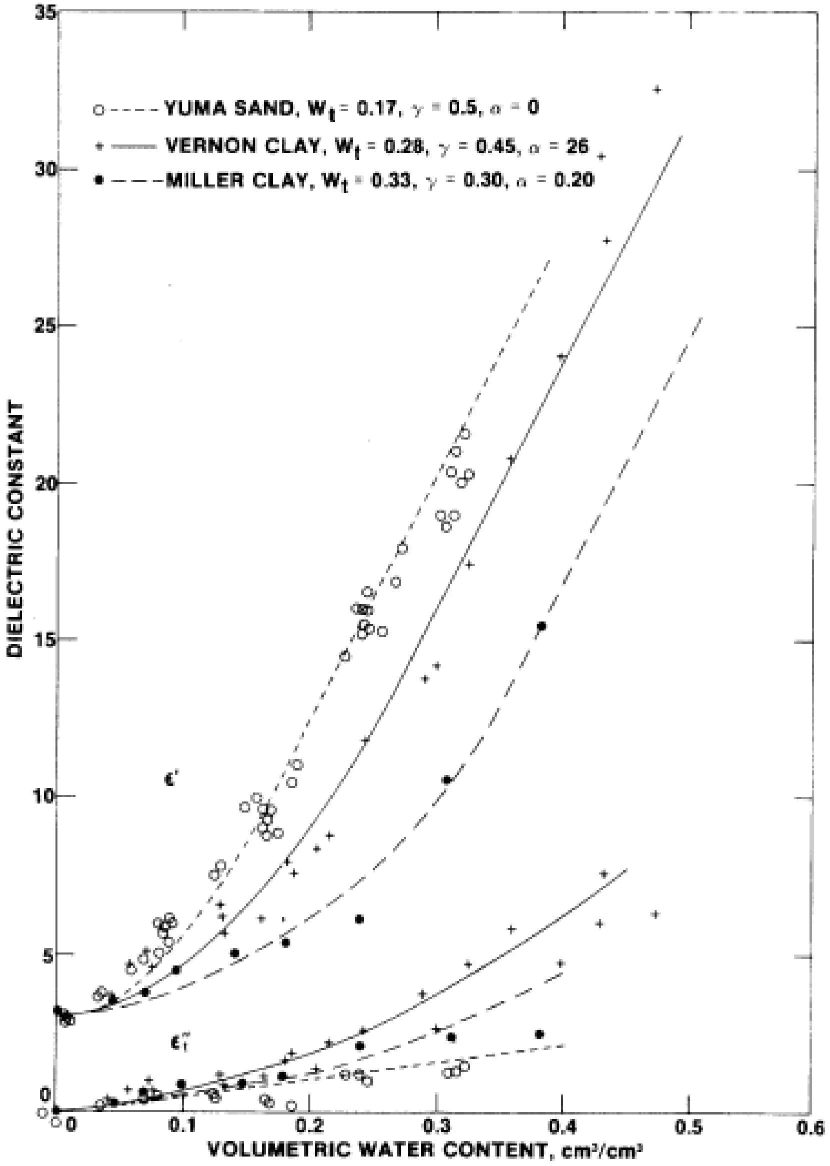

ig. 6. A comparison between the calculated dielectric constants from the empirical model and the measured values at 5 GHz.

Sensitivity to soil moisture and surface roughness

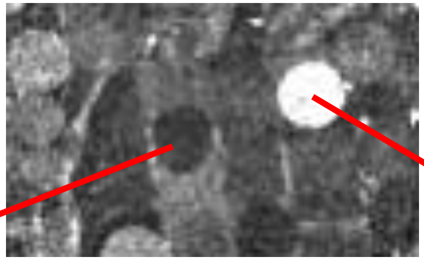

Low backscatter
➔ dry soil

High backscatter
➔ Wet soil

For constant roughness

BUT :

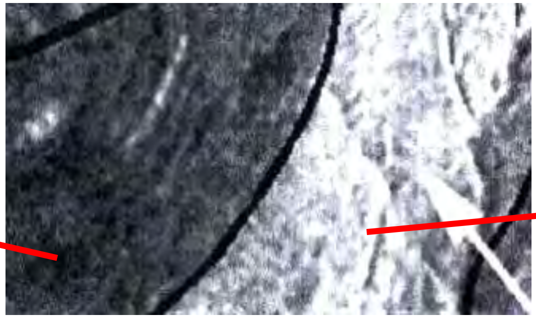

Low backscatter
➔ Smooth surface

High backscatter
➔ rough surface

For constant moisture

Simultaneous effect of roughness and moisture on the radar signal

Our first ERS experiment in 1992 on irrigated area in Gharb, Morocco

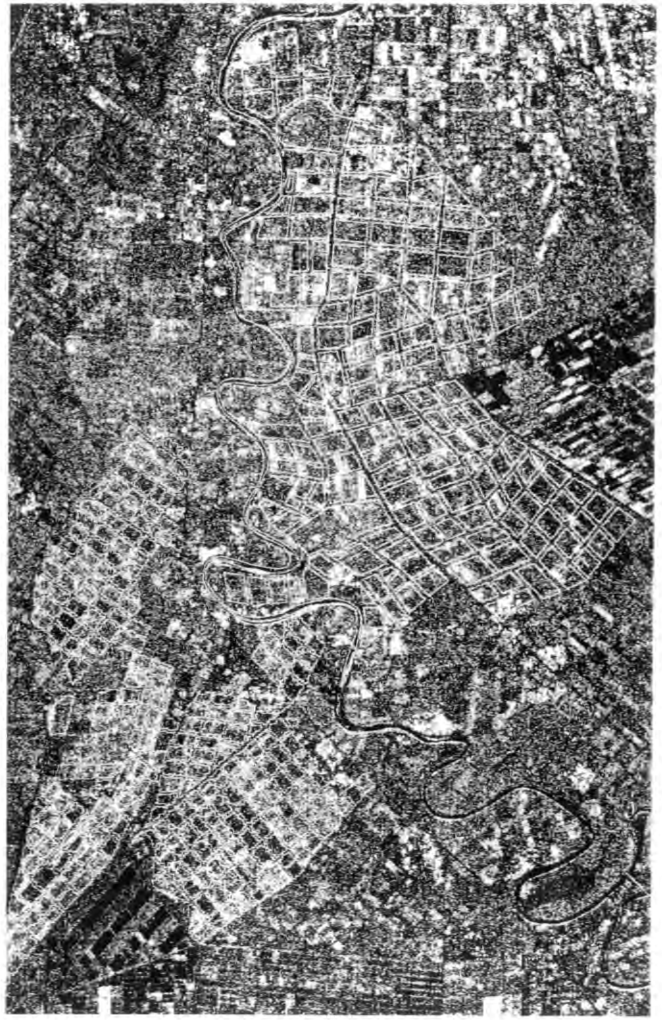

We mapped irrigated fields, but to retrieve soil moisture was found hard with a single ERS data!

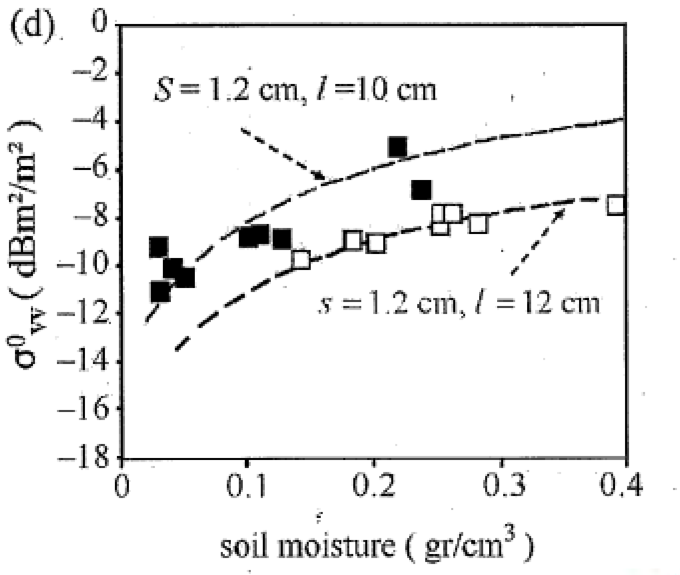

Le Toan, T, J.C. Souyris and P. Macchia,

Polarisation in surface scattering

Smooth surface

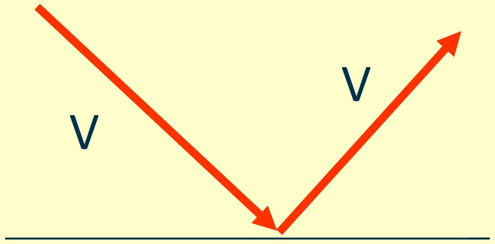

- no depolarisation
no HV or VH backscatter

- Fresnel Reflectivity $R_H > R_V$

Rough surface

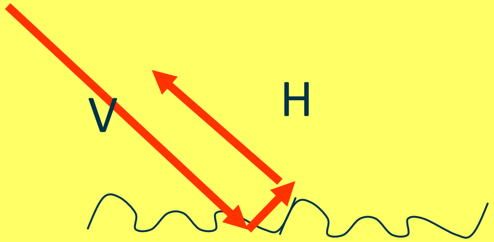

- some depolarisation
HV or VH backscatter > 0

- Fresnel Reflectivity $R_H = R_V$

Interactions mechanisms of a vegetation cover

* Order 0

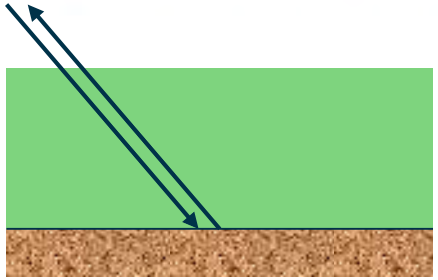

Attenuated surface scattering

* Order 1: Simple scattering

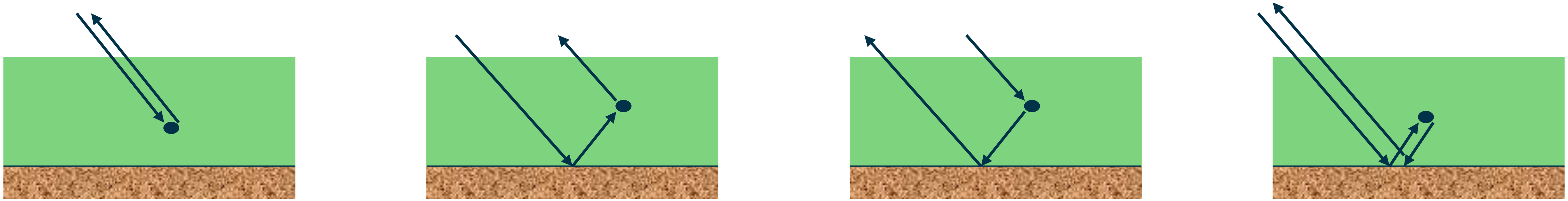

Volume scattering

Surface-volume scattering

$$\sigma^0 = \sigma^0_{soil} + \sigma^0_{veg.} + \sigma^0_{soil-veg.}$$

Volume scattering

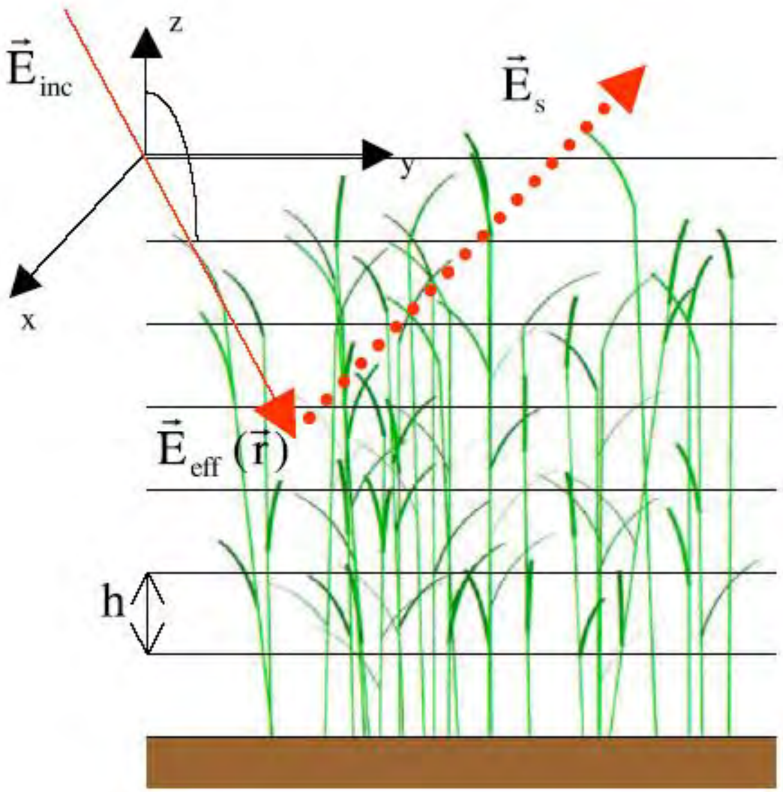

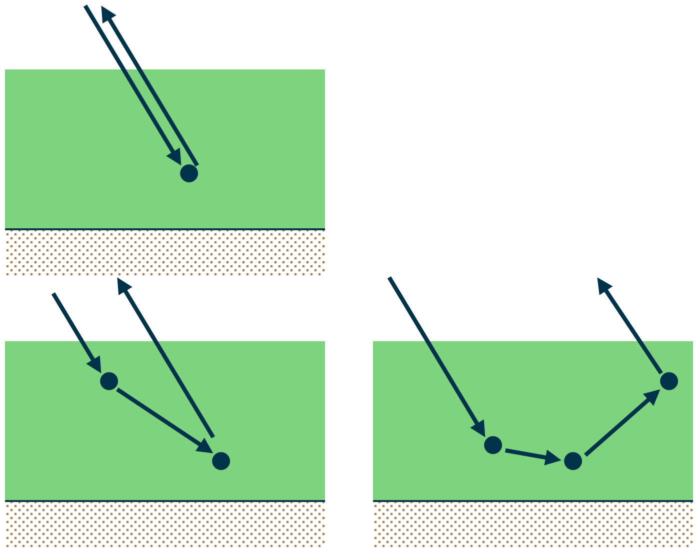

Single and multiple scattering

Polarisation in volume scattering

Point scatterer

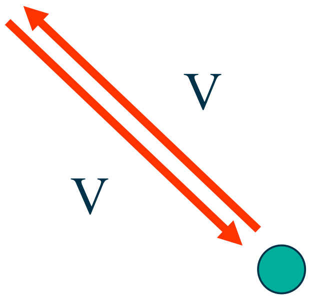

-> no depolarisation

Anisotropic scatterer

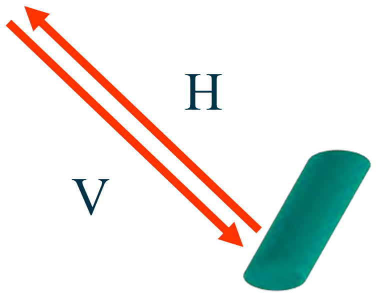

-> depolarisation

Multiple scattering

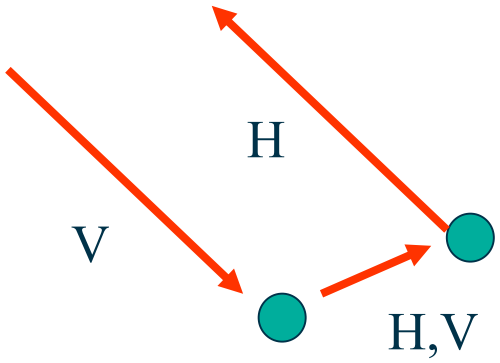

-> depolarisation

HV or VH: high backscatter of vegetation canopy

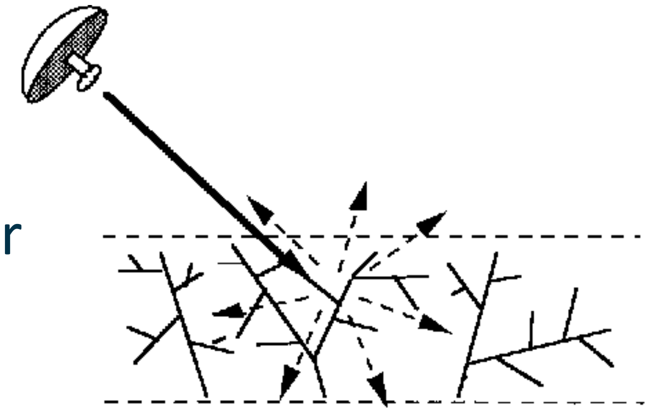

Optical image
Sentinel-2

Contents lists available at ScienceDirect

Remote Sensing of Environment

journal homepage: www.elsevier.com/locate/rse

Understanding the temporal behavior of crops using Sentinel-1 and Sentinel-2-like data for agricultural applications

Amanda Veloso *,[1], Stéphane Mermoz, Alexandre Bouvet, Thuy Le Toan, Milena Planells, Jean-François Dejoux, Eric Ceschia

CESBIO, Université de Toulouse, CNES/CNRS/IRD/UPS, Toulouse, France

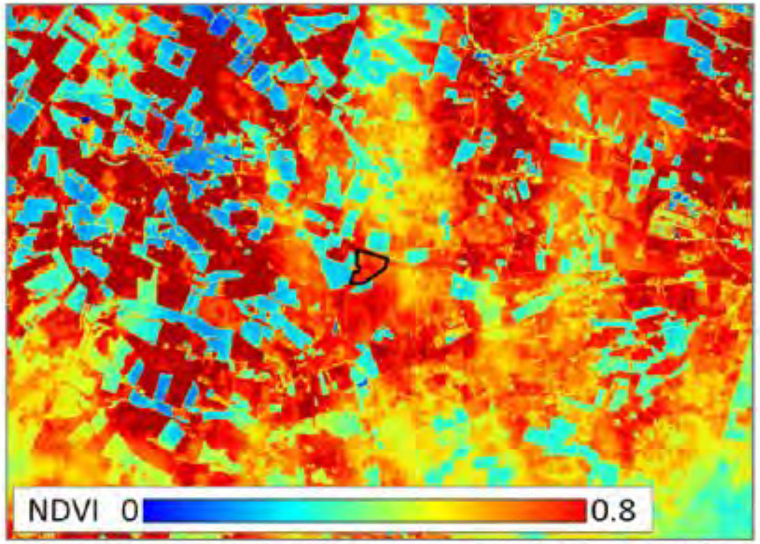

Radar image
Sentinel-1

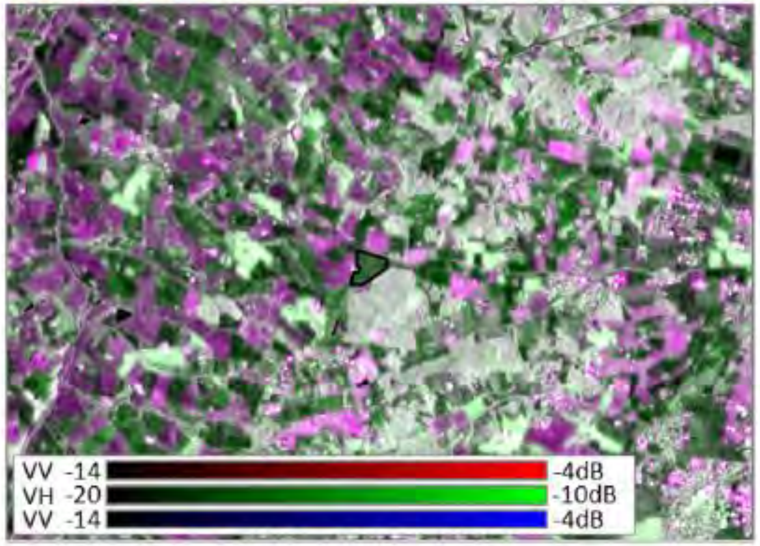

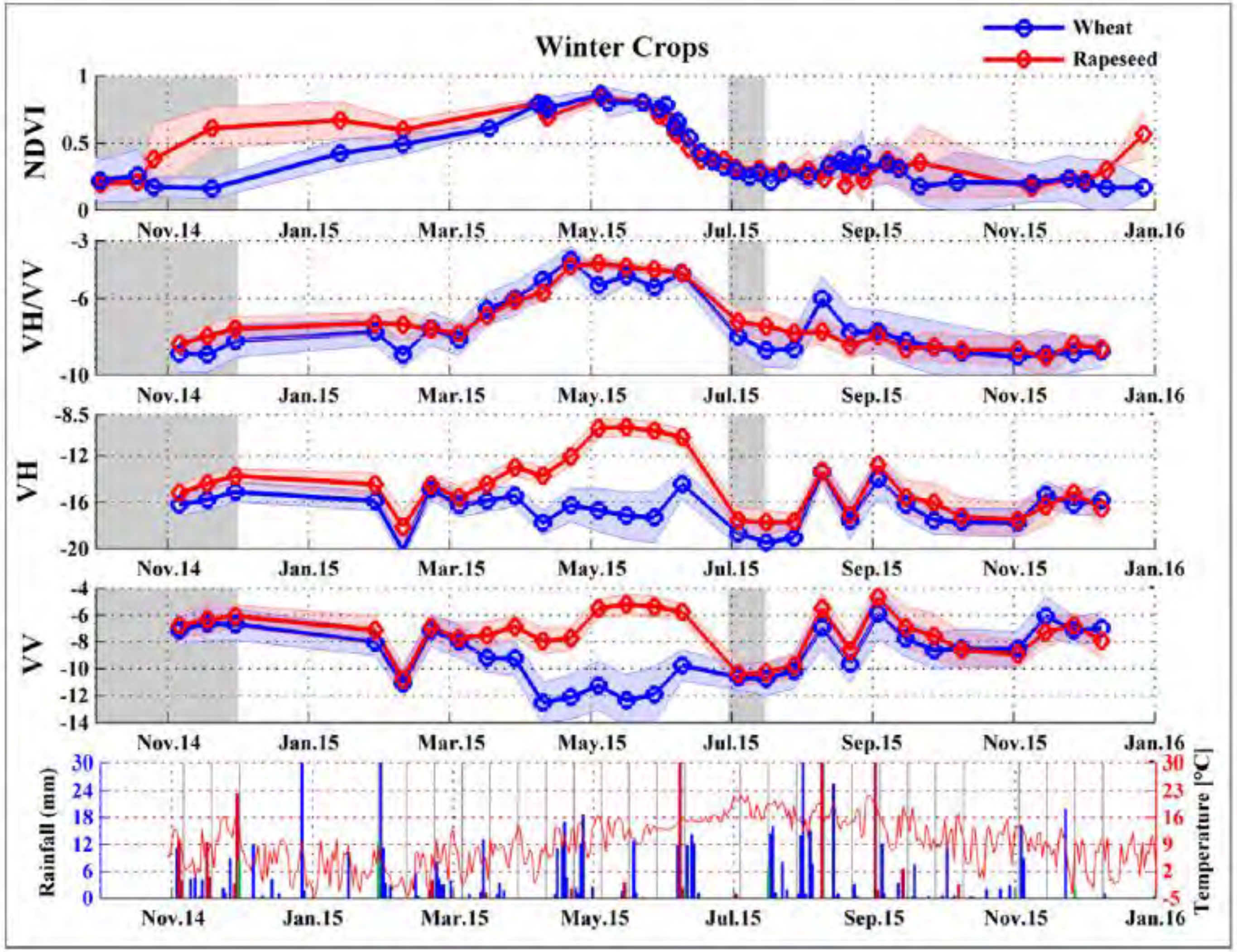
Winter Crops
Wheat
Rapeseed
NDVI
VH/VV
VH
VV
Rainfall (mm)
Temperature [°C]
Nov.14
Jan.15
Mar.15
May.15
Jul.15
Sep.15
Nov.15
Jan.16

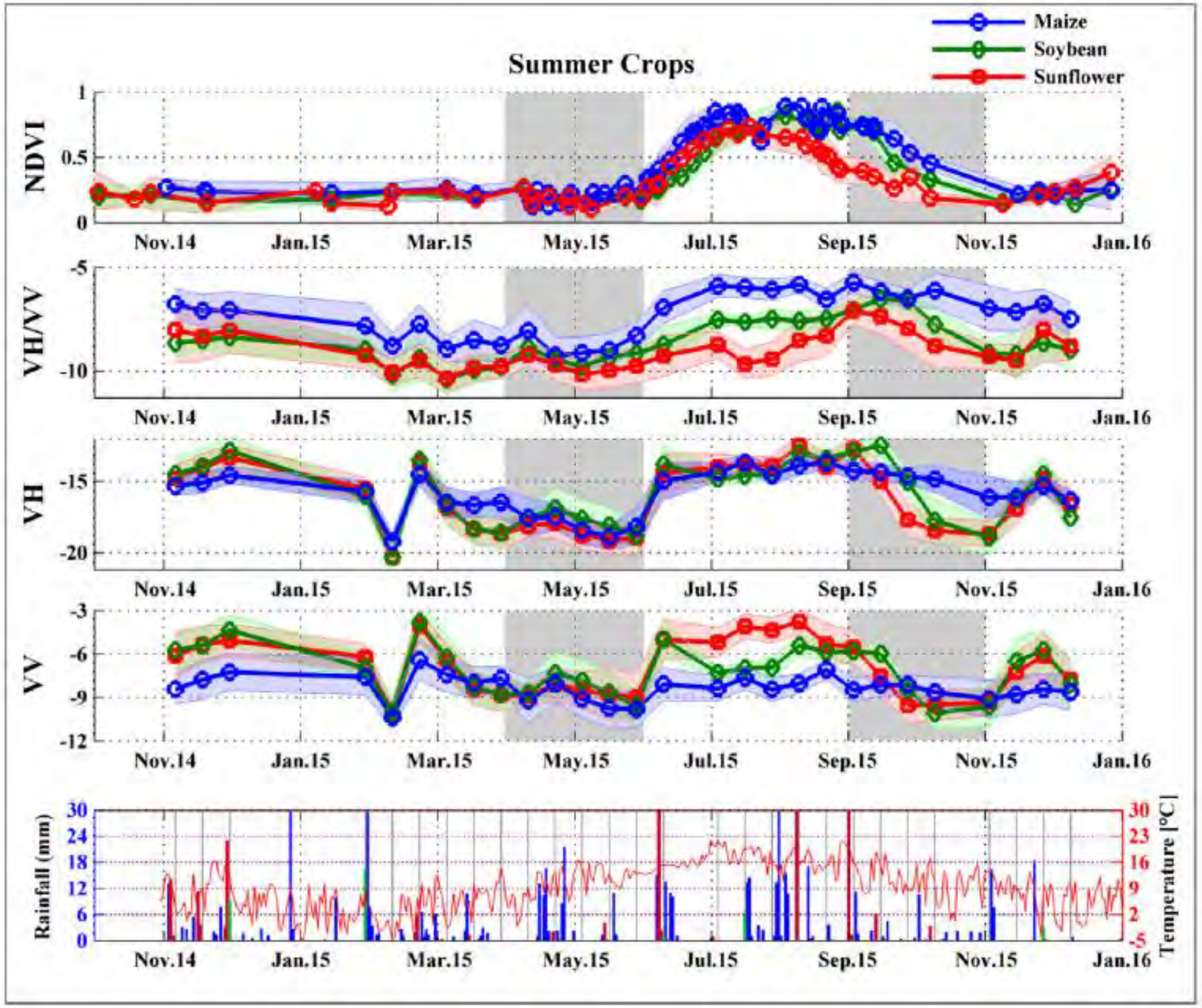
Summary Crops
Maize
Soybean
Sunflower
NDVI
VH/VV
VH
VV
Rainfall (mm)
Temperature [°C]
Nov.14
Jan.15
Mar.15
May.15
Jul.15
Sep.15
Nov.15
Jan.16

Contents

How do the radars see the trees ?

Austrian pine	X band λ= 3 cm	C band λ= 6 cm	L band λ= 27 cm	P band λ= 70 cm	VHF λ > 3 m

Interaction mechanisms in a forest

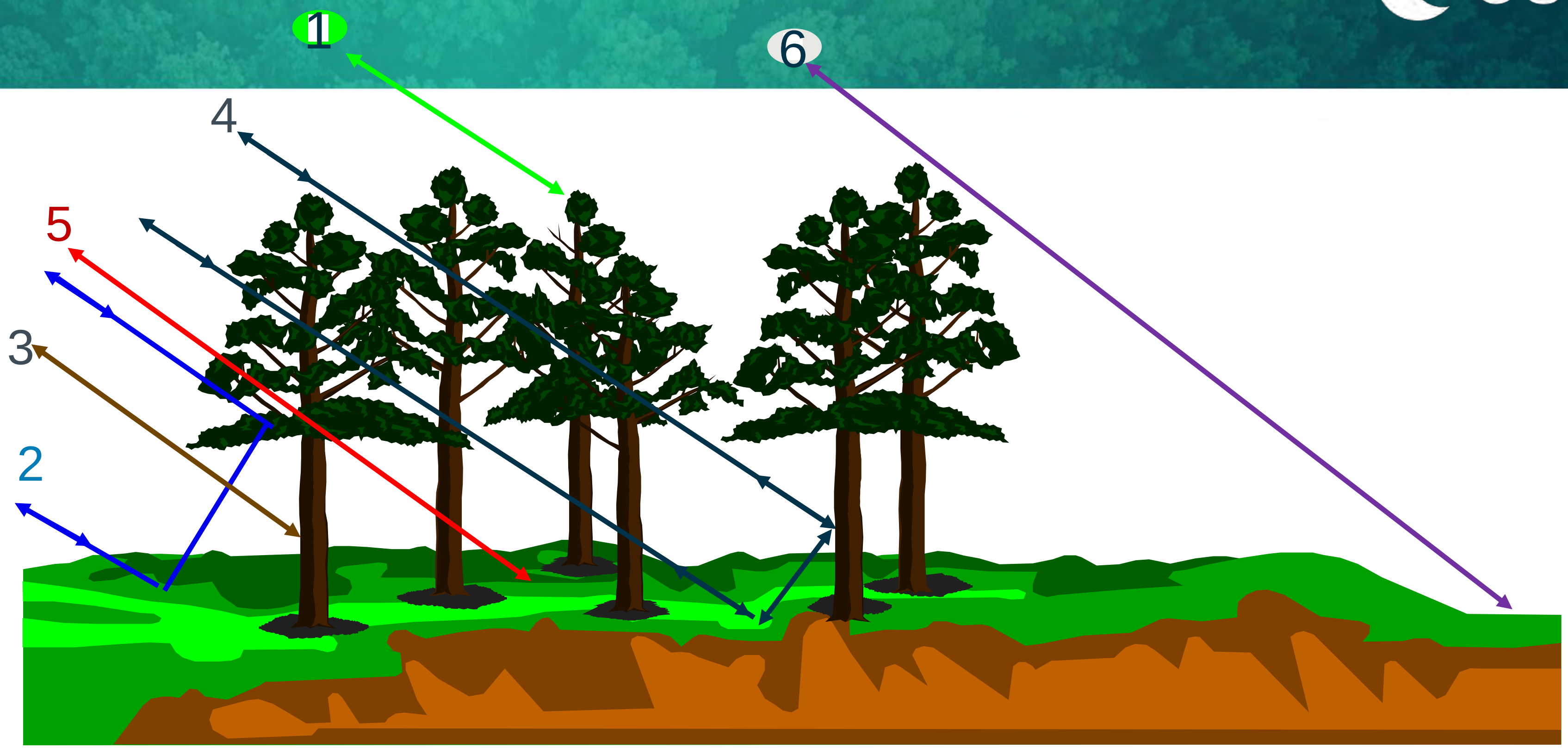

Scatterers contribution

Leaves, Needles

Primary Branches

Secondary branches

Higher order branches

Trunk

1) Direct Crown scattering
2) Direct trunk-ground
3) Trunk scattering
4) Multiple trunk-ground
5) Attenuated ground
6) Direct ground scattering

Interactions mechanisms in a forest – C-band

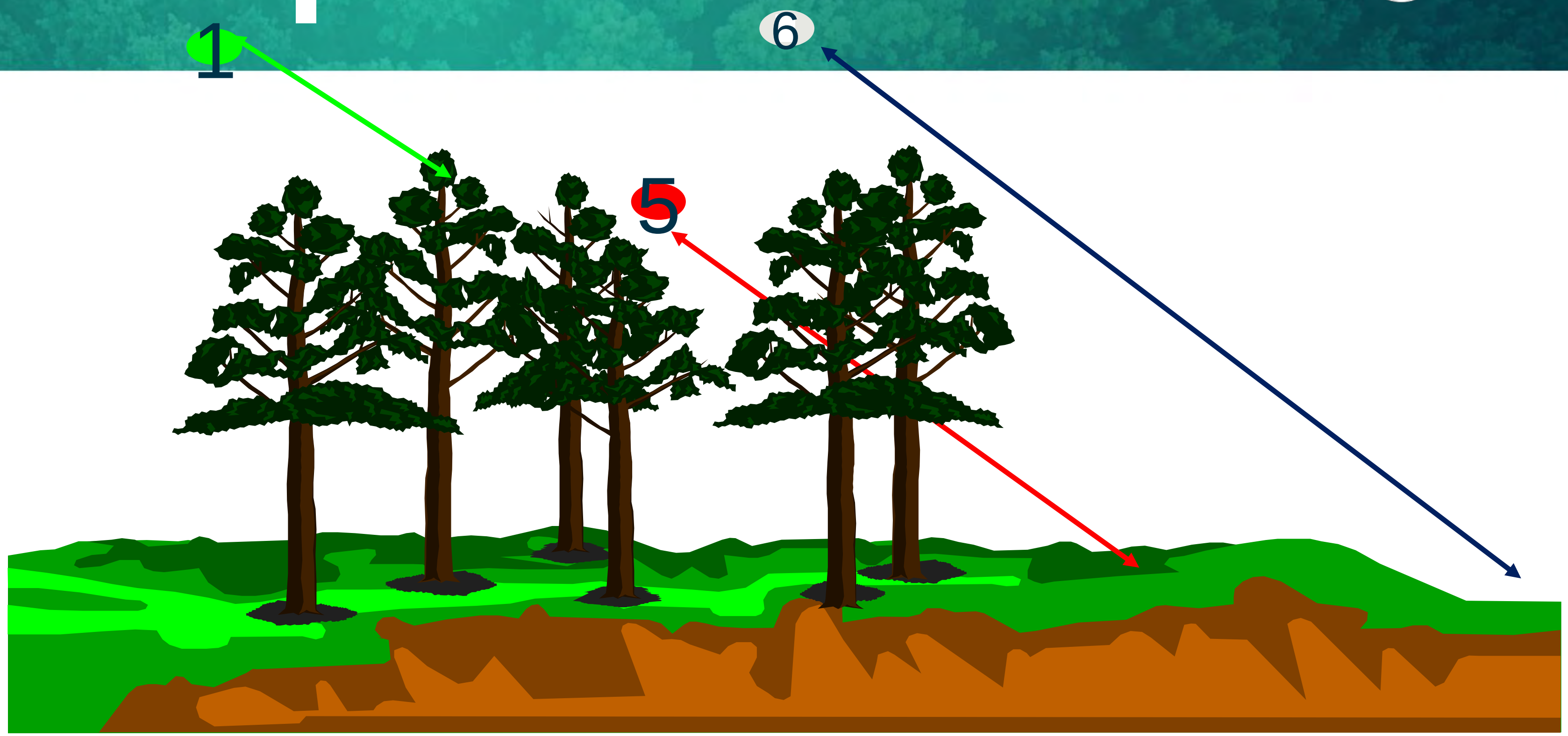

Scatterers contribution

Leaves, Needles

1) Direct Crown scattering

5) Attenuated ground

6) Direct ground scattering

Scattering mechanisms simulated by a R.T. model

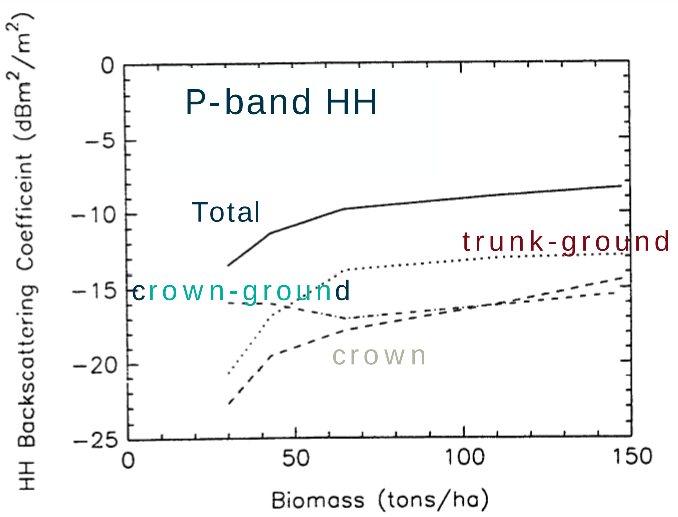

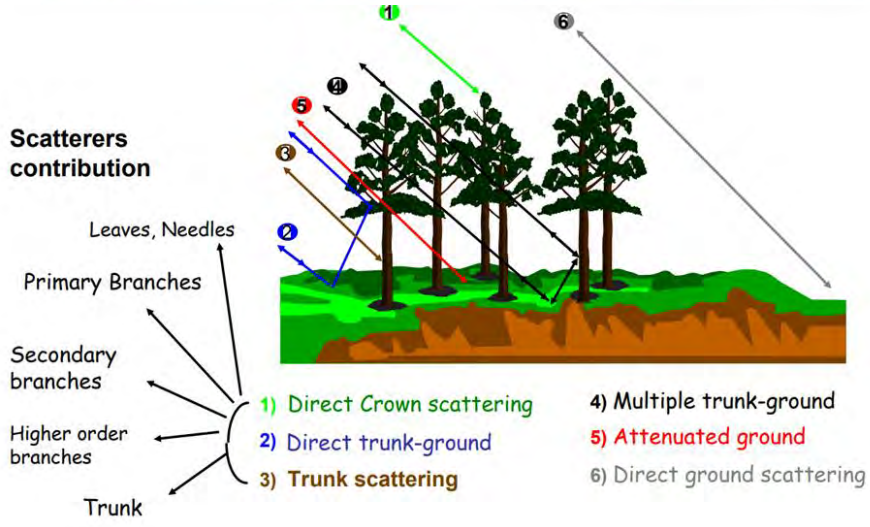

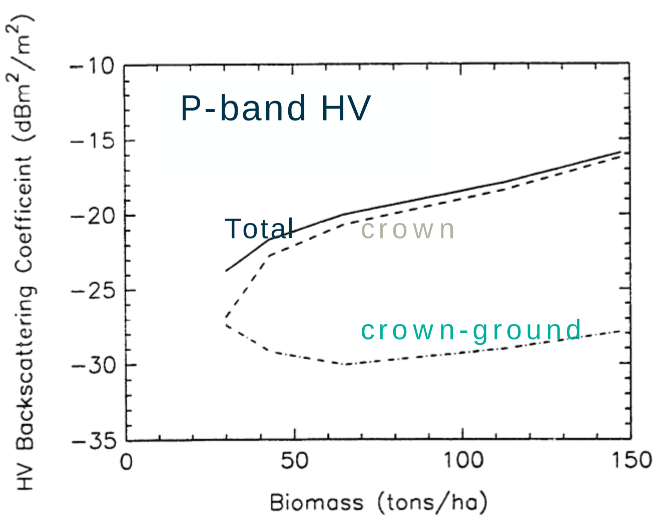

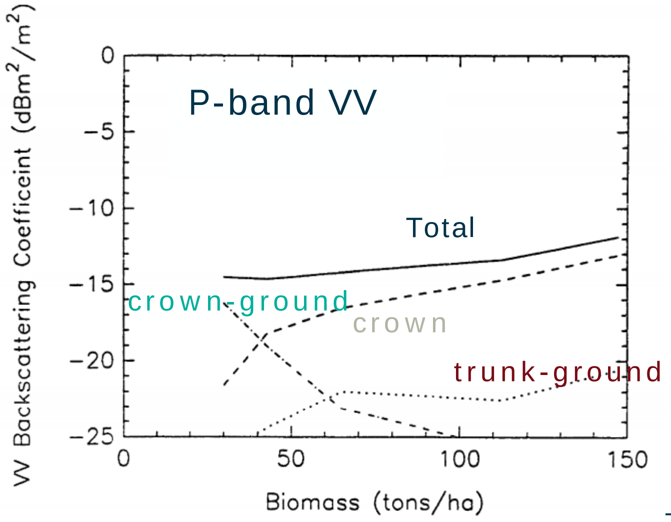

- Le Toan, T., Beaudoin, A., Riom, J., & Guyon, D. (1992). Relating forest biomass to SAR data. *IEEE Transactions on Geoscience and Remote Sensing*, *30*(2), 403-411.
- Hsu, C. C., Han, H. C., Shin, R. T., Kong, J. A., Beaudoin, A., & Le Toan, T. (1994). Radiative transfer theory for polarimetric remote sensing of pine forest at P band. *International Journal of Remote Sensing*, *15*(14), 2943-2954.
- Beaudoin, A., Le Toan, T., Goze, S., Nezry, E., Lopes, A., Mougin, E., ... & Shin, R. T. (1994). Retrieval of forest biomass from SAR data. *International Journal of Remote Sensing*, *15*(14), 2777-2796.

Change in dominant mechanism

Varzea Dry

Varzea Wet Season

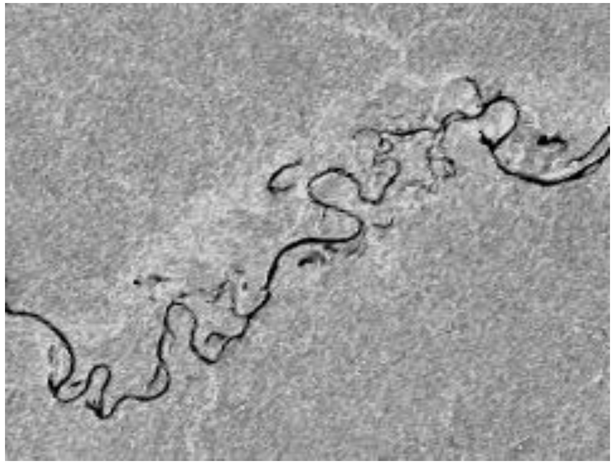

SAR image (L- HH)

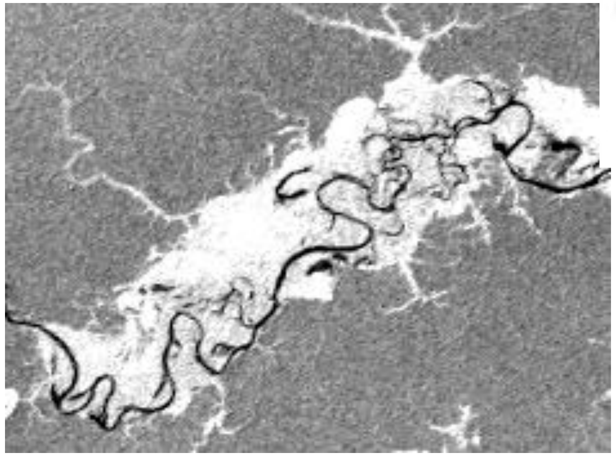

SAR image (L-HH)

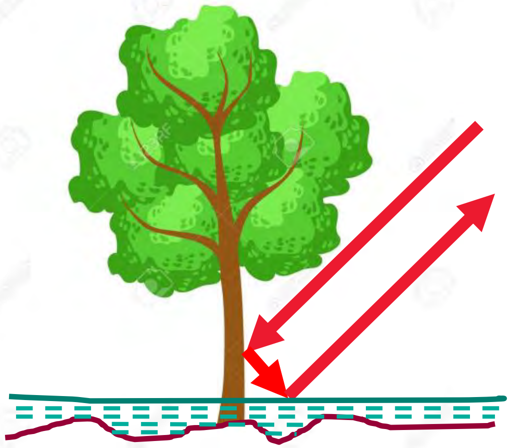

Forest structure- Boreal vs Tropical rain forest

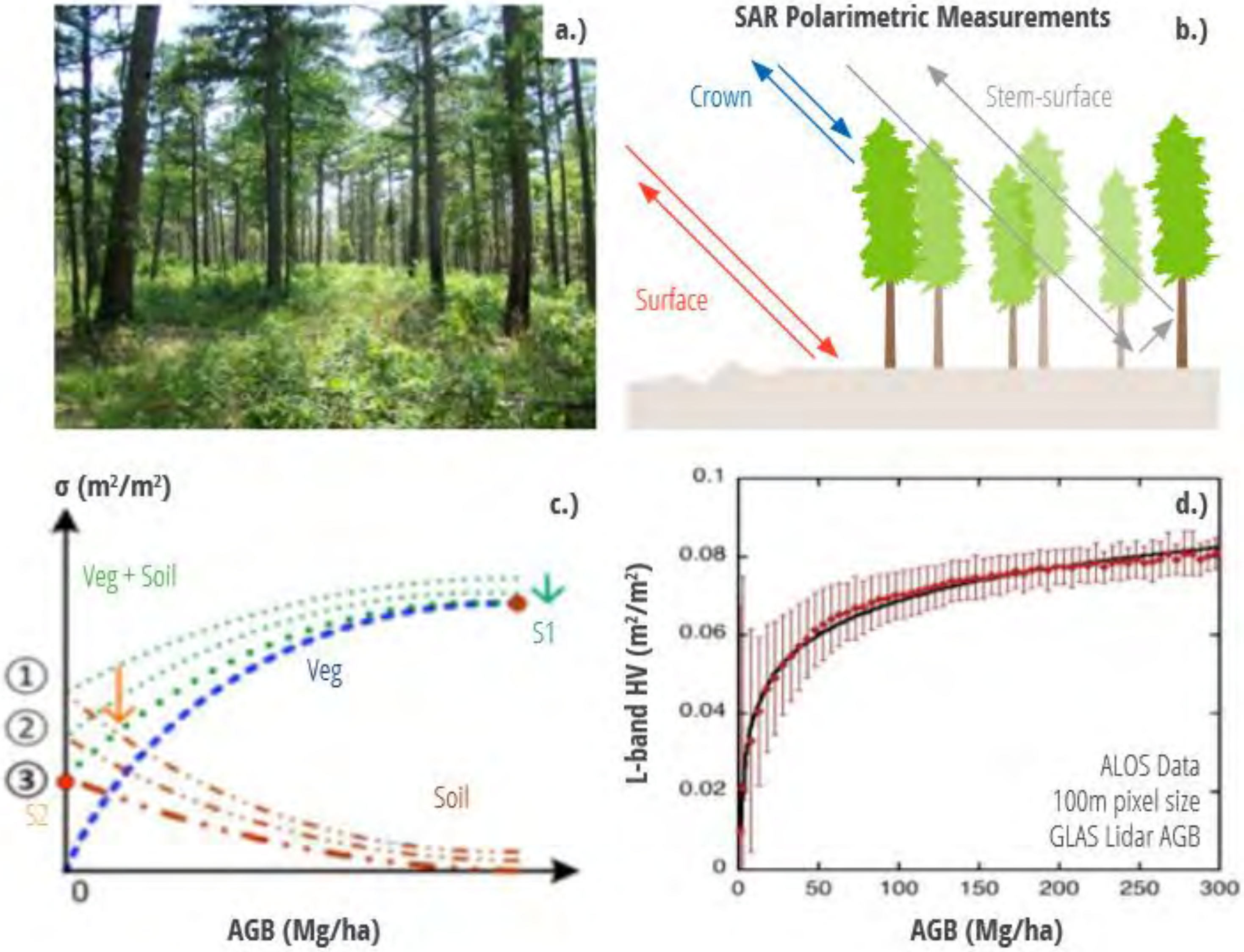

Yu & Saatchi S., 2016

Dielectric constant of wood material

Francois Demontoux, Wood Sci Technol, DOI 10.1007/s00226-017-0935-4, 2017

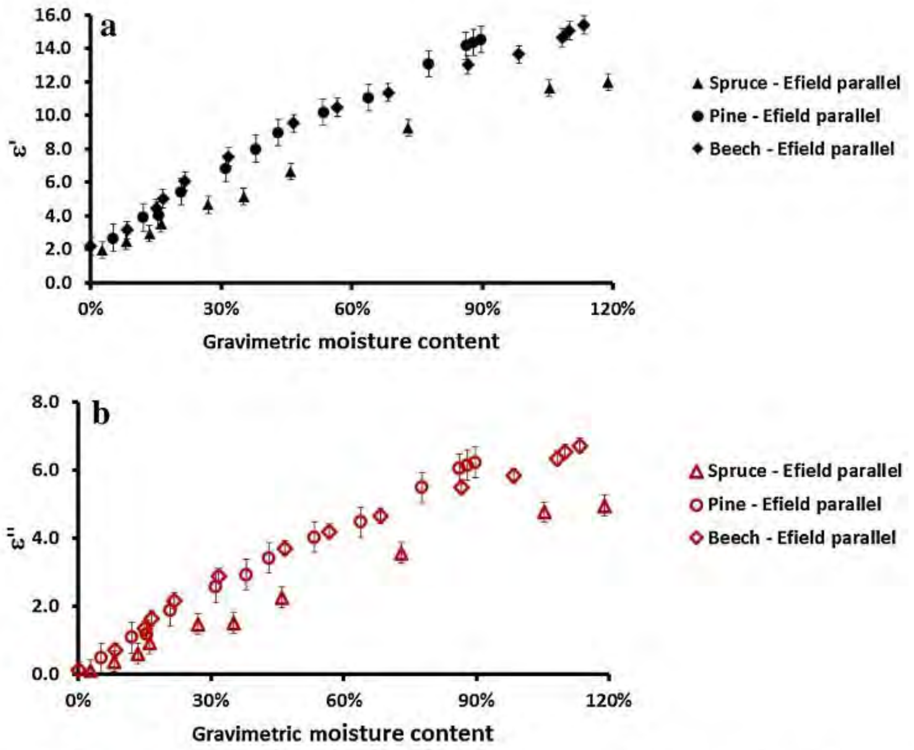

Fig. 1 ε' (**a**) and ε'' (**b**) versus gravimetric moisture content for spruce, pine and beech for E_{field} parallel to fiber direction and frequency of 1.26 GHz

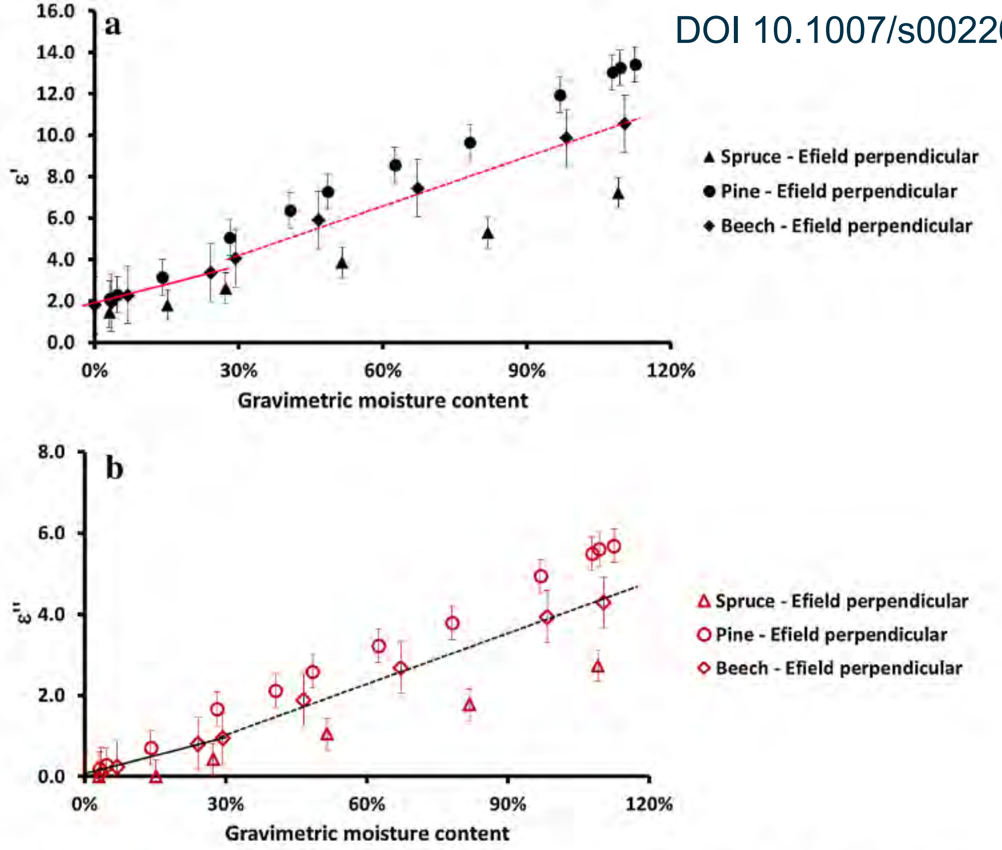

Fig. 2 ε' (**a**) and ε'' (**b**) versus gravimetric moisture content for spruce, pine and beech for E_{field} perpendicular to fiber direction and frequency of 1.26 GHz. Linear behavior of permittivity versus MCg is indicated by *straight lines* which are shown before (*plain*) and after (*dashed*) the fiber saturation point for beech data, indicating changes of slopes for ε' (**a**) and ε'' (**b**)

Dielectric constant of living wood

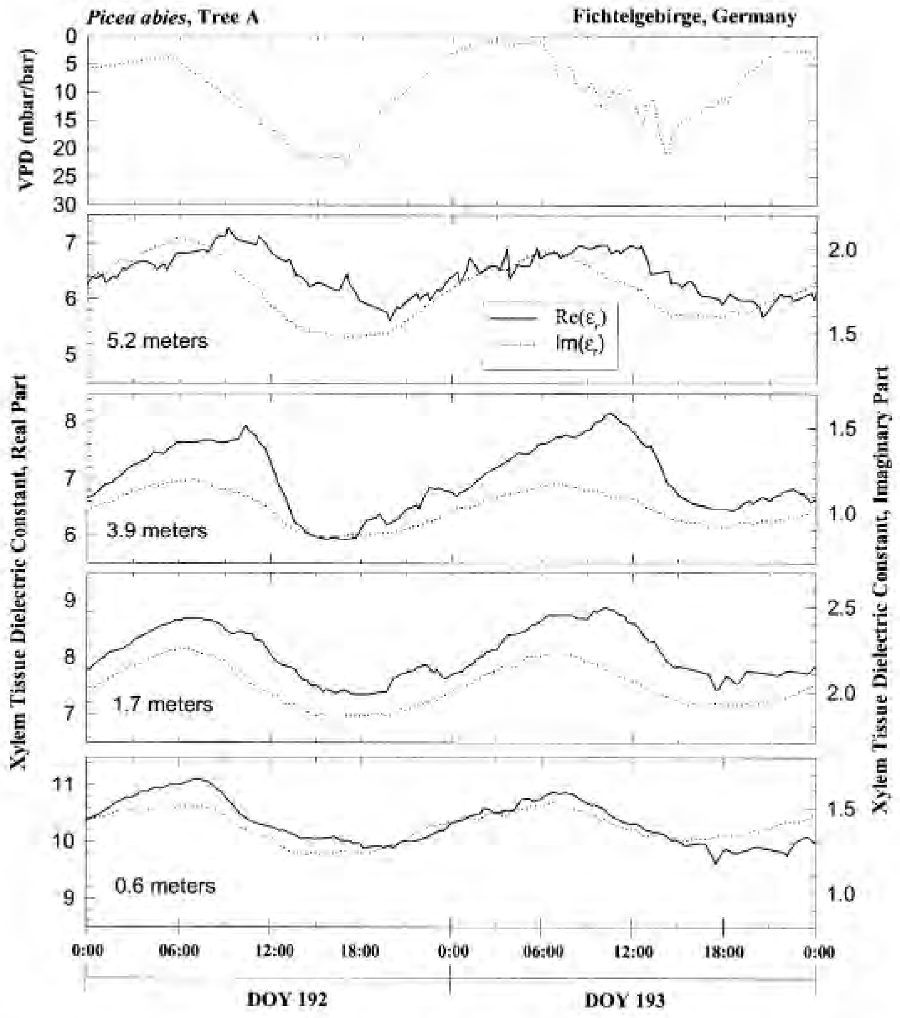

Fig. 7. Plots of VPD, $Re(\epsilon_r)$, and $Im(\epsilon_r)$ at four heights in the trunk of Tree A for DOY 192 and DOY 193. VPD is plotted with the zero reference placed at the top of the graph. No rain occurred during this period. Significant rainfall had last occurred on DOY 185. Dielectric constant was monitored at P band. VPD (mbar/bar) is the measured vapor pressure deficit (in mbar) normalized to standard atmospheric conditions at sea level (1013 mbar) (1 mbar/bar is equivalent to 1 Pa/kPa) [23].

IEEE TRANSACTIONS ON GEOSCIENCE AND REMOTE SENSING, VOL. 40, NO. 9, SEPTEMBER 20022063
Diurnal and Spatial Variation of Xylem DielectricConstant in Norway Spruce (Picea abies[L.] Karst.)as Related to Microclimate, Xylem Sap Flow, andXylem Chemistry, Kyle C. McDonald,, Reiner Zimmermann, and John S. Kimball

The TropiSCAT campaign

A ground-based radar observing a tropical forest

- Located in French Guyana – same site as TropiSAR
- Team members from ONERA, CNES, CESBIO, POLIMI
- 20 antennas installed on top of the Guyaflux tower (55 m)
- Fully polarimetric (HH, HV, VH and VV)
- Vertical resolution capabilities
- One image every 15 minutes over a time span of one year

⇒ Access to the vertical structure of temporal decorrelation

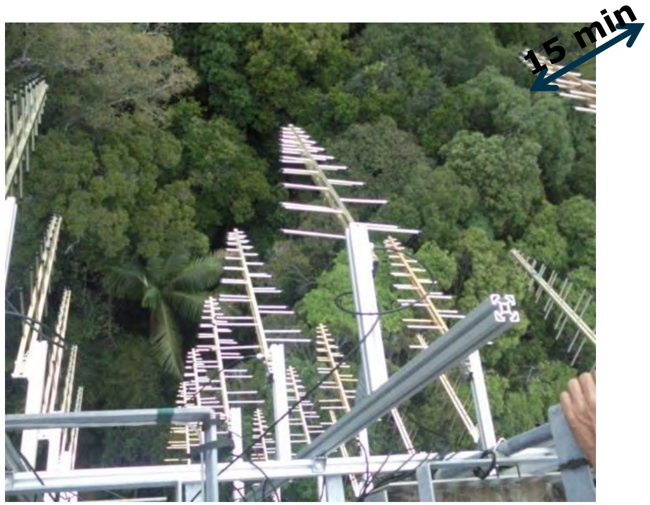

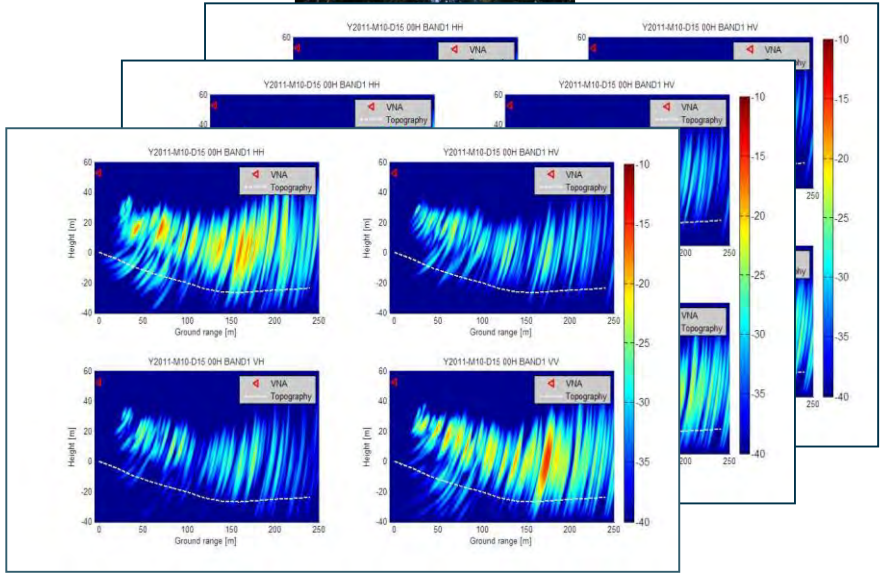

Diurnal variation of Radar center of mass

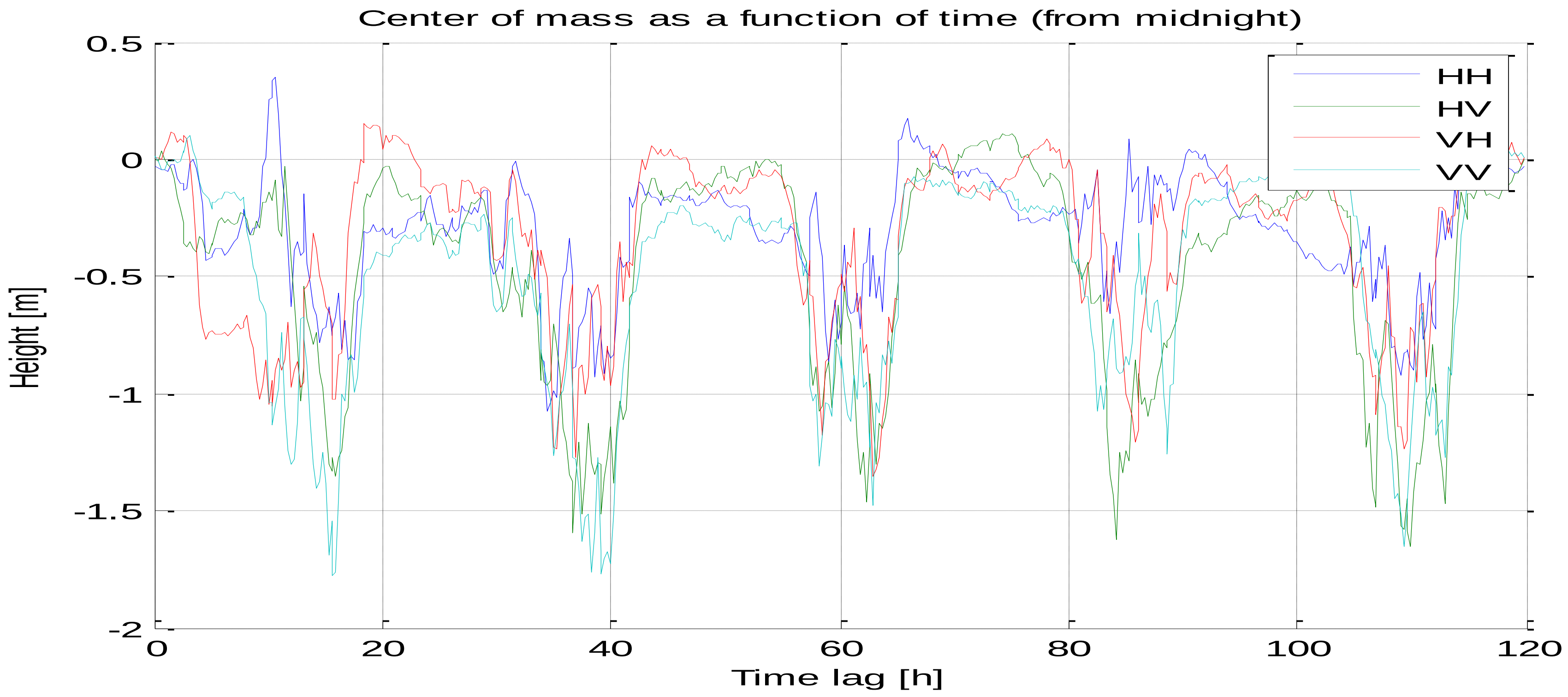

TropiScat 'centre of mass'

Height is relative to the height observed at midnight (about 20 m).

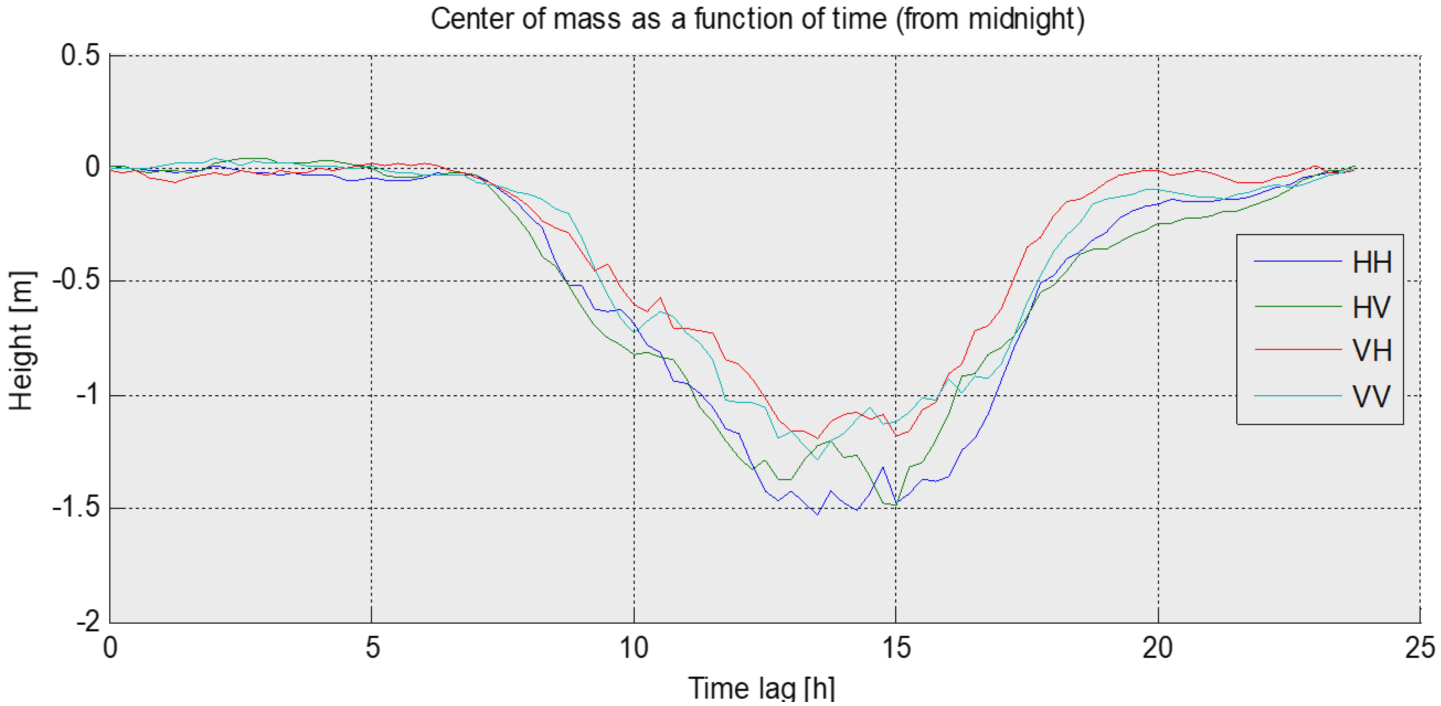

The center of mass is going down, from 7am , with minimum at 13-15 pm
and up again to original height at 22-23 h
The amplitude is about 1.5 m inside the forest.

Average of 10 dry days (without rain) during the period from 8 to 31 December 2011

Diurnal cycle of radar intensity

Tour Guyaflux
Equipe Guyafor

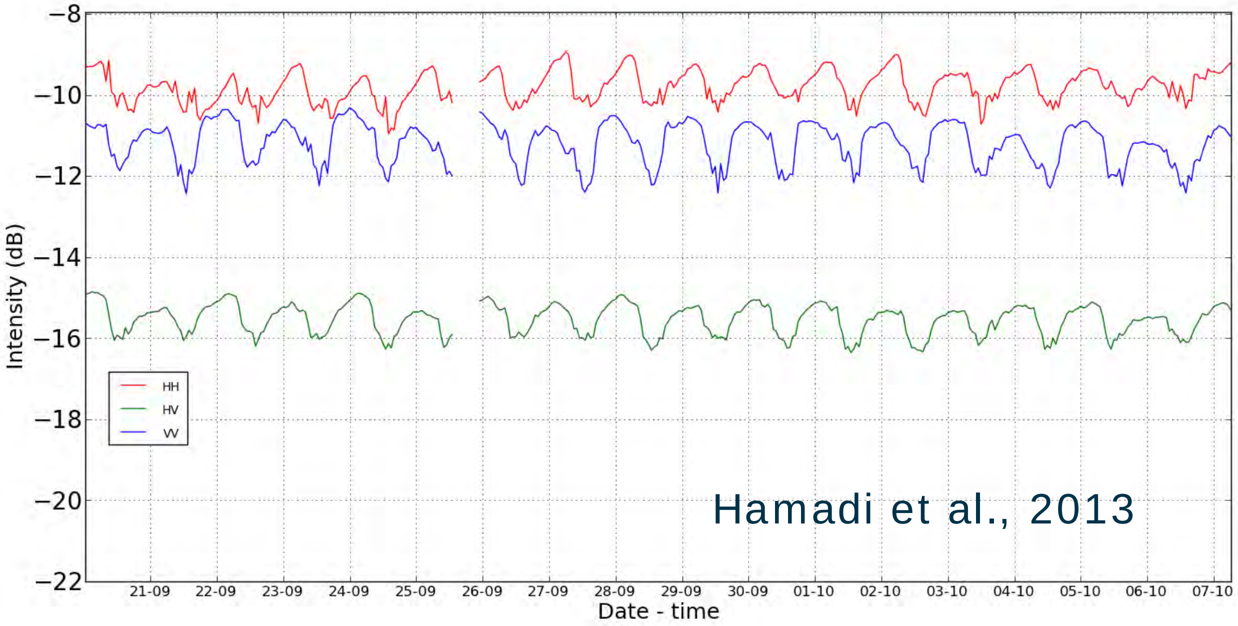

THE EUROPEAN SPACE AGENCY

Research infrastructure:

- A 50-m high radar tower in a hemi-boreal forest site in southern Sweden.
- Acquires tomographic P/L/C-band radar data
- On-site weather station and moisture sensors: dendrometers, sap flow, and soil moisture
- More details at www.borealscat.se

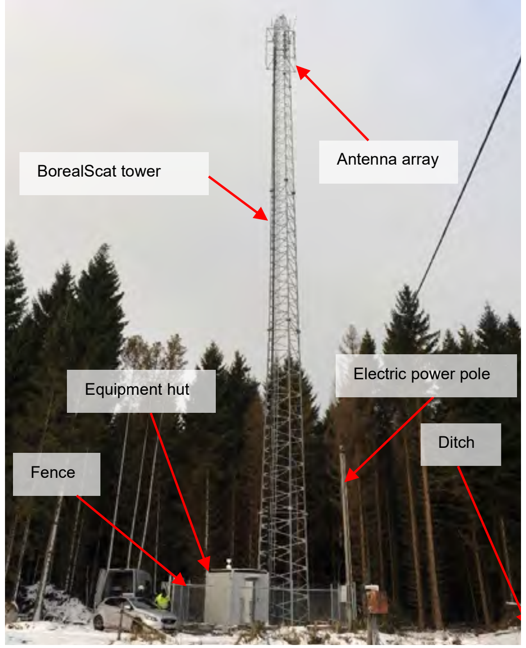

Antenna arrays

Mature spruce stand

L. Ulander, A. Monteilh, 2020

Backscatter variability caused by freeze/thaw in boreal forest

esa

Backscatter Jun 2017- Jun 2019: Canopy, Ground and Full forest

HH

VV

VH

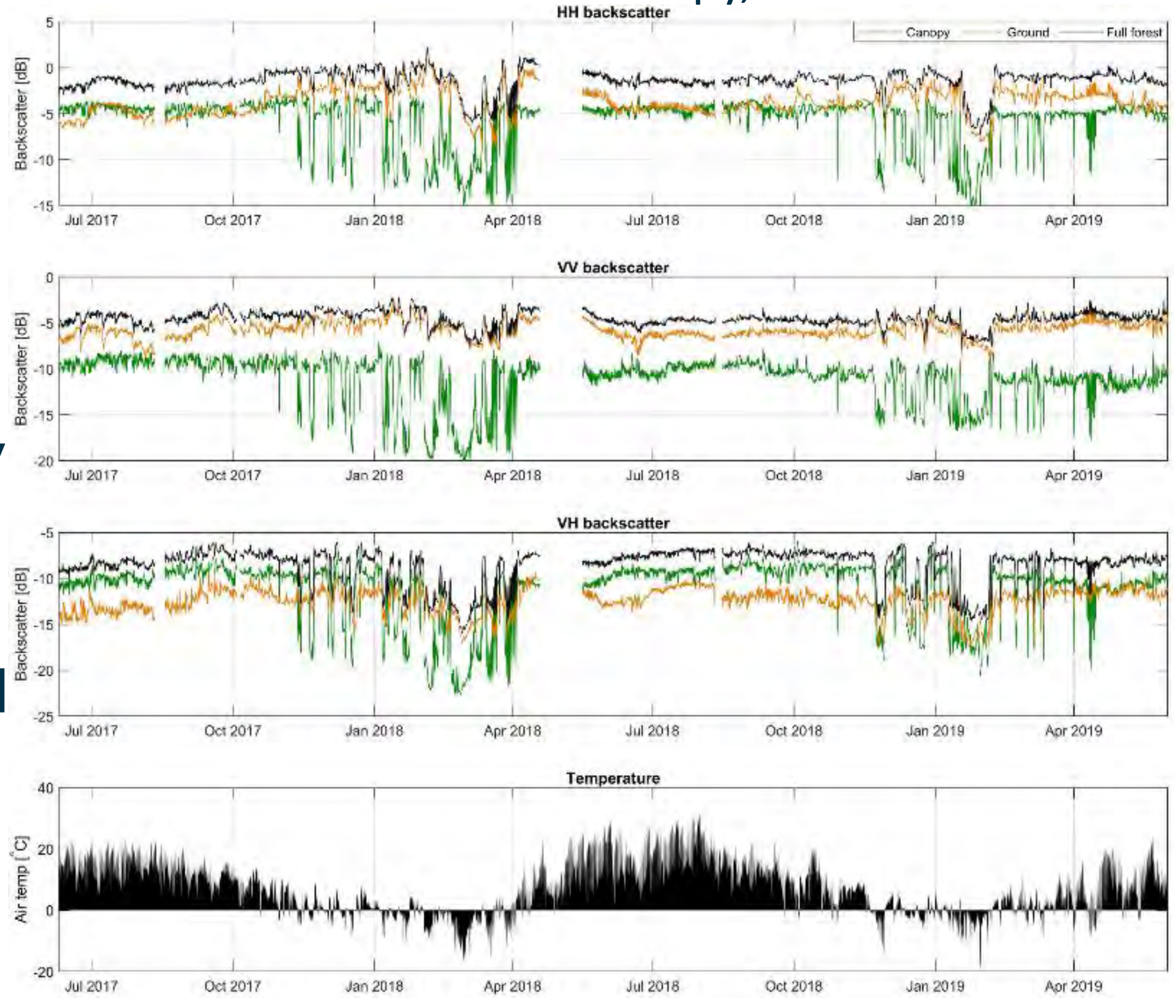

Monthly range of canopy backscatter

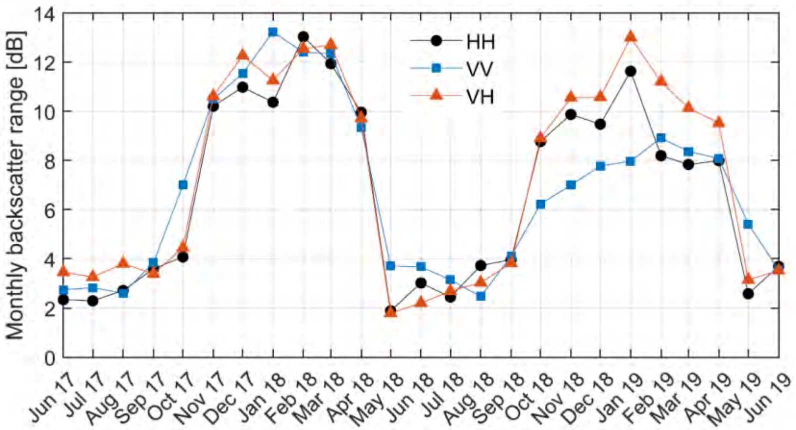

Backscatter varies 2-4 dB during summer, whereas much larger variability during winter (freeze/thaw).

L. Ulander, A. Monteilh, 2020

Monteith & Ulander, IEEE J-STARS, 14, 1967-1984, 2021 (open access)

Forest biomass is a key element in the carbon cycle

Biomass is an ECV (Essential Climate Variable) of the ESA CCI (Climate Change Initiative)

1. Biomass consists of approximately 50% carbon

2. Forests account for 70-90% of the terrestrial above-ground biomass, and the majority are located in the tropics

3. The forest biomass stocks and their change remain poorly quantified

Biomass = dry weight of woody matter (in tons/ha)

Forests are a major carbon sinks, but can be C sources

Carbon sinks

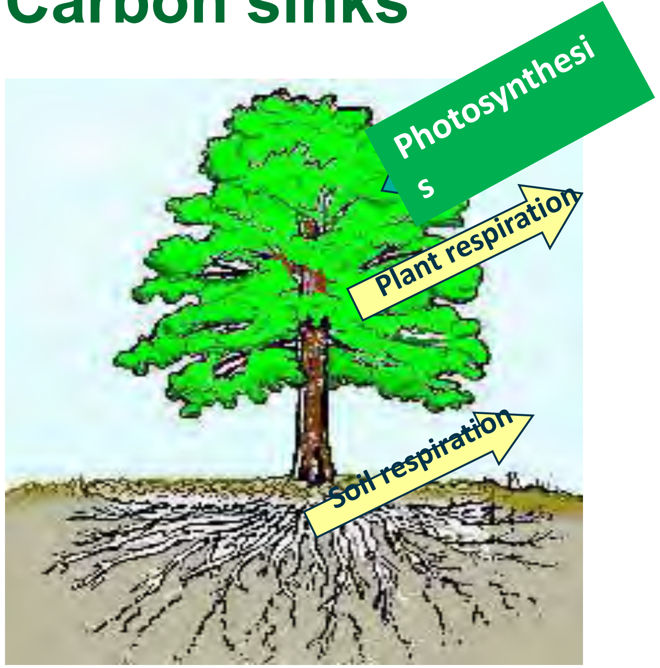

Carbon sources

International Conventions and National Determination on the forests aim at:

- o Increase C sequestration
- o Reduce the emissions

→ need to quantify C losses and gains for the carbon cycle

SAR intensity increases with biomass

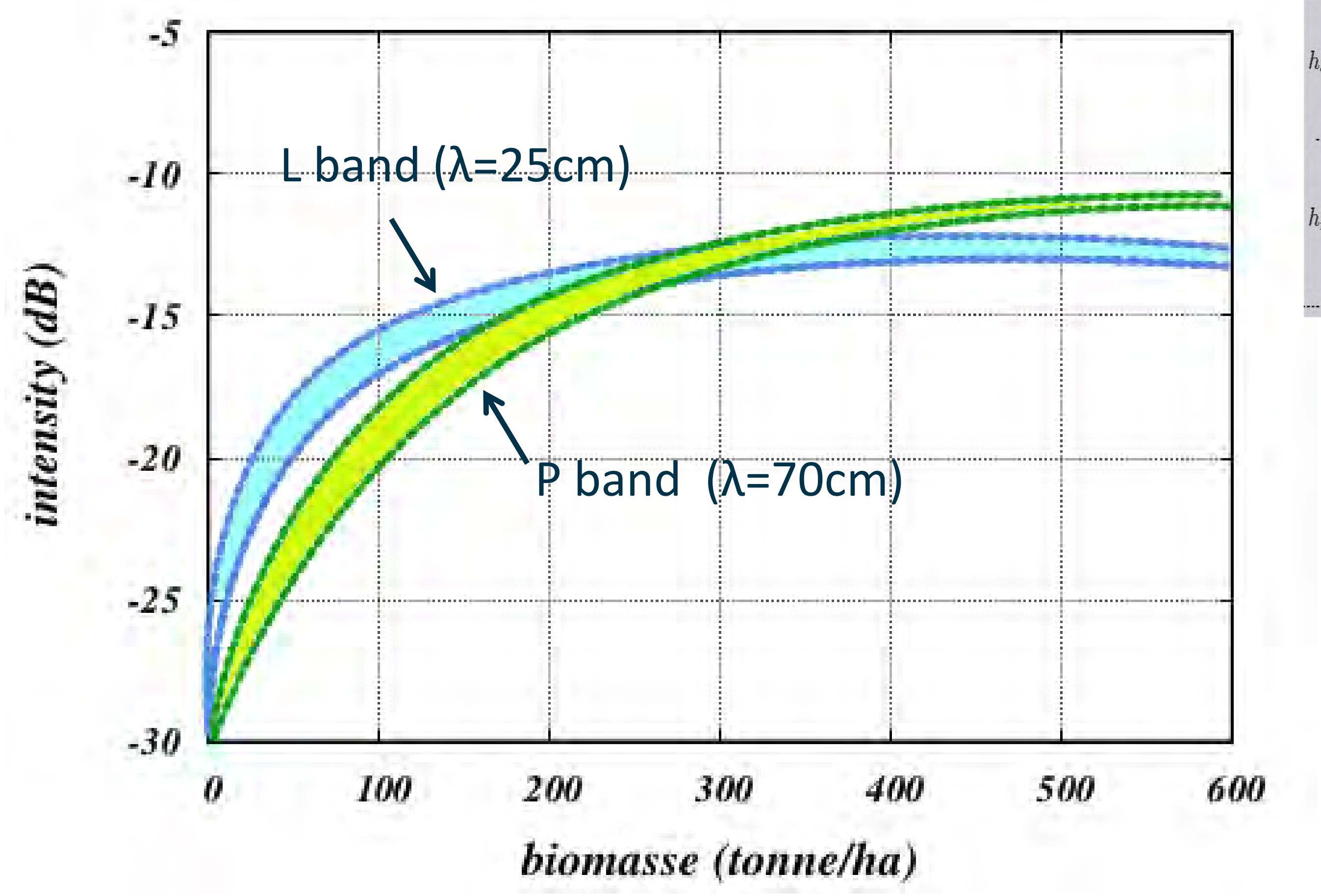

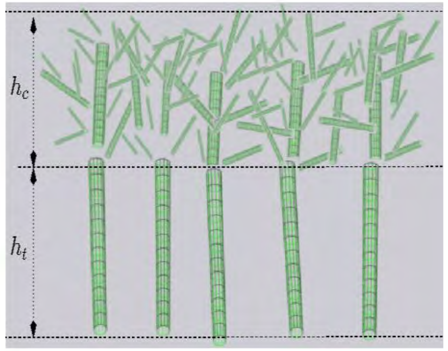

SAR intensity increases with biomass

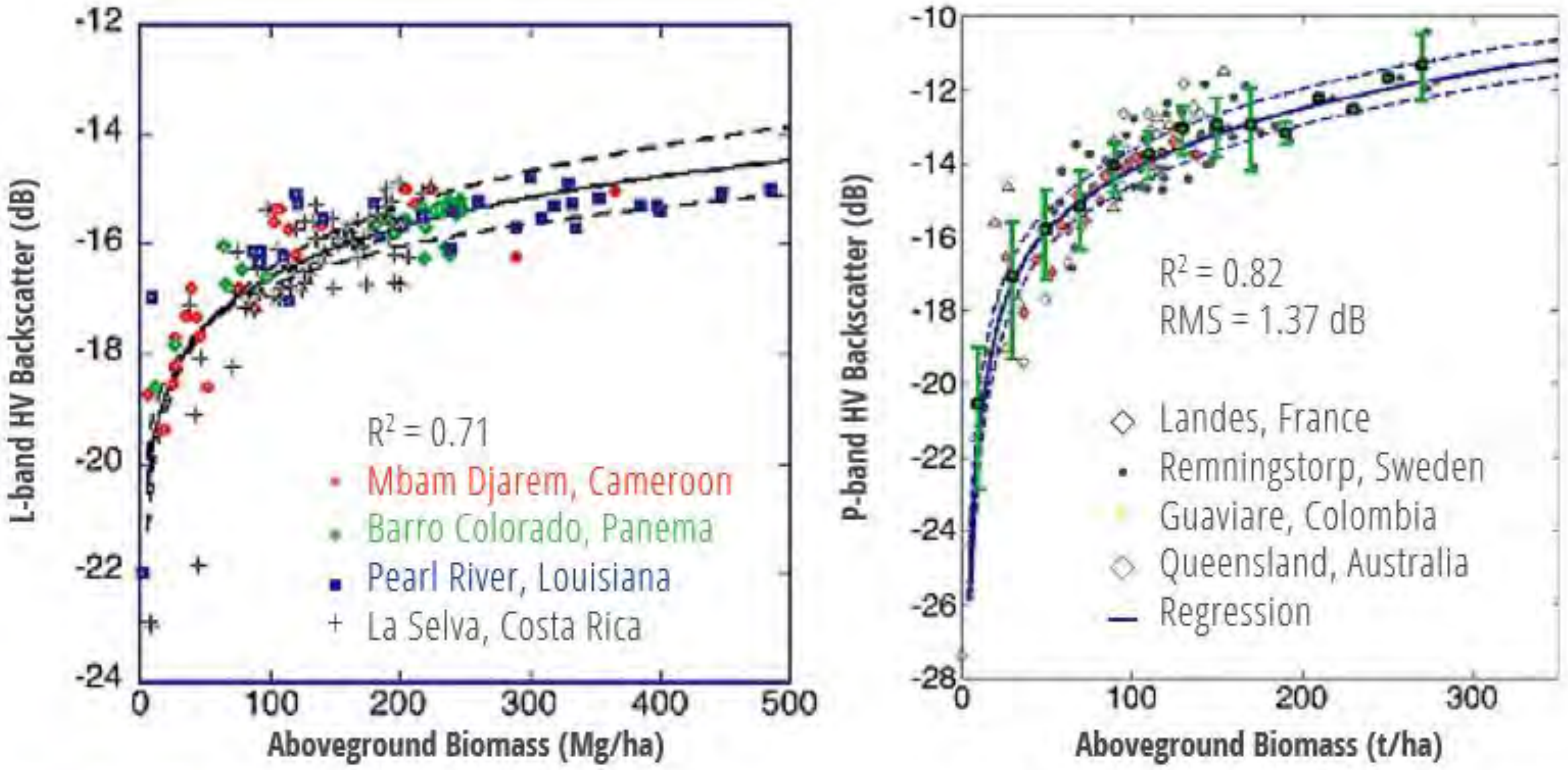

Figure 5.22 *Sensitivity of radar backscatter measurement at L-band and P-band frequencies and HV polarization to forest AGB over sites distributed in boreal, temperate, and tropical ecosystems (Shugart et al. 2010).*

Scattering mechanisms simulated by a R.T. model

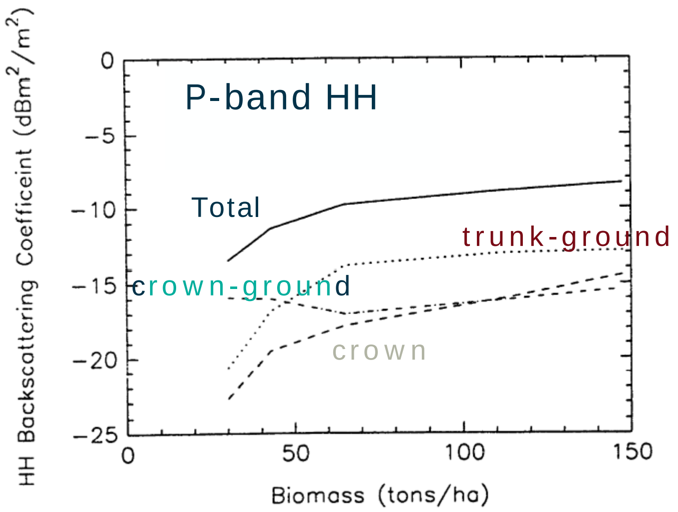

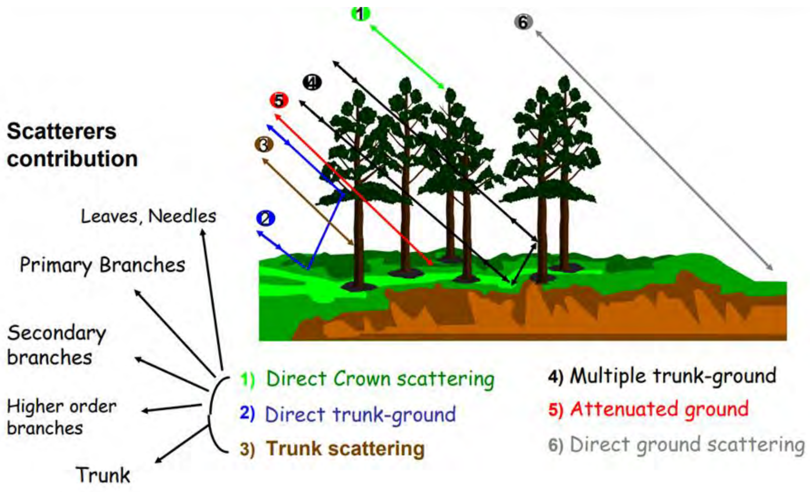

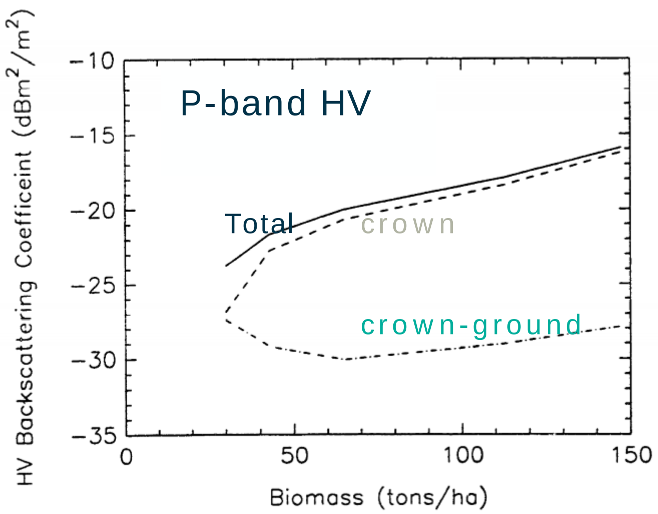

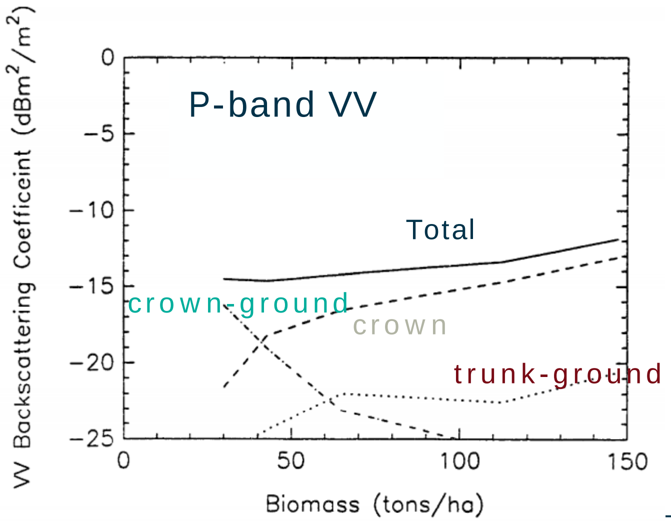

- Le Toan, T., Beaudoin, A., Riom, J., & Guyon, D. (1992). Relating forest biomass to SAR data. *IEEE Transactions on Geoscience and Remote Sensing*, *30*(2), 403-411.
- Hsu, C. C., Han, H. C., Shin, R. T., Kong, J. A., Beaudoin, A., & Le Toan, T. (1994). Radiative transfer theory for polarimetric remote sensing of pine forest at P band. *International Journal of Remote Sensing*, *15*(14), 2943-2954.
- Beaudoin, A., Le Toan, T., Goze, S., Nezry, E., Lopes, A., Mougin, E., ... & Shin, R. T. (1994). Retrieval of forest biomass from SAR data. *International Journal of Remote Sensing*, *15*(14), 2777-2796.

Crucial point: for biomass inversion to perform well, data must be processed to retain only the volume component of the forest canopy

SAR measurement modes-BIOMASS

PolSAR

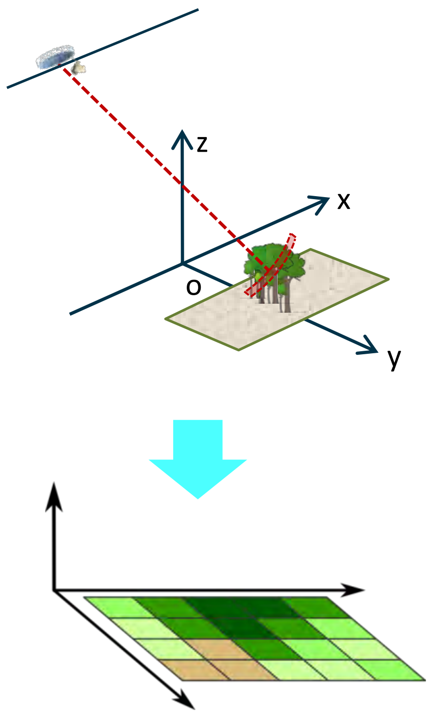

Pol-InSAR

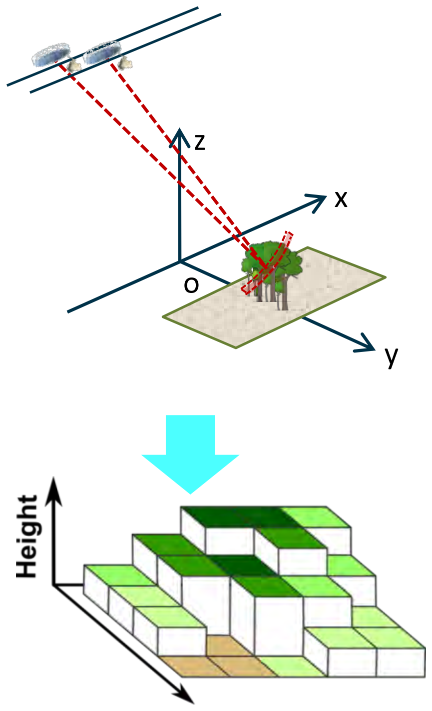

TomoSAR

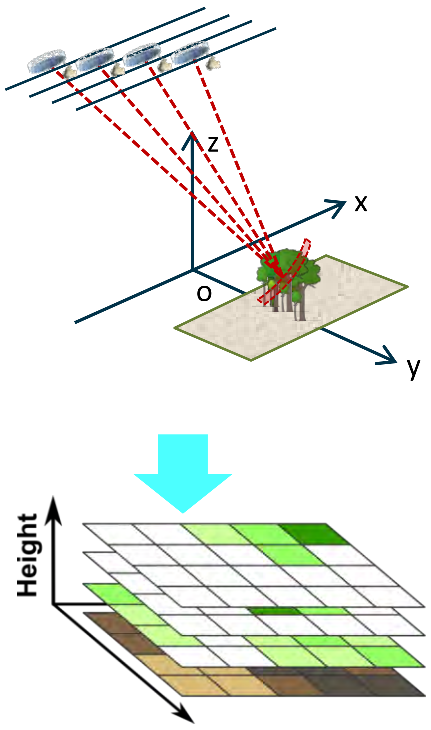

SAR tomography, a new concept to explore 3D forest structure

Generates images of different forest layers from multi-orbit SAR images

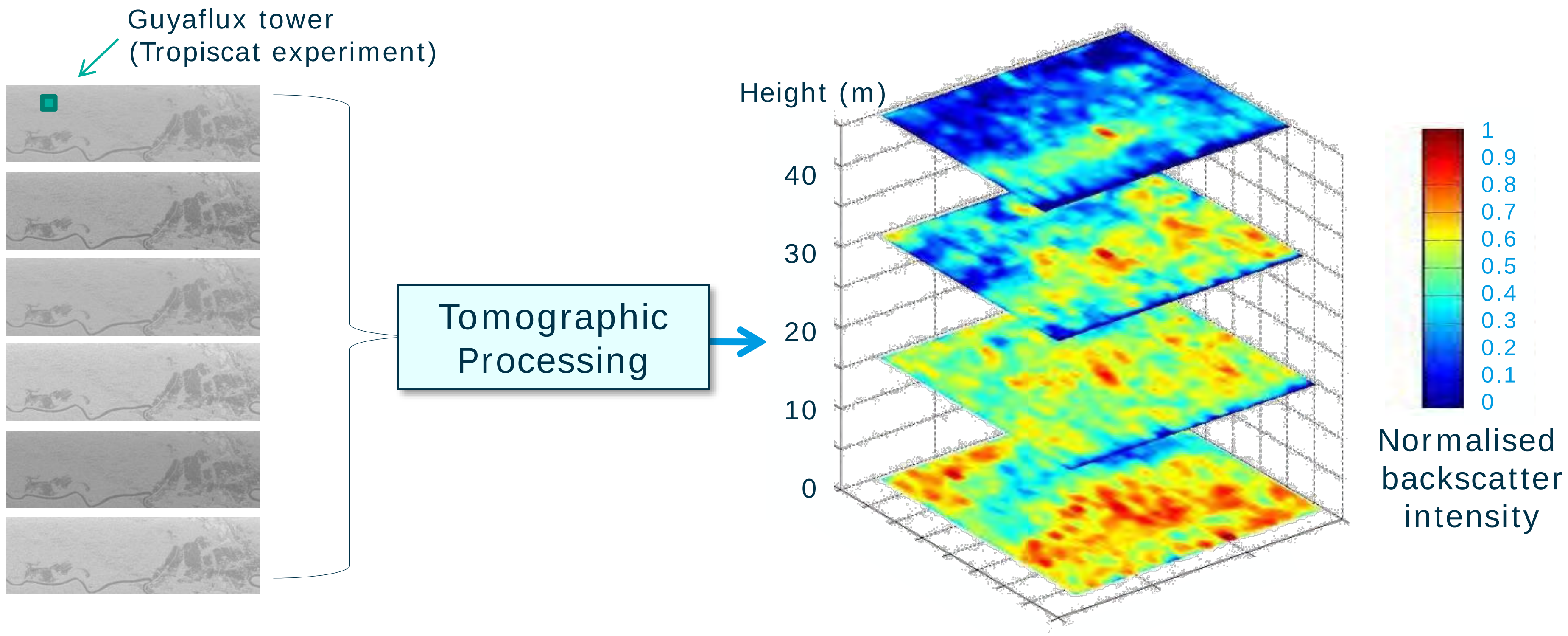

Tomography to understand scattering mechanisms

Provides the most complete description of all contributions to the radar signal through 3D reconstruction of forest backscatter.

Boreal forest

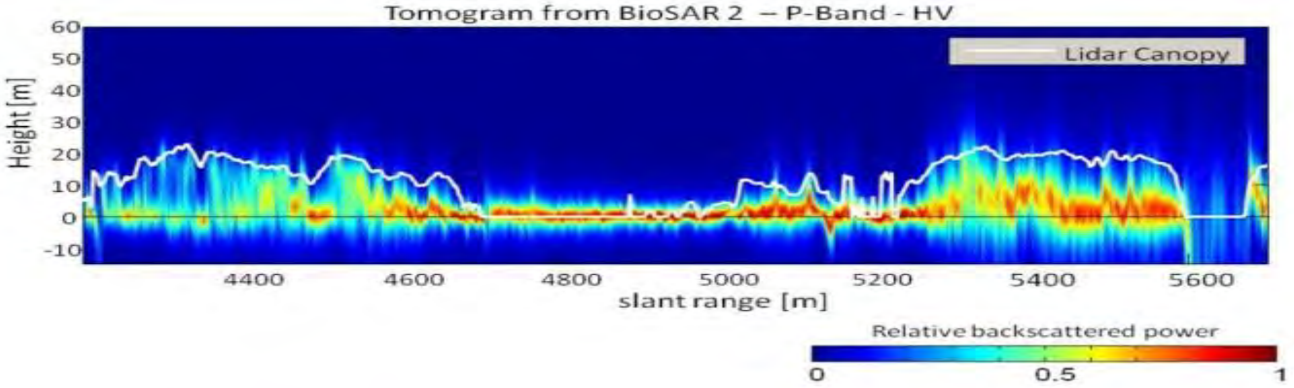

Tropical forest

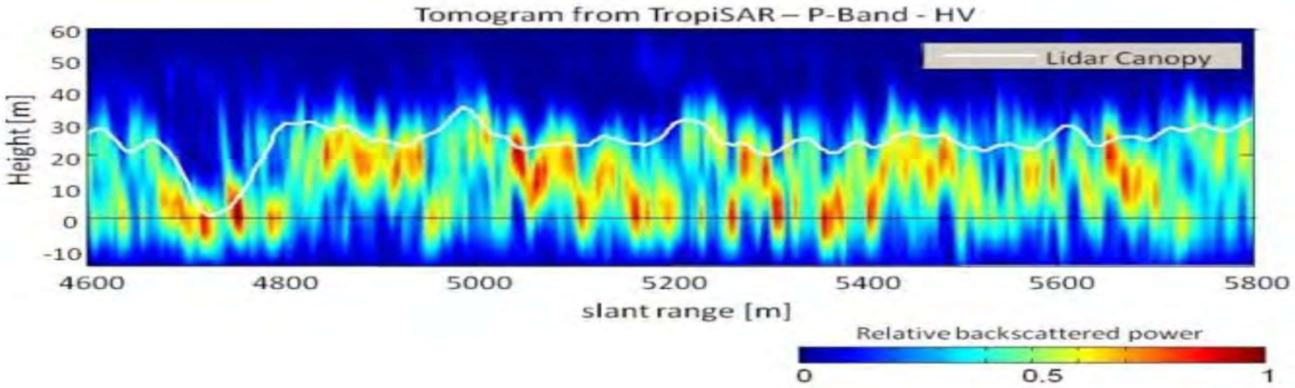

Scattering mechanisms in tropical forests

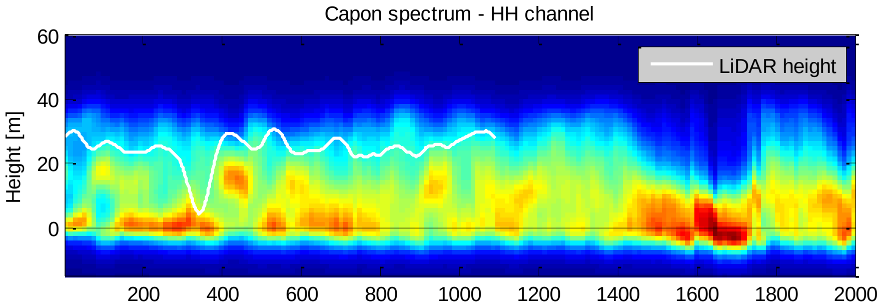

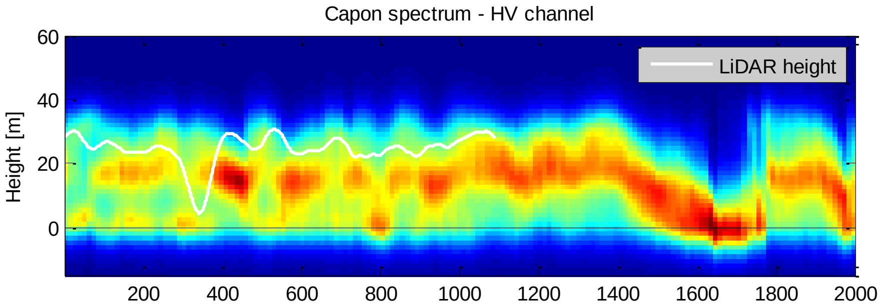

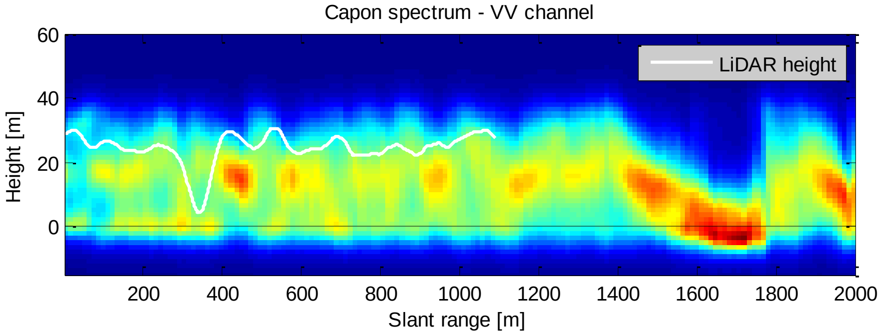

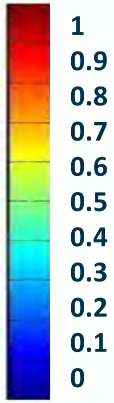

Normalised backscatter intensity

Tomography to understand scattering mechanisms

Boreal forest

Tropical forest

Provides the most complete description of all contributions to the radar signal through 3D reconstruction of forest backscatter.

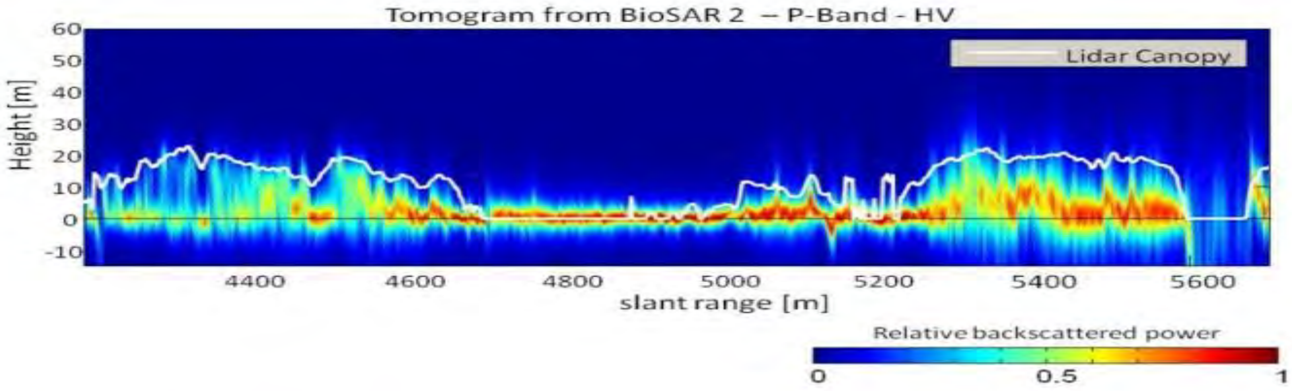

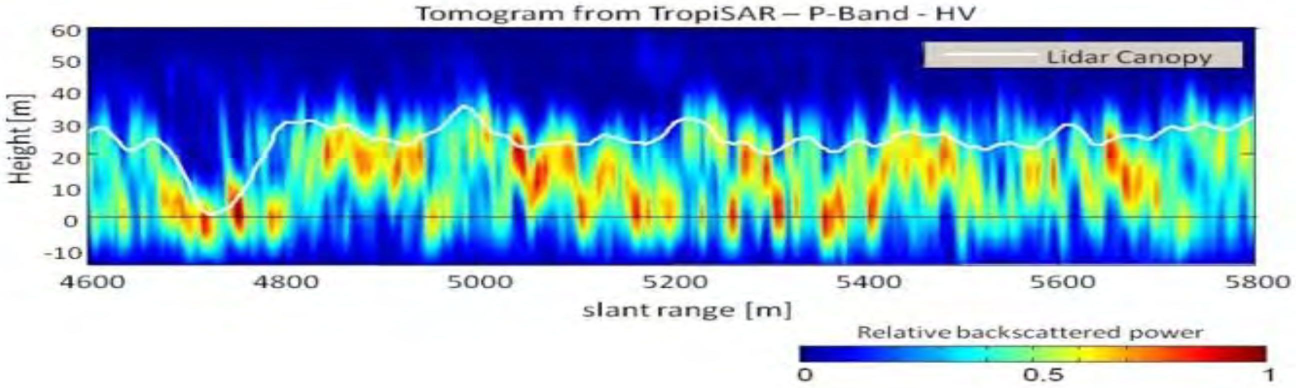

Isolate the layer not containing ground scattering

.. Whose biomass related to AGB

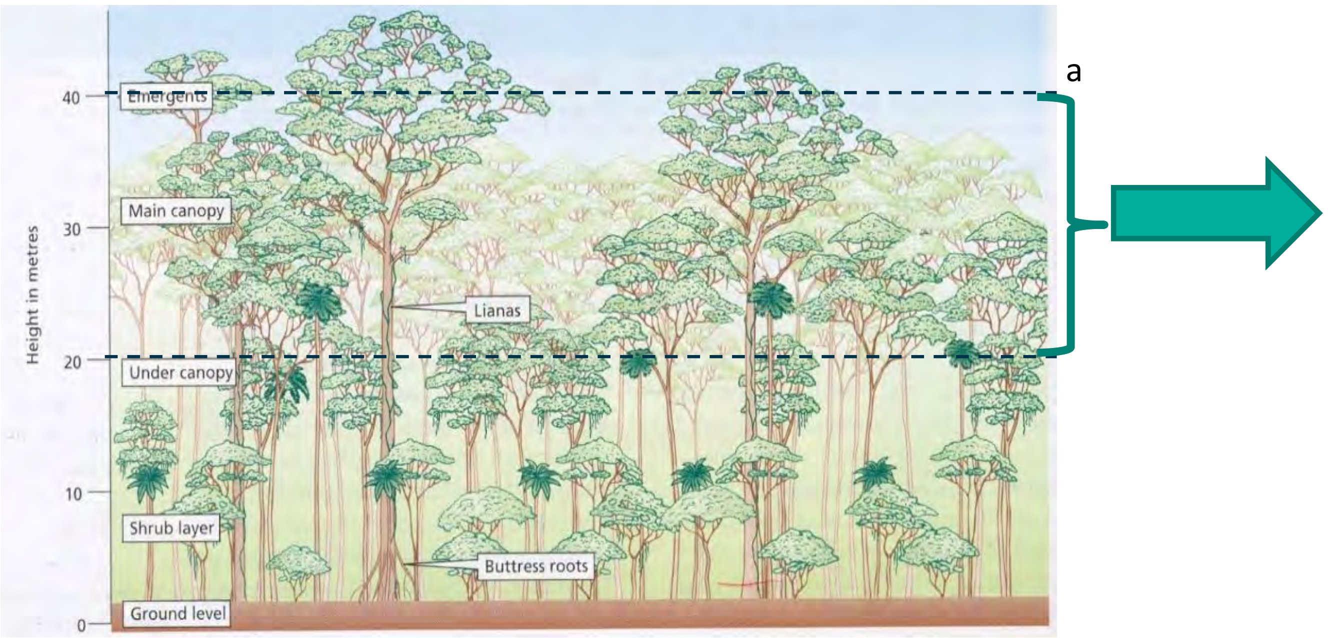

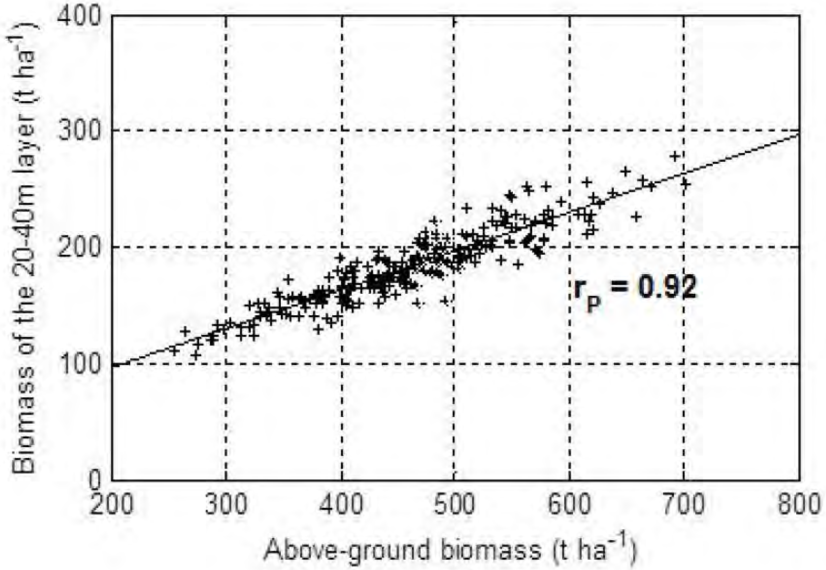

Using Troll model (from Chave, 1999)

Tebaldini, S., Minh, D. H. T., d'Alessandro, M. M., Villard, L., Le Toan, T., & Chave, J. (2019). The status of technologies to measure forest biomass and structural properties: State of the art in SAR tomography of tropical forests. *Surveys in Geophysics*, *40*(4), 779-801.

MINH, Dinh Ho Tong, LE TOAN, Thuy, ROCCA, Fabio, *et al.* Relating P-band synthetic aperture radar tomography to tropical forest biomass. *IEEE Transactions on Geoscience and Remote Sensing*, 2013, vol. 52, no 2, p. 967-979.

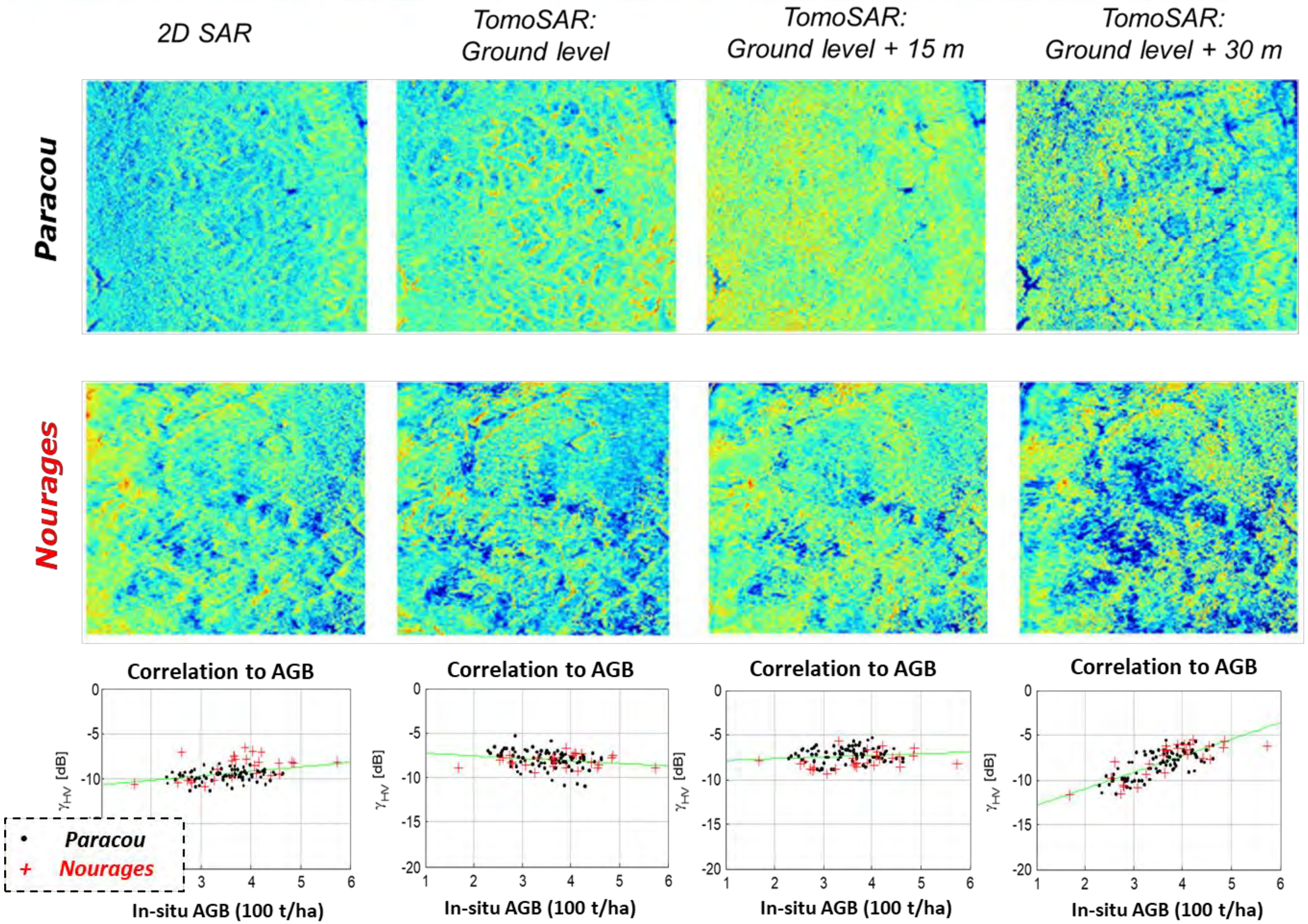

Ho Tong Minh Dinh et al., 2013, 14

La biomasse des forêts tropicales (≥ 500 t/ha) mesurable par le SAR bande P de Biomass

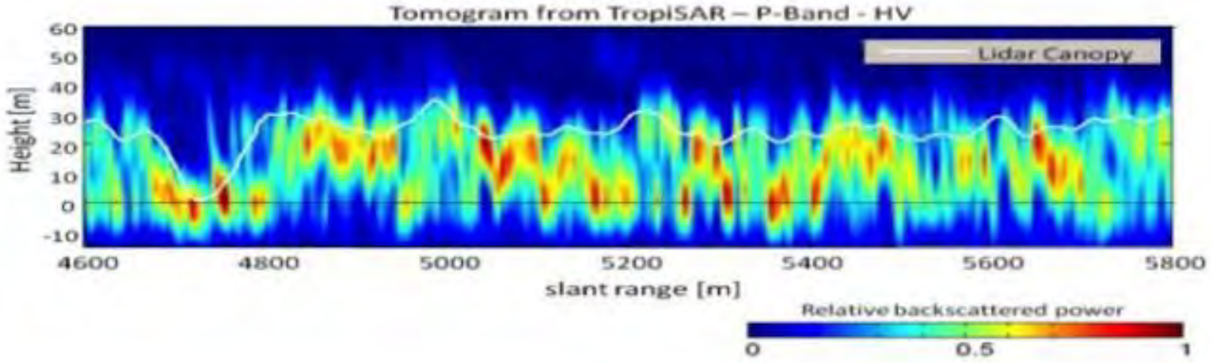

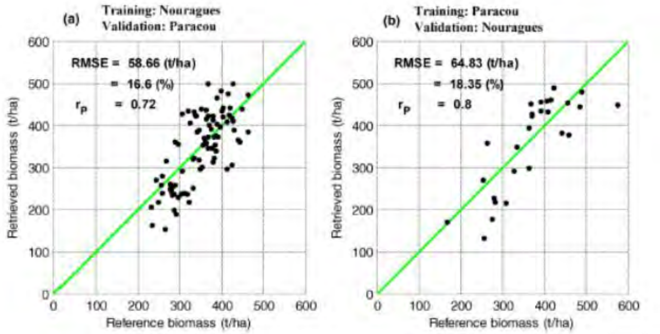

Contents lists available at ScienceDirect

Remote Sensing of Environment

journal homepage: www.elsevier.com/locate/rse

SAR tomography for the retrieval of forest biomass and height: Cross-validation at two tropical forest sites in French Guiana

Dinh Ho Tong Minh [a,b,*], Thuy Le Toan [b], Fabio Rocca [c], Stefano Tebaldini [c], Ludovic Villard [b], Maxime Réjou-Méchain [d,e], Oliver L. Phillips [f], Ted R. Feldpausch [g], Pascale Dubois-Fernandez [h], Klaus Scipal [i], Jérôme Chave [d]

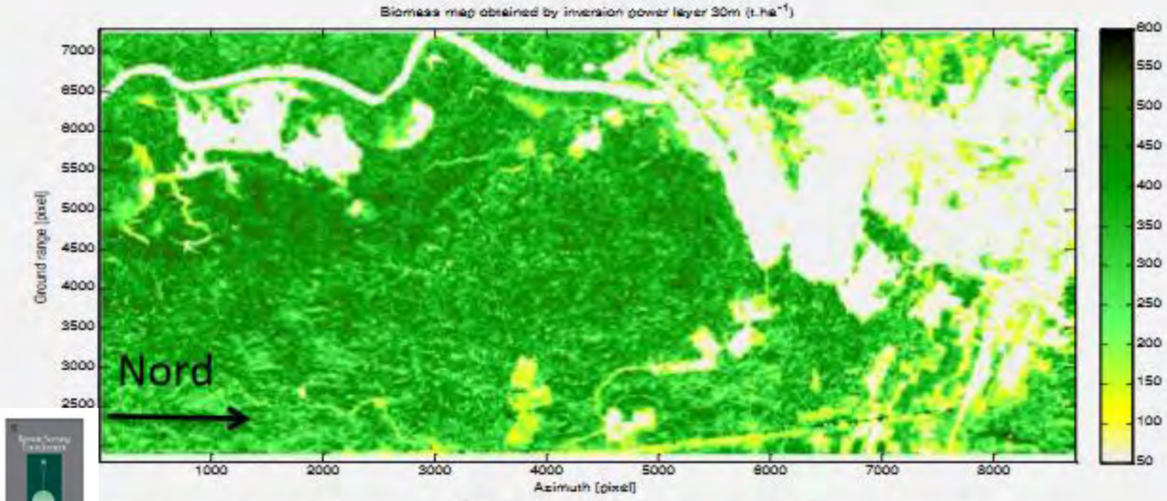

Carte de biomasse à 50 m dérivée de la tomographie

Tomography techniques allow AGB up to 500t/ha

Cross-continental robustness and transferability of tropical forest biomass estimation by SAR tomography

LPS, 2018

Yen-Nhi Ngo[a,1], Dinh Ho Tong Minh[a,1,2], Doyle McKey[b], Ludovic Villard[c], Stefano Tebaldini[d], Mauro Mariotti d'Alessandro[d], Jérôme Chave[e], Clément Albinet[f], Klaus Scipal[g], and Thuy Le Toan[c]

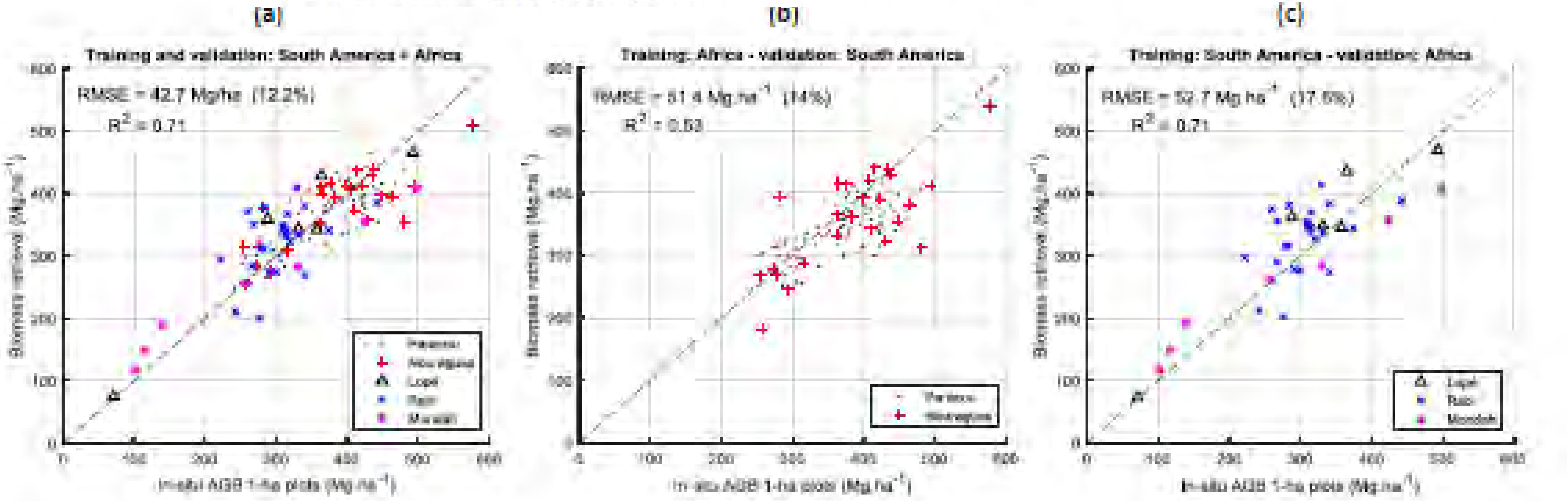

Fig. 3. Results for TomoSAR biomass retrieval based on cross-validations: comparison of retrieved AGB and In-situ AGB. (a) training and validation samples from the same study site. (b) training samples from Africa and validation samples from South America. (c) training samples from South America and validation samples from Africa.

Isolating the volume by ground cancellation

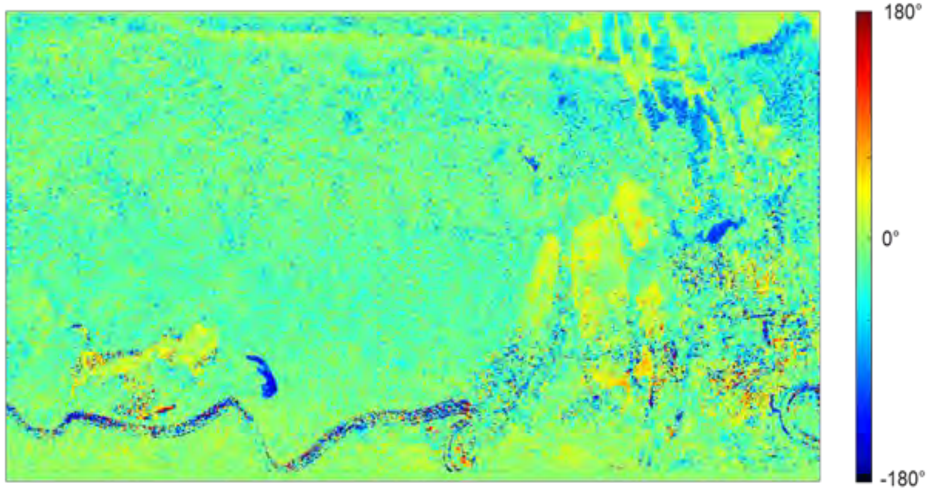

HH-VV phase difference:

30 m height

Tomographic section at terrain height

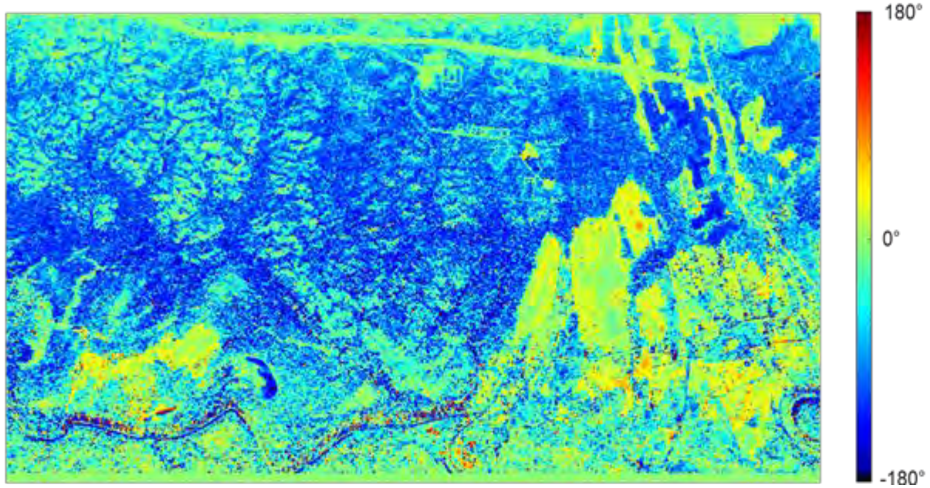

Ground level

More by: S. Tebaldini

Biomass estimation

1. Strong evidence that the volume layer 25-35 m above the ground in tropical forest is strongly correlated with the total AGB.
2. Development of methods for ground cancellation using **tomography or Pol-InSAR** to isolate volume scattering.
3. Development of an approach to solve the volume scattering equation that minimizes the need for reference data.

Summary

1. An introduction on radar remote sensing has been given, with focus on agriculture and forests.

2. It is essential to understand the statistical properties of SAR images, and the physical content of the SAR data , to interpret and to analyse the images, and to develop retrieval and mapping algorithms.

3. Lectures and training on advanced SAR polarimetry, Pol-InSAR and TomoSAR will be provided in the following sessions.